九州工業大学大学院生命体工学研究科

令和 2 年度　博士学位論文

Regulatory effects of lignocellulose derived compounds on the growth and metabolism of microalga *Euglena gracilis*

（リグノセルロース由来成分による微細藻類ユーグレナの成長と代謝の調節作用に関する研究）

令和 3 年 3 月

ZHU JIANGYU

Content

Chapter 1. Introduction

1.1 Microalgae: source of high value-added products

Microalgae are a diverse group of unicellular photosynthetic microorganisms comprising eukaryotic protists and prokaryotic cyanobacteria that live in saline and freshwater environments [1]. They are the major primary producers in water bodies, and play important roles in the material circulation and energy flow of aquatic ecosystems [2]. They can carry out photosynthesis for autotrophic growth, converting solar energy and carbon dioxide into available algal biomass, and producing oxygen [3]. According to the reports, microalgae consume a considerable amount of greenhouse gases and produce approximately half of the atmosphere oxygen, which have a significant positive effect on the environment and ecology [4]. On the other hand, microalgae are one of the bases of the food chain, which are able to provide energy for all the trophic levels above them, and play a role in energy flow and circulation [2]. It is reported that the species of microalgae is between 200,000 and 800,000, of which about 50,000 species have been isolated and identified. These microalgae are widely distributed in aquatic ecosystems, and most of them are easy to artificially propagate and rich in an abundant of trace elements and biologically active substances, thus they have broad application prospects in food, feed, supplements, cosmetics, pharmaceutical, biofuel, environmental protection and other industries. Although the potential of microalgae in production and life is extremely huge, their development level is still relatively low at this stage which is in its infancy. It is urgent to replace the increasingly depleted traditional raw materials with renewable microalgae in various fields.

In recent decades, with the development of modern biotechnology and the improvement of separation and identification methods, the research and application of microalgae has entered a whole new era. It is reported that, over 15,000 new compounds derived from algal biomass have been structure-determined [5]. Recently, microalgae have been regarded as the novel and sustainable alternatives to conventional microbial cell factories (such as bacteria), since they are able to produce a vast quantity of bioactive products at high efficiency through photosynthesis [6]. These high-value-added products from microalgae include primary metabolites such as

proteins, carbohydrates and lipids, and secondary metabolites including chlorophylls, carotenoids, phycocyanin, sterols, plant hormones, phenylpropanes, with various biological properties, such as nutrition, neuroprotection, anti-oxidation, antibacterial, anti-inflammatory, anti-tumor properties. It is predicted that the global market of microalgal products will increase to 1.14 billion dollars by 2024 [7]. However, there are still many major challenges, to quantify the benefits obtained from microalgae, fully understand the potential adverse effects of some by-products, and ensure the sustainable supply of microalgal biomass for large-scale industrial production [8].

1.1.1 The freshwater microalga *Euglena gracilis*

Euglena gracilis is one of the most widely and successfully cultivated commercial microalgae, amd usually found in quiet inland waters. When its population reaches a certain number, the ponds and ditches will be greened. The micrograph of *E. gracilis* was shown in Figure 1-1. The cell surface of *E. gracilis* is soft, lacking cell wall, and there is only one film composed of protein layers supported by microtubule structure [9]. This film spirals around the cells and can slide on each other. It is one kind of metabolite polysaccharides, giving excellent flexibility and contractility to the *E. gracilis* cells, so that the cells can regulate their cell morphologies according to the external environments and the biological clock [10]. The morphology of the microalgae cells can often reflect the living state of the cells. When the cell state is needle-shaped, the algae cells tend to have stronger cell vigor and metabolic activity. Therefore, the cell aspect ratio of *E. gracilis* is often used as a biological indicator to evaluate the physiological state of algae cells.

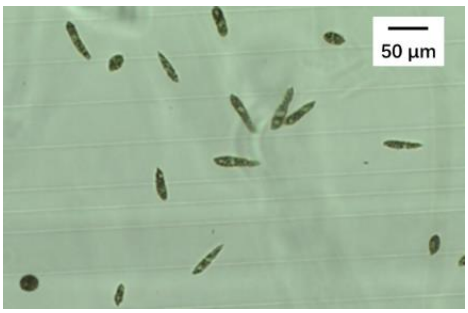

Figure 1-1. Micrograph of *Euglena gracilis* cells.

The lifestyle of the *E. gracilis* is quite special. It has both plant and animal characteristics: on the one hand, when there is sufficient sunlight, it can use chloroplasts containing chlorophyll

a and b to synthesize carbohydrates for living. On the other hand, it can also absorb external nutrients through osmosis and grow like animals. In the microalgae cells, it contains an organelle composed of carotenoid particles called an eye point. The eye point itself is not photosensitive, but it filters out the sunlight that falls on the light-detecting structure at the bottom of the flagella, allowing the cells to find and move toward the light, which is also the reason for the phototropism of *E. gracilis* cells [11].

Due to its faster growth rate than terrestrial plants and many other advantanges, *E. gracilis* has been widely used as a model microorganism in physiological and biochemical research. In addition, this alga has the special phylogenetic position, and is easy to cultivate, thus, *E. gracilis* is a suitable protozoa to work with [12]. Different from bacteria and other protists, *E. gracilis* has no pathological risks to humanbeings, and it is safe to conduct large-scale cultivation outdoors. *E. gracilis* can grow autotraphically through photosynthesis and heterophically by phagocytosis. Different carbon sources can be assimilated by the microalgal cells in a wide pH range. Moreover, it can utilize the abandoned phosphorus and nitrogen from the wastewater containing chemical and organic pollutants [13]. Thus, it is also an important species of microalga for the purification of aquatic environment.

1.1.2 Valuable metabolites in *E. gracilis* and the application fields

The metabolic capacities of *E. gracilis* is complicated, and comparable to those of multicellular organisms, which provides extansive opportunities for the production of high-value-added metabolites [12]. According to the report of literature [14], the dry cell biomass of *E. gracilis* contains around 23.1% proteins, 7.5% lipids and 64.9% total carbohydrates. In addition, alga contains 21.68 $\mu g \cdot g^{-1}$ total carotenoids, of which the most abundant is β-carotene (10.48 $\mu g \cdot g^{-1}$). The GC-MS analysis of the extract of *E. gracilis* illustrates that the content of sugar alcohol and free amino acid are 28.1% and 17.8% of the dry biomass weight, respectively. Among them, mannitol is the most important sugar alcohol, known as the important osmotic regulator, which can regulate the inflammation. Other important sugars detected from GC-MS analysis were glucose and trehalose. The major composition of amino acids is L-leucine, L-valine and L-proline, with concentrations of 2.4%, 1.8% and 1.5% respectively.

Table 1-1. Metabolites in the dried cell biomass of *E. gracilis* [11].

Major metabolites in dried *E. gracilis* cells	Content (%DW)	Secondary metabolites in dried alga cells analyzed by HPLC	Content ($\mu g \cdot g^{-1}$)	Secondary metabolites in dried alga cells analyzed by GC-MS	Content (%DW)
Proteins	23.1	Total reported carotenoids	21.68	D-mannitol	27.96
Lipids	7.5	Total β-carotene	10.48	Phosphate	5.21
Total carbohydrates	64.9	Total canthaxanthin	4.86	D-glucose	3.28
		β-Cryptoxantin	6.04	L-leucine	2.42
		trans-Lutein	3.7	L-valine	1.76
		Total vitamin A	10.48	L-proline	1.55
		trans-β-carotene	6.16	L-alanine	1.53
		cis-β-carotene	4.32	L-lysine	1.20
		α-carotene	0.78	Succinic acid	1.19
		cis-Lutein and zea	0.38	L-phenylalanine	1.16
				L-threonine	1.09
				Pyroglutamic acid	1.06
				Serine	0.94
				Trehalose	0.82
				L-tyrosine	0.77
				Aspartic acid	0.7

The potential of *E. gracilis* in commercialization has been recognized after the discovery of the rich proteins content and amino acid profiles [15]. *Euglena gracilis* can produce an unique metabolite called paramylon (β-1,3 glucan) as well, which is a glucose polymer with β-1,3 linkages structurally similar to starch. Recently, its medical potential has been reported, for instance, paramylon and its chemically modified derivatives exhibit a certain degree of anti-HIV activity [16], antitumor activity [17], and anti-infection activity [18]. Thus, its biomass production has been greatly encouraged due to the biomedical applications of paramylon [19]. It has been reported that there are a lot of carbohydrate-active enzymes in *E. gracilis* cells and its ability of synthesizing complex polysaccharides is exceptional for unicellular organisms. In addition, *E. gracilis* contains a variety of essential nutrients such as vitamins, minerals, and unsaturated fatty acids including docosahexaenoic acid (DHA), eicosapentaenoic acid (EPA), and these high-value added metabolites are easy to be digested and absorbed by human body due to lack of cell wall in *E. gracilis*, implying its great potentia as a valuable resource of health supplements [20]. In recent decades, *E. gracilis* derived bioproducts have been extensively studied, which fostered a rise in the number of research papers regarding the new metabolites identification, physiological functions exploration, and their promising applications.

Apart from the conventional application fields of food, feed and health products, *E. gracilis* is also an emerging alternative to biofuel production, due to the fast growth rate and high lipid productivity. Meanwhile, *E. gracilis* has positive impacts on the environment, since it is able to allievite the greenhouse effect by producing fresh oxygen and consuming carbondioxide. In addition, *E. gracilis* also has a prominent role in the purification of organic matter and radioactive substances in the aquatic environment. In addition to its application in bioremediation, *E. gracilis* is also a cultivable microalga for the accumulation of various metabolites and bioproducts with mulyiple applications. Thence, the market of E. gracilis is expected to continue to increase in the future.

1.2 Bottleneck of Commercialization

With the development of modern separation and identification technology, the application of microalgae has entered a new stage. A large number of microalgae are used in food, health care

products, pharmaceuticals, cosmetics, animal feed, biofuels and many other fields. It has become increasingly important to replace the increasingly scarce traditional resources with inexhaustible microalgae resources. In the process of commercialization (Figure 1-2), microalgae have to undergo strains screening, cultivation, harvesting, extraction and purification. However, the production of algal biomass and metabolites are strictly limited by the external environments, such as light, pH, temperature, salt concentration, radiation, pesticides, heavy metal pollution, etc., which will greatly limit the growth of microalgae [21-25]. Open culture can also lead to severe evaporation of water and insufficient supply of carbon dioxide, resulting in slower accumulation of metabolites. Open-air culture will also lead to severe evaporation of water and insufficient supply of carbon dioxide, resulting in a slower accumulation of metabolites in microalgae. In the face of unfavorable growth environment, algae cells will enter an oxidative stress state, and a large amount of active oxygen is generated in the cells, resulting in redox imbalance, and protein, membrane lipids and other cellular components are destroyed. Eventually the growth and metabolism of algal cells is adversely affected.

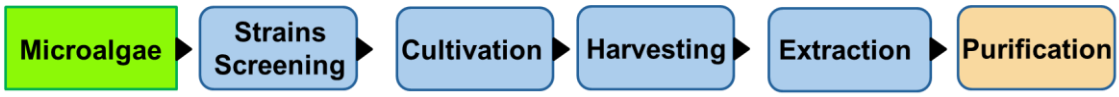

Figure 1-2. The process of commercialization of microalgae

On the other hand, the accumulation of high-value-added bioproducts in microalgae is often not conducive to the growth of microalgae, which is a potential contradiction in microalgae biomass production. This implies that while increasing the accumulation of beneficial metabolites, the production of algal biomass is often hindered, which greatly limits the development of the microalgae industry. Therefore, finding an approach that can effectively shorten the microalgae culture cycle, safely and efficiently promote the growth of microalgae, and simultaneously increase the accumulation of high-value-added bioproducts in *E. gracilis* is essential for the development of microalgae commercialization, and it has become a top priority to satisfy the increasing demands of customers for microalgae production.

1.3 Approaches to improving the algal biomass yield

Researchers have spent a significant amount of time and efforts to overcome these problems.

From a micro perspective, gene editing seems to be a good solution and this topic is now very popular. Theoretically, by modifying some functional genes, we can stably enhance yield and even improve the properties against bacteria or diseases. From a practical perspective, however, the cost of this method is extremely high and the process is more complex than normal approaches. More importantly, the safety of the genetically modified microorganisms is still controversial and the method should be severely restricted [26]. From a macro point of view, the most common method used to improve growth and metabolism is supplementing with various types of additives, for example, exogenous nutrients [27] and plant hormones [28]. Nevertheless, these additives are still costly. It was reported that 1,000 mg/L of alginate oligosaccharides derived from macroalgae could promote the growth of *Spirulina platensis* 3.68-fold [29], and 5,000 mg/L of steel-making slag, a byproduct of steel processing, could increase the growth of *S. platensis* 1.12-fold [30]. These studies suggested a new and promising strategy to enhance microalgae yield at a low cost with high efficiency by simply adding unutilized or waste materials.

1.4 Potential candidates from lignocellulosic materials

Lignocellulosic biomass, which is widely present in land plants, is a potential alternative to the conventional growth additives because it is one of the most abundant and renewable carbon resources in nature. Its composition is relatively complicated, mainly composed of cellulose, hemicellulose and lignin, of which the structure was as shown in Figure 1-3. The hydrolyzed monomers of cellulose, hemicellulose and lignin are glucose, pentose and hexose, and phenolic substances, respectively. Research on the utilization of cellulose to microalgae cultivation has been widely reported. For example, the enzymatic hydrolysate of rice straw could be utilized as an alternative carbon source for the cultivation of *Chlorella pyrenoidosa* and can significantly increase its lipid productivity [31]. Similarly, straw cellulose hydrolysate could promote the growth of *Chlorella* and *Scenedesmus* species, and increase the intracellular polyunsaturated fatty acid content [32]. In these reports, the monosaccharides (mainly glucose) in cellulosehe palyed the main role in the microalgal growth promotion.

As for hemicellulose and lignin, which have more complex components in lignocellulose, they are not fully utilized. Because of the complex linkages between these components, they are

usually discarded/abandoned in large quantities. However, a variety of active ingredients from these biomass have been identified and they have a variety of physiological functions. If these lignocellulosic compounds, which are largely discarded in nature, can be utilized for microalgae cultivation, this will help alleviate the burden on the aquatic environment and contribute to the production and industrialization of microalgal biomass.

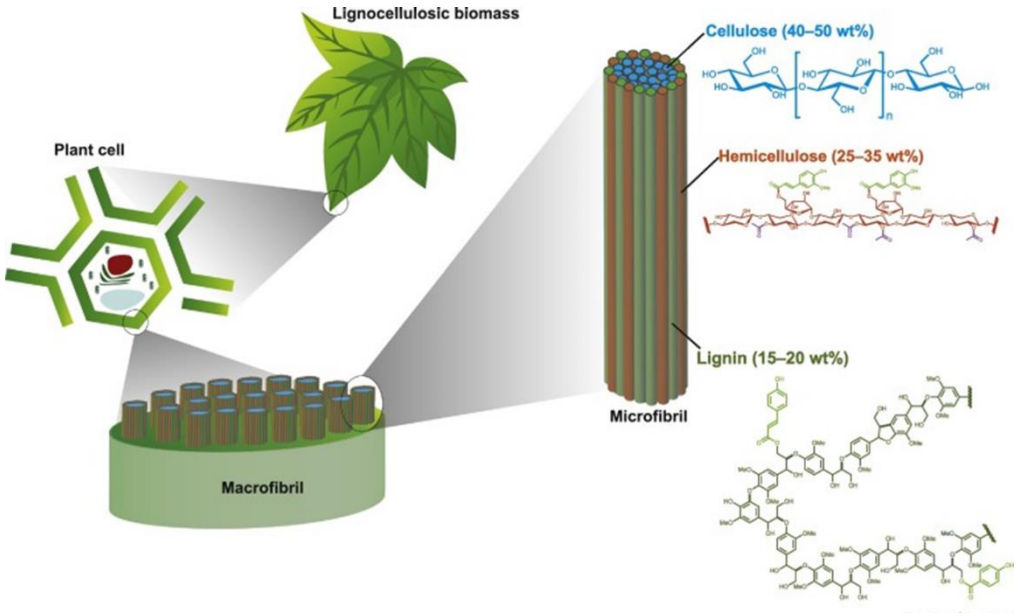

Fig. 1-3 Composition of lignocellulose and their content.

(Copyright: https://www.cell.com/trends/chemistry/S2589-5974(20)30055-1)

1.4.1 Cellulose derived elicitors

It has been proved to be a novel and effective way to cultivate microalgae by using cellulose hydrolysate as the organic carbon sources, because the glucose derived from cellulose can be easily utilized by most microalgae, and the cells enter the mixtrophic growth mode. Under mixtrophic nutrient conditions, the presence of glucose substrate can make the growth of microalgae cells not strictly dependent on photosynthesis, and the final biomass yield can exceed the sum of those under photoautotrophism and heterotrophism [33]. The potential of hydrolysates from rice straw and sweet sorghum as cheap carbon sources for microalgae growth have already been confirmed and the result showed that biomass and lipid production of *Chlorella pyrenoidosa* and *Chlorella vulgaris* were greatly improved under mixotrophic culture with the hydrolysates [34,35]. Similar report has also been reported on *E. gracilis*. Kim et al. found that industrial waste

byproducts, corn steep liquor and brewer's spent grains, were able to be used for heterotrophic cultivation of *E. gracilis*, and significantly increase the production of paramylon [36]. This implies that the utilization of glucose derived from the cellulose hydrolysate for the cultivation of *E. gracilis* is feasible and related researches have been extensively studied. Therefore, this issue was not considered in this study.

1.4.2 Hemicellulose derived elicitors

Although the glucose in these hydrolysates of cellulose can be easily utilized by microalgae, other pentoses and hexoses from the hemicellulose are not fully used by the microalgae. For example, xylose was reported as a difficult substrate for microalgae growth, and only few species of wild-type microalgae were able to utilize xylose naturally [37,38]. In some cases, toxicity of xylose to some microalgae was even observed, including inhibition of photosynthesis [39], inactivation of hexokinase inhibiting of glycolysis [40], and substantial pigment loss [38], etc. Hence, screening microalgae strains containing multiple organic carbon metabolism pathways was essential for the production of microalgal biomass using lignocellulosic materials. In this study, two hemicellulose hydrolysate related sugar alcohols, mannitol and xylitol, were selected as the carbon sources for the growth of *E. gracilis*.

Therefore, two hemicellulose hydrolysate related sugar alcohols, mannitol and xylitol, were selected as the carbon sources for the growth of *E. gracilis*. Mannitol is one of the most abundant energy and carbon storage molecules in nature, which could be produced by a plethora of organisms, including bacteria, yeasts, fungi, macroalgae (especially brown algae), lichens, and many other plants [41]. It is also the major component of hemicellulose in soft wood [42]. However, there have been no reports of utilizing mannitol as the carbon source for the growth of *E. gracilis* cells [43]. The metabolic pathway of mannitol in yeast has been identified, and it is very likely that similar pathways also exist in *E. gracilis* cells [41]. In addition, xylitol is a hydrogenated product of xylose, which also has a wide range of sources. In most xylose assimilating microorganisms, xylose was first reduced to xylitol and finally oxidized to xylulose in cells [37]. However, some microalgae that lack xylose reductase were unable to assimilate xylose, usage of xylitol as the carbon source for microalgae can avoid this disadvantage. Thus, it

is necessary to analyze the availability of mannitol and xylitol to *E. gracilis* cells and their effects on the metabolites biosynthesis.

1.4.3 Lignin derived byproducts

Lignocellulose is one of the most abundant raw materials in nature, but its utilization rate is relatively low, and the current development mainly focused on the use of cellulose, while the utilization of hemicellulose and lignin is very limited, especially for lignin, as it is a cross-linked phenolic polymer which is resistant to degradation and acid- and base-catalyzed hydrolysis [44]. The development of lignocellulosic raw materials inevitably leads to a large amount of lignin being discarded. Especially in the paper industry, a large amount of lignin is removed from wood pulp in the form of lignosulfonates and becomes the major by-product in sulfite pulping waste liquor. Meanwhile, due to the improper discharge, it has also become the source of significant environmental concerns. In order to solve this problem, making full use of LIGNs is helpful to alleviate the environmental stress and improve the economic benefits of pulping waste liquor.

Researchers have keenly discovered the phytohormone-like regulatory role of LIGNs in the cultivation of a variety of higher plants, but there was no report that LIGNs could affect the growth of microalgae. If LIGNs are able to serve as stimulants for the growth of *E. gracilis*, it will achieve multiple benefits, not only to improve the economic benefits of *E. gracilis* cultivation, but also to reduce the environmental burden caused by pulping liquor.

1.4.4 Lignin derived elicitors

Lignins are mainly composed of three basic monolignols which was oxidative coupled (as building blocks), including guaiacyl, p-hydroxyphenyl, and syringyl alcohols. Because it contained an abundant of phenolic compounds, thus there are a lot of phenols in the wastewater from downstream industries of lignin. A variety of physiological activities, such as antioxidant, antibacterial, anti-tumor and anti-diabetic have been reported, however, there is little research on the effects of phenolic compounds on the growth and biochemical synthesis of *E. gracilis*. Therefore, investigation of the effects of phenols, as the predominant phenolic derivatives in waste streams, on the physiological and biochemical parameters of *E. gracilis*, are important.

1.5 Objective of the research

The aim of this study is to explore the effects of various components in lignocellulosic materials and its related by-products on the growth and metabolism of *E. gracilis*, mainly on the lipid biosynthesis. Therefore, the focus is on the hexose and pentose sugars from hemicellulose, the industrial by-product calcium lignosulfonate, and phenolic acid and aldehydes from the lignin hydrolysate with three basic structures. Effects of these growth additives were evaluated by parameters such as cell density, dry weight, cell morphology, photosynthetic pigment content and ratio, and macromolecular metabolite content. In addition, we also compared the metabolic profiles by Fourier transform infrared spectroscopy combined with multivariate analysis. This will help to better regulate the accumulation of high value-added products in *E. gracilis* cells. This experiment mainly focuses on the use of some basic structures from lignocellulose, and there is still a lack of exploration on the direct utilization of industrial waste lignocellulose. However, this research provides a direction and basis for the further utilization of abandoned lignocellulosci materials. Therefore, in future work, we are committed to improving this part of the work.

References

[1] Day, J. G., Benson, E. E., & Fleck, R. A. (1999). In vitro culture and conservation of microalgae: applications for aquaculture, biotechnology and environmental research. *In Vitro Cellular & Developmental Biology-Plant*, *35*(2), 127-136.

[2] Kay, R. A., & Barton, L. L. (1991). Microalgae as food and supplement. *Critical reviews in food science & nutrition*, 30(6), 555-573.

[3] Ruane, J., Sonnino, A., & Agostini, A. (2010). Bioenergy and the potential contribution of agricultural biotechnologies in developing countries. *Biomass and Bioenergy*, *34*(10), 1427-1439.

[4] Tabatabaei, M., Tohidfar, M., Jouzani, G. S., Safarnejad, M., & Pazouki, M. (2011). Biodiesel production from genetically engineered microalgae: future of bioenergy in Iran. *Renewable and Sustainable Energy Reviews*, *15*(4), 1918-1927.

[5] Gong, Y., Hu, H., Gao, Y., Xu, X., & Gao, H. (2011). Microalgae as platforms for production of recombinant proteins and valuable compounds: progress and prospects. *Journal of*

industrial microbiology & biotechnology, *38*(12), 1879-1890.

[6] Shalaby, E. (2011). Algae as promising organisms for environment and health. *Plant signaling & behavior*, *6*(9), 1338-1350.

[7] Mehta, P., Singh, D., Saxena, R., Rani, R., Gupta, R. P., Puri, S. K., & Mathur, A. S. (2018). High-value coproducts from algae—an innovational way to deal with advance algal industry. In *Waste to wealth* (pp. 343-363). Springer, Singapore.

[8] Wells, M. L., Potin, P., Craigie, J. S., Raven, J. A., Merchant, S. S., Helliwell, K. E., ... & Brawley, S. H. (2017). Algae as nutritional and functional food sources: revisiting our understanding. *Journal of applied phycology*, *29*(2), 949-982.

[9] Mahltig, B., Soltmann, U., & Haase, H. (2013). Modification of algae with zinc, copper and silver ions for usage as natural composite for antibacterial applications. *Materials Science and Engineering: C*, *33*(2), 979-983.

[10] Lonergan, T. A. (1983). Regulation of Cell Shape in Euglena gracilis: I. Involvement of the biological clock, respiration, photosynthesis, and cytoskeleton. *Plant physiology*, *71*(4), 719-730.

[11] Krinsky, N. I., & Goldsmith, T. H. (1960). The carotenoids of the flagellated alga, *Euglena gracilis*. *Archives of biochemistry and biophysics*, *91*(2), 271-279.

[12] O'neill, E. C., Trick, M., Hill, L., Rejzek, M., Dusi, R. G., Hamilton, C. J., ... & Field, R. A. (2015). The transcriptome of Euglena gracilis reveals unexpected metabolic capabilities for carbohydrate and natural product biochemistry. *Molecular BioSystems*, *11*(10), 2808-2820.

[13] Mahapatra, D. M., Chanakya, H. N., & Ramachandra, T. V. (2013). *Euglena* sp. as a suitable source of lipids for potential use as biofuel and sustainable wastewater treatment. *Journal of Applied Phycology*, *25*(3), 855-865.

[14] Phillips, F. C., Jensen, G. S., Showman, L., Tonda, R., Horst, G., & Levine, R. (2019). Particulate and solubilized β-glucan and non-β-glucan fractions of *Euglena gracilis* induce pro-and anti-inflammatory innate immune cell responses and exhibit antioxidant properties. *Journal of inflammation research*, *12*, 49.

[15] Kottuparambil, S., Thankamony, R. L., & Agusti, S. (2019). *Euglena* as a potential natural

source of value-added metabolites. A review. *Algal Research*, *37*, 154-159.

[16] Sakagami, H., Kushida, T., Makino, T., Hatano, T., Shirataki, Y., Matsuta, T., ... & Mimaki, Y. (2012). Functional analysis of natural polyphenols and saponins as alternative medicines. In *A Compendium of Essays on Alternative Therapy*. InTech.

[17] Xiao, Z., Trincado, C. A., & Murtaugh, M. P. (2004). β-Glucan enhancement of T cell IFNγ response in swine. *Veterinary immunology and immunopathology*, *102*(3), 315-320.

[18] Chan, G. C. F., Chan, W. K., & Sze, D. M. Y. (2009). The effects of β-glucan on human immune and cancer cells. *Journal of hematology & oncology*, *2*(1), 25.

[19] Briand, J., & Calvayrac, R. (1980). Paramylon synthesis in heterotrophic and photoheterotrophic *Euglena* (*Euglenophyceae*). *Journal of Phycology*, *16*(2), 234-239.

[20] Hayashi, M., Toda, K., Misawa, Y., Kitaoka, S. (1993). Preparation of ***Euglena gracilis*** enriched with eicosapentaenoic and docosahexaenoic acids. *Aquaculture Science*, *41*(2), 169-176.

[21] Ogbonna, J. C., Yada, H., & Tanaka, H. (1995). Kinetic study on light-limited batch cultivation of photosynthetic cells. *Journal of fermentation and Bioengineering*, *80*(3), 259-264.

[22] Danilov, R. A., & Ekelund, N. G. A. (2001). Effects of pH on the growth rate, motility and photosynthesis inEuglena gracilis. *Folia microbiologica*, *46*(6), 549-554.

[23] Kitaya, Y., Azuma, H., & Kiyota, M. (2005). Effects of temperature, CO2/O2 concentrations and light intensity on cellular multiplication of microalgae, *Euglena gracilis*. *Advances in Space Research*, *35*(9), 1584-1588.

[24] Jahnke, L. S., & White, A. L. (2003). Long-term hyposaline and hypersaline stresses produce distinct antioxidant responses in the marine alga *Dunaliella tertiolecta*. *Journal of Plant Physiology*, *160*(10), 1193.

[25] Prasad, S. M., & Zeeshan, M. (2005). UV-B radiation and cadmium induced changes in growth, photosynthesis, and antioxidant enzymes of cyanobacterium Plectonema boryanum. *Biologia Plantarum*, *49*(2), 229.

[26] Araki, M., Nojima, K., & Ishii, T. (2014). Caution required for handling genome editing

technology. *Trends in biotechnology*, *32*(5), 234-237.

[27] Ogbonna, J. C., Tomiyamal, S., & Tanaka, H. (1998). Heterotrophic cultivation of *Euglena gracilis* Z for efficient production of α-tocopherol. *Journal of Applied Phycology*, *10*(1), 67-74.

[28] Noble, A., Kisiala, A., Galer, A., Clysdale, D., & Emery, R. N. (2014). *Euglena gracilis* (*Euglenophyceae*) produces abscisic acid and cytokinins and responds to their exogenous application singly and in combination with other growth regulators. *European journal of phycology*, *49*(2), 244-254.

[29] Nogami, R., Nishida, H., Hong, D. D., & Wakisaka, M. (2017). Growth promotion effect of alginate oligosaccharides on *Spirulina* analyzed by repeated batch culture. *Journal of the Japan Institute of Energy*, *96*(9), 352-356.

[30] Nogami, R., Nishida, H., Hong, D. D., & Wakisaka, M. (2016). Growth promotion of Spirulina by steelmaking slag: application of solubility diagram to understand its mechanism. *AMB Express*, *6*(1), 96.

[31] Li, P., Miao, X., Li, R., & Zhong, J. (2011). In situ biodiesel production from fast-growing and high oil content *Chlorella pyrenoidosa* in rice straw hydrolysate. *Journal of Biomedicine and Biotechnology*, *2011*.

[32] Zhang, T. Y., Wu, Y. H., Wang, J. H., Wang, X. X., Deantes-Espinosa, V. M., Dao, G. H., ... & Hu, H. Y. (2019). Heterotrophic cultivation of microalgae in straw lignocellulose hydrolysate for production of high-value biomass rich in polyunsaturated fatty acids (PUFA). *Chemical Engineering Journal*, *367*, 37-44.

[33] Cheirsilp, B., & Torpee, S. (2012). Enhanced growth and lipid production of microalgae under mixotrophic culture condition: effect of light intensity, glucose concentration and fed-batch cultivation. *Bioresource technology*, *110*, 510-516.

[34] Li, P., Miao, X., Li, R., & Zhong, J. (2011). In situ biodiesel production from fast-growing and high oil content *Chlorella pyrenoidosa* in rice straw hydrolysate. *Journal of Biomedicine and Biotechnology*, *2011*.

[35] Sibi, G. (2015). Low cost carbon and nitrogen sources for higher microalgal biomass and

lipid production using agricultural wastes. *Journal of Environmental Science and Technology*, *8*(3), 113-121.

[36] Kim, S., Lee, D., Lim, D., Lim, S., Park, S., Kang, C., ... & Lee, T. (2020). Paramylon production from heterotrophic cultivation of *Euglena gracilis* in two different industrial byproducts: Corn steep liquor and brewer's spent grain. *Algal Research*, *47*, 101826.

[37] Yang, S., Liu, G., Meng, Y., Wang, P., Zhou, S., & Shang, H. (2014). Utilization of xylose as a carbon source for mixotrophic growth of *Scenedesmus obliquus*. *Bioresource technology*, *172*, 180-185.

[38] Leite, G. B., Paranjape, K., & Hallenbeck, P. C. (2016). Breakfast of champions: Fast lipid accumulation by cultures of *Chlorella* and *Scenedesmus* induced by xylose. *Algal Research*, *16*, 338-348.

[39] Hassall, K. A. (1958). Xylose as a specific inhibitor of photosynthesis. *Nature*, *181*(4618), 1273-1274.

[40] Fernandez, R., Herrero, P., & Moreno, F. (1985). Inhibition and inactivation of glucose-phosphorylating enzymes from *Saccharomyces cerevisiae* by D-xylose. *Microbiology*, *131*(10), 2705-2709.

[41] Ghoreishi, S. M., & Shahrestani, R. G. (2009). Innovative strategies for engineering mannitol production. *Trends in food science & technology*, *20*(6-7), 263-270.

[42] Miazek, K., Remacle, C., Richel, A., & Goffin, D. (2014). Effect of lignocellulose related compounds on microalgae growth and product biosynthesis: a review. *Energies*, *7*(7), 4446-4481.

[43] Osafune, T., Sumida, S., Ehara, T., Ueno, N., Hase, E., & Schiff, J. A. (1990). Lipid (wax) and paramylum as sources of carbon and energy for the early development of proplastids in dark-grown *Euglena gracilis* cells transferred to an inorganic medium. *Microscopy*, *39*(5), 372-381..

[44] Wang, W., Tan, X., Yu, Q., Wang, Q., Qi, W., Zhuang, X., ... & Yuan, Z. (2018). Effect of stepwise lignin removal on the enzymatic hydrolysis and cellulase adsorption. *Industrial Crops and Products*, *122*, 16-22.

Chapter 2. Effect of hemicellulose-derived sugar alcohols on the growth and metabolites biosynthesis of *Euglena gracilis*

It is an effective solution to overcome the bottlenecks of commercial production of microalgal biomass by providing cost-effective and environment-friendly organic carbon sources for microalgal mixotrophic growth. In this chapter, effects of lignocellulose-related mannitol and xylitol on the growth, photosynthetic pigment content, cell morphology, and metabolites biosynthesis of freshwater microalga *Euglena gracilis* were investigated. The results revealed that both mannitol and xylitol effectively promoted the growth of *E. gracilis*, and at the optimal dosage of 4 $g \cdot L^{-1}$, the biomass yield was increased by 4.64-fold and 3.18-fold, respectively. Increase of cell aspect ratio was only observed in mannitol treatment groups, indicating that *E. gracilis* had different physiological responses to mannitol and xylitol. Fourier transform infrared spectroscopy combined with multivariate analysis was applied to analyze the cellular components. The lipid content of *E. gracilis* was significantly promoted by these two sugar alcohols, which would increase its potential in biofuel production.

2.1 Introduction

With the growth of world population, the impact of global warming and the depletion of petroleum fuels, people are facing threats from food, energy and environment. In recent years, microalgae which were widely distributed in aquatic environment have attracted attention because of their ability as cell factories for various natural products [1]. *Euglena gracilis* is a common freshwater microalga, and viable with both phagotrophic and phototrophic modes. *E.gracilis* can produce a large number of products with high nutritional value or economic benefits, such as β-1,3-glucan, polyunsaturated fatty acids, amino acids, α-tocopherols, chlorophylls, carotenoids and wax esters, etc., used as a promising feedstock in many fields such as food, pharmaceuticals, supplements, animal feed, and cosmetics [2,3]. In addition, its potential as biodiesel or aviation biofuel has also been greatly exploited to increase the lipid content by changing the culture modes [4]. However, a number of technical challenges remained before it can be fully applied in the highly competitive biofuel market, including optimization and improvement of culture conditions,

complete understanding of the biofuel production mechanisms, and effective techniques for large-scale cultivation of microalgae [5-7]. Generally, due to the restriction of illumination, conventional autotrophic cultivation has being suffering from the low biomass density, which resulted in the great increase in the cost of microalgae cultivation, and impeded the large-scale commercial algal production [8]. In face of the increasing market demand for *E. gracilis*, cost-effective, environment-friendly and practical solution to enhance biomass yield of *E. gracilis* are expected.

Improving the microalgal growth and beneficial metabolites accumulation by additives derived from abandoned biomass was recognized as a cheap and effective strategy [9]. It was reported that, 5 $g \cdot L^{-1}$ steelmaking slag, the industrial by-product, could increase the growth and lipid production of *Botryococcus braunii* by 1.74 and 2.16 times, respectively, and found that the elusion of iron from the slag played a key role [10]. In addition, ferulic acid and phytic acid from agro-waste rice bran were also reported to promote the growth of *E. gracilis* at most 1.6 and 3.6 times, respectively [11,12]. The former might serve as the available phosphorus source for the growth of *E. gracilis*, while the latter might play a role similar to phytohormones. Generally, supplementing carbon sources in the microalgal cultivation has been proven to be the most effective method to promote the microalgal growth and increase the final productivity of metabolites, since the algal cells under the mixotrophic culture can yield more ATP and biomass than that under the autotrophic cultivation [7]. However, the addition of organic carbon to the microalgae cultures could significantly increase the operational cost. Therefore, exploitation of cheap organic carbon sources from waste biomass is essential.

Lignocellulosic biomass widely distributed in land plants is one of the most abundant and renewable carbon resources in nature [13]. However, the vast majority of these carbon resources are abandoned. It is a novel and promising method to culture microalgae by using carbon sources derived from lignocellulose materials. The potential of hydrolysates from rice straw and sweet sorghum as cheap carbon sources for microalgae growth have already been explored and the result showed that biomass and lipid production of *Chlorella pyrenoidosa* and *Chlorella vulgaris* were greatly improved under mixotrophic culture with the hydrolysates [14,15]. Although the glucose

in these lignocellulosic hydrolysates can be easily used by microalgae, other pentoses and hexoses are not all fully utilized by microalgae. For example, xylose was reported as a difficult substrate for microalgae growth, and only few species of wild-type microalgae were able to utilize xylose naturally [16,17]. In some cases, toxicity of xylose to some microalgae was even observed, including inhibition of photosynthesis [18], inactivation of hexokinase inhibiting of glycolysis [19], and substantial pigment loss [17], etc. Hence, screening microalgae strains containing multiple organic carbon metabolism pathways was essential for the production of microalgal biomass using lignocellulosic materials. In this study, two hemicellulose hydrolysate related sugar alcohols, mannitol and xylitol, were selected as the carbon sources for the growth of *E. gracilis*. Mannitol is one of the most abundant energy and carbon storage molecules in nature, which could be produced by a plethora of organisms, including bacteria, yeasts, fungi, macroalgae (especially brown algae), lichens, and many other plants [20]. It is also the major component of hemicellulose in soft wood [13]. However, there have been no reports of utilizing mannitol as the carbon source for the growth of *E. gracilis* cells [21]. The metabolic pathway of mannitol in yeast has been identified, and it is very likely that similar pathways also exist in *E. gracilis* cells [20]. In addition, xylitol is a hydrogenated product of xylose, which also has a wide range of sources. In most xylose assimilating microorganisms, xylose was first reduced to xylitol and finally oxidized to xylulose in cells [16]. However, some microalgae that lack xylose reductase were unable to assimilate xylose, usage of xylitol as the carbon source for microalgae can avoid this disadvantage.

Aim of this study is to investigate the availability of mannitol and xylitol to *E. gracilis* cells and their effects on the metabolites biosynthesis. To better understand the cellular status and physiology in response to different sugar alcohols, cell growth, photosynthetic pigments content and cell morphology were evaluated under mixotrophic cultures with mannitol and xylitol. Furthermore, high-throughput Fourier transform infrared spectroscopy (FT-IR) combined with multivariate analysis was used to analyze the changes in the intracellular macromolecular pool, so as to determine the effect of different sugar alcohols on the product biosynthesis of *E. gracilis*.

2.2 Materials and methods

2.2.1 Microalga and culture conditions

Freshwater microalga *E. gracilis* Klebs (NIES-48) was purchased from National Institute for Environmental Studies, Japan. Algal cells were pre-cultured in Cramer–Myers (CM) medium with the following composition (mg·L^{-1}): $(NH_4)_2HPO_4$, 1000; KH_2PO_4, 1000; $MgSO_4 \cdot 7H_2O$, 200; $CaCl_2 \cdot 2H_2O$, 20; $FeSO_4 \cdot 7H_2O$, 3; $MnCl_2 \cdot 4H_2O$, 1.8; $CoSO_4 \cdot 7H_2O$, 1.5; $ZnSO_4 \cdot 7H_2O$, 0.4; $Na_2MoO_4 \cdot 2H_2O$, 0.2; $CuSO_4 \cdot 5H_2O$, 0.02; Vitamin B_{12}, 0.0005; Thiamine HCl, 0.1.

Mannitol and xylitol stock solutions were pre-configured and sterilized by filtering using vaccum filters (Nalgene, Thermo Fisher Scientific, USA). Different concentrations of sugar alcohol solutions were obtained by diluting the pre-configured stock solution with fresh CM medium. When the algal cells entered the exponential growth phase, 10 mL of cell suspension were inoculated to a 300 mL Erlenmeyer flask, and different concentrations of mannitol and xylitol solution and CM medium were added, with a final culture volume of 100 mL. The final concentrations of mannitol and xylitol treatment groups were 0, 0.1, 0.5, 2 and 4 g·L^{-1}. All groups were cultured at 25 ± 1 °C and illuminated by the cool white fluorescent lamps at the light intensity of 5000 lx with a 12-12 h light and dark cycle. To avoid cell aggregation and ensure uniform light exposure, flasks were manually shaken three times per day.

2.2.2 Growth parameters

Cell density was measured periodically using a hemocytometer (Thoma, Hirschmann, Germany). Aliquot 300 μL of cell suspension from the cultures was picked and 200 μL of ethanol was added to fix the cells. The cell density was counted under the light microscope (Motic, BA210, Japan). Specific growth rate μ (d^{-1}) and doubling time (*DT*, d) were also calculated according to Eq. (1) and Eq. (2) [22].

$$\mu = \frac{ln(D2) - ln(D1)}{t2 - t1} \quad (1)$$

$$DT = ln2/\mu \quad (2)$$

Where *t1* and *t2* are the beginning and end times of the log growth phase, and *D1* and *D2* are the cell density at the time of *t1* and *t2*, respectively.

The pH of culture filtrate was regularly determined by pH meter (LAQUA-2103AL, Horiba, Japan). At the end of cultivation, cell dry weight of each group was also measured. Algal cells were harvested by filtering 5 mL of cell suspension through filter paper of which the pore size was smaller than 0.45 μm (GC-50, Advantec, Japan). The deposited cells were rinsed with deionized water twice to remove the remained salts, and then were dried in the oven (AVO-250N, As one, Japan) at 80°C overnight. After being transferred to the desiccator and cooled to room temperature, cell dry weight was obtained by calculating the difference between the final and initial weight of the filter papers.

In addition to the algal biomass, chlorophyll content and ratio of carotenoids to total chlorophyll were also determined according to modified Lichtenthaler's method [23]. Five milliliter of algal suspension was collected by the filtration and harvested cells were washed with deionized water. Hereafter, cells were ground with glass sand and 80% acetone solution was added to extract the pigments. Until the cell debris was colorless, the homogenate of extract was filtered and the filtrate was collected in the volumetric flask and made up to 10 mL with 80% acetone. Chlorophyll a, chlorophyll b, and carotenoids content ($mg \cdot L^{-1}$) were determined by the spectrophotometer (Genesys 10S UV-Vis, Thermo Fisher Scientific, USA) at the wavelength of 663 nm, 645 nm and 470 nm, respectively. Their specific content was calculated via Eq. (3), Eq. (4) and Eq. (5).

$$Chl_a = 12.21Abs_{663} - 2.81Abs_{646} \quad (3)$$

$$Chl_b = 20.13Abs_{646} - 5.03Abs_{663} \quad (4)$$

$$C_{x+c} = (1000Abs_{470} - 3.27Chl_a - 104Chl_b)/229 \quad (5)$$

Where Chl_a, Chl_b, and C_{x+c} denote the chlorophyll a, chlorophyll b, and carotenoids content, and Abs_{470}, Abs_{646}, and Abs_{663} are the absorbance of extract at the wavelength of 470 nm, 646 nm, and 663 nm, respectively.

2.2.3 Quantification of cell morphological changes

E. gracilis cells exhibit changes in cell morphologies (such as spindled, spherical, and elongated shapes) in different physiological states, so it is considered as an important indicator to evaluate growth [24]. Cell morphologies of more than 100 cells were observed and recorded by

light microscope (BA210, Motic, Japan) and the corresponding software (Motic Image Plus 2.2S). Micrographs were then imported into image processing software ImageJ (open source) and analysis of particle size was carried out. Feret's diameter (the longest distance between any two points along the selection boundary) denote the cell length, and MinFeret (the minimum caliper diameter) denote the cell width. The ratio of Feret's diameter to MinFeret is approximated as the cell aspect ratio.

2.2.4 Cellular component analysis by FT-IR

FT-IR spectroscopy analysis was carried out to analyze the changes in intracellular macromolecule pools. As a sensitive and high-throughput technology, FT-IR spectra could reflect the changes in carbon allocation of *E. gracilis* in response to different external environments and nutrition modes. To better analyze the product biosynthesis in different treatment groups, FT-IR spectroscopy analysis was performed following the method of Meng et al. [25]. Cell samples were collected by centrifuging aliquot 10 mL of cell suspension at 6000 rpm and then rinsed with deionized water for five times to eliminate the interference of mineral salts to the spectra. The washed cells were pre-frozen with liquid nitrogen and then dried in a vacuum freeze dryer (FDU-1200, EYELA, Japan) at -50 ℃overnight. Freeze-dried cells were mixed with potassium bromide (KBr) powder at a weight ratio of 1:200, and the mixture was ground until the samples were evenly dispersed in KBr. After the mixture powder was pressed into thin sheet by a hand press, the samples were analyzed by the FT-IR spectrometer (Nicolet iZ10, Thermo Fisher Scientific, USA). The absorbance spectra of samples were acquired in the region of 4000-400 cm^{-1} at a resolution of 4 cm^{-1} with 32 scans, and the spectra were narrowed to 1800-1000 cm^{-1} and then analyzed by the corresponding spectrum software (OMINIC, Thermo Fisher Scientific, USA). Spectrum of KBr thin sheet was acquired as the background. The experiment was performed in triplicate and the analysis was repeated three times (n=9). After the baseline correction and atmospheric correction according to the automatic correction algorithms, the collected spectra were normalized to the amide I band at 1655 cm^{-1} to eliminate the difference in the deposit thickness [25,26]. Relative lipid and carbohydrate content was accessed by calculating lipid/amide I peak height ratios and carbohydrate/amide I peak height ratios [27].

2.2.5 Multivariate statistical analysis

Myriad changes in product biosynthesis would be caused by different culture modes (such as autotroph, heterotroph and mixotroph) and conditions (such as pH, temperature, light intensity, nutrient concentrations, and air conditions, etc.) [28]. To provide important biochemical information and find further biological evidence, FT-IR spectra combined with multivariate data analysis were performed by SIMCA-P version 13.0 (Umetrics, Sweden). Non-supervised principal components analysis (PCA) and supervised orthogonal partial least squares discriminant analysis (OPLS-DA) were employed to rapidly compare metabolic fingerprints and observe the discrete trend in metabolites from different culture conditions

2.2.6 Statistical analysis

All groups were cultured in triplicate and the results were expressed as mean ± standard deviation. Significance was analyzed by the statistical software SPSS version 16.0 (IBM, USA) and one-way analysis of variance (ANOVA) was employed to determine the statistical difference in the growth and metabolic parameters at different treatment groups. For pairwise comparisons, post hoc Tukey's honest significant difference (HSD) test and Tamhane T2 test were used under equal variance and unequal variance conditions, respectively. The significant level was set at $p < 0.05$.

2.3 Results and discussion

2.3.1 Growth profiles of *E. gracilis* with two sugar alcohol treatment

Significant promotion effects on *E. gracilis* were observed with both mannitol and xylitol as shown in Fig. 2-1, but the specific changes in cell density and pH caused by various sugar alcohols were different.

Mannitol showed a significant growth promotion effect for *E. gracilis* at different concentrations ($P < 0.05$), and it was in a dose-dependent manner. On day 6, the cell density of 4 $g \cdot L^{-1}$ mannitol treatment group was 9.05 times higher than that of the control group. Although the promotion effect of 4 $g \cdot L^{-1}$ mannitol treatment group decreased somewhat at day 16, which was due to depletion of nutrients in the medium, it was still 4.17 times that of the control group, showing an extremely superior growth promotion. The specific growth rate as shown in Table 2-

1 increased to double while cell doubling time reduced to half at 4 $g \cdot L^{-1}$ mannitol treatment group compared to control. However, there was no significant difference in the growth of 2 $g \cdot L^{-1}$ and 4 $g \cdot L^{-1}$ mannitol treatment group ($P > 0.05$). Both of these two groups reached the end of exponential growth on the 9th day of culture, after which the cell density began to decline. Results of specific growth rate, doubling time and biomass yield were consistent. It indicated that although mannitol could promote the growth of *E. gracilis*, the amounts of other nutrients, such as nitrogen, phosphorus, and mineral salts, etc. were limited, therefore the difference of cell density between 2 $g \cdot L^{-1}$ and 4 $g \cdot L^{-1}$ mannitol treatment groups was not significant.

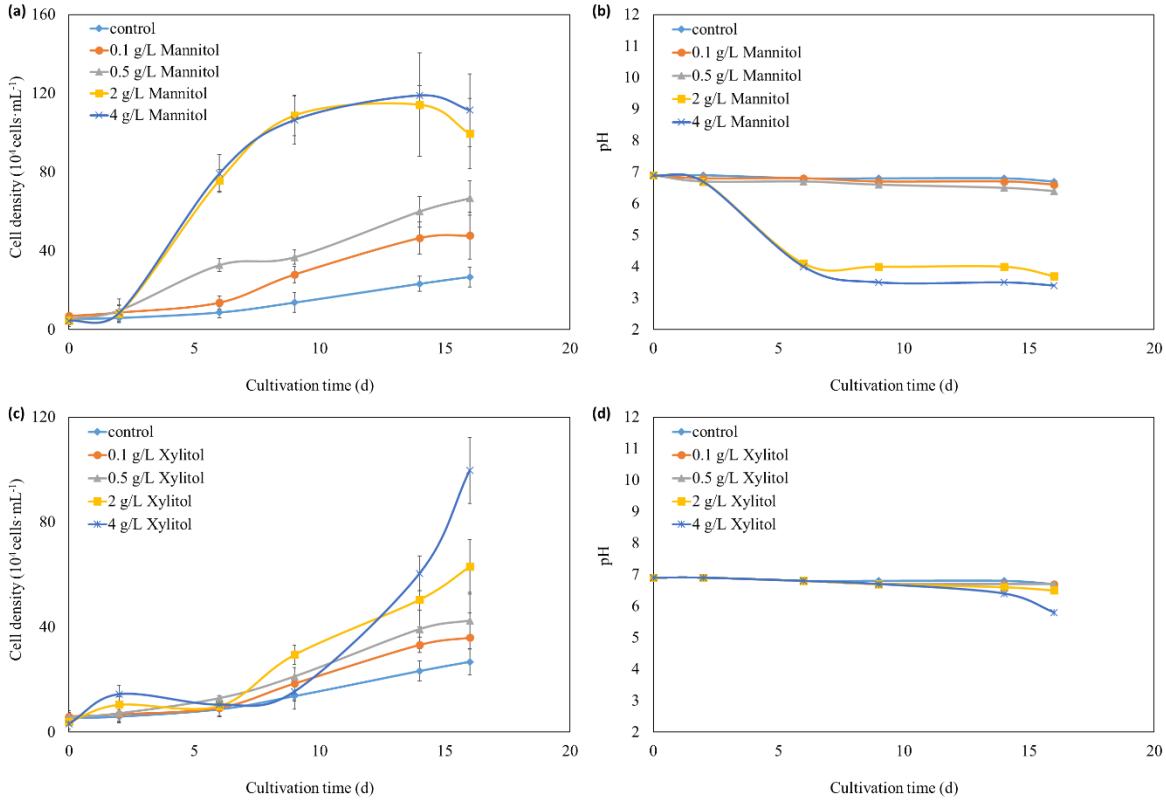

Fig. 2-1. Growth curves of *E. gracilis* cells and pH changes of the media under different concentrations of mannitol and xylitol. Error bars represent the standard deviation (n=3). (a): growth curves under different concentrations of mannitol; (b): pH changes under different concentrations of mannitol; (c): growth curves under different concentrations of xylitol; (b): pH changes under different concentrations of xylitol.

In addition, the pH of the medium (Fig. 2-1b) was found declined sharply at higher

concentrations of mannitol. In the 16-day-culture period, the pH of the 4 $g \cdot L^{-1}$ mannitol treatment group decreased from 6.9 to 3.4. Generally, optimal pH for *E. gracilis* is around 7, and remain stable (or slight decrease) during the growth process as shown in the control group. It was reported that pH of the cultures depended on the culture modes and nutrient concentration [7]. Here the metabolic process of the autotrophic cells was different from that of mixotrophic growth by mannitol. The decrease in pH was mainly attributed to the rapid consumption of ammonium salts and increase of carbon dioxide. Due to the decrease in pH, the cultivation with mannitol was considered more suitable for open culture systems since normal bacterial contamination would be suppressed under such an acidic pH [29].

Effect of xylitol differed from that of mannitol. On day 2, xylitol showed a concentration-dependent stimulating effect (Fig. 2-1c), with the highest cell density at 4 $g \cdot L^{-1}$. The subsequent cell growth showed a lag for about 4 days, suggesting that the *E. gracilis* cells need an adaption process to xylitol exposure. Similar adaptation phenomenon was reported to occur when cells were exposed to environment changes such as culture medium, pH, temperature, light, etc. [30,31]. However, the addition of xylitol significantly extended the lag phase of cells, indicating that *E. gracilis* need to adjust their physiological state and metabolic mode to adapt to the xylitol environment. After the lag phase, xylitol also showed an excellent promotion effect on *E. gracilis* growth, but not significant at lower concentrations ($P > 0.05$). When xylitol concentration increased to 4 $g \cdot L^{-1}$, cell specific growth rate and dry biomass yield showed the maximum of 0.23 d^{-1} and 0.70 $g \cdot L^{-1}$, respectively. The change of pH in xylitol treatment group was much smaller than that of mannitol. The pH remained almost stable under lower concentrations of xylitol treatment, which was similar to the control group, but then slightly decreased to 5.8 in the 4 $g \cdot L^{-1}$ xylitol group.

This is the first report that both mannitol and xylitol serve as carbon sources for promoting growth of *E. gracilis*, which indicated that the metabolic pathways for both mannitol and xylitol exist in *E. gracilis*. A metabolic pathway of mannitol to fructose which eventually involved glycolysis has been discovered in some species of red algae (*Caloglossa leprieurii*, and *C. continua*) [32,33] and brown algae (*Eisenia bicyclis*, and *Ectocarpus siliculosus*) [34,35].

Mannitol cycle was known in fungi, and it is highly possible that other microorganisms (such as *E. gracilis*) also employ similar pathways [20]. On the other hand, many microalgae species were unable to assimilate xylose, and even photosynthesis was inhibited [16,18]. In this study, xylitol serving as the organic carbon source for mixotrophic growth of *E. gracilis* was observed for the first time. Although *E. gracilis* showed a long lag phase on xylitol, the final biomass yield was greatly improved (as shown in Table 2.1). The extension of the lag phase caused by xylitol might be due to the metabolic energy required for *E. gracilis* cells when xylitol was used as the single substrate to induce the xylitol pathway [16].

Table 2-1. Specific growth rate (d^{-1}), doubling time (d) and biomass yield ($g \cdot L^{-1}$) of *E. gracilis* cultured under different concentrations of mannitol and xylitol.

Concentrations ($g \cdot L^{-1}$)	Mannitol			Xylitol		
	Specific growth rate (d^{-1})	Doubling time (d)	Biomass yield ($g \cdot L^{-1}$)	Specific growth rate (d^{-1})	Doubling time (d)	Biomass yield ($g \cdot L^{-1}$)
0	0.10 ± 0.02^{b}	10.18 ± 2.35^{a}	0.22 ± 0.05^{c}	0.10 ± 0.02^{b}	10.18 ± 2.35^{a}	0.22 ± 0.05^{b}
0.1	0.12 ± 0.00^{b}	8.37 ± 0.23^{ab}	0.37 ± 0.04^{c}	0.11 ± 0.03^{b}	9.54 ± 3.24^{a}	0.20 ± 0.07^{b}
0.5	0.16 ± 0.02^{ab}	6.42 ± 0.79^{bc}	0.49 ± 0.16^{bc}	0.12 ± 0.02^{b}	8.24 ± 1.50^{ab}	0.27 ± 0.06^{b}
2	0.19 ± 0.02^{a}	5.17 ± 0.53^{c}	0.82 ± 0.24^{ab}	0.19 ± 0.07^{ab}	5.83 ± 2.02^{ab}	0.44 ± 0.20^{ab}
4	0.21 ± 0.05^{a}	4.90 ± 1.05^{c}	1.02 ± 0.02^{a}	0.23 ± 0.05^{a}	4.55 ± 0.89^{b}	0.70 ± 0.17^{a}

Data (mean ± standard deviation) with the different letters (superscript) in each column showed significant difference from each other ($p < 0.05$), and data with the same letter in each column showed no significant difference from each other ($p > 0.05$).

2.3.2 Analysis of photosynthetic pigments

The total chlorophyll content and chlorophyll to carotenoids ratio in *E. gracilis* cells were summarized in Table 2-2. The total chlorophyll content increased with the mannitol, which supported the growth promotion effect of mannitol. In addition, the ratio of total chlorophyll to

carotenoids was negatively correlated with mannitol concentrations, and decreased from 5.36 in the control group to 3.94 in the 4 $g \cdot L^{-1}$ mannitol treatment group. Generally, decrease in chlorophyll/carotenoid ratio is the indicator of senescence, stress or damage to the photosynthetic apparatus [36]. On the one hand, as the chlorophyll structure was sensitive, it would be damaged under pH or osmotic stresses. When the pH was low, the magnesium ions in the porphyrin ring of the chlorophyll molecules would be replaced by hydrogen ions, and the chlorophyll content would decrease [37]. In addition, mannitol increased osmotic pressure in the medium, which might also decrease the chlorophyll content [38]. On the other hand, carotenoids, as an auxiliary pigment, were able to achieve energy dissipation and chlorophyll protection through non-photochemical quenching. The increase in carotenoids content was the stress response which could help to protect the photosynthesis under pH and osmotic stress [38,39]. Although high concentrations of mannitol treatment lowered the pH and created osmotic stress in the medium led to a decline in chlorophyll to carotenoids ratio, the total production of chlorophyll and biomass content were significantly increased. Thus, mannitol was still considered as an effective growth promotor for *E. gracilis* cells. For xylitol, the total chlorophyll yield has also been improved, but no significant difference was found in the ratio of chlorophyll to carotenoids, which might be due to the relatively stable pH and osmotic environment in the xylitol treatment group.

Table 2-2. Total chlorophyll content ($mg \cdot L^{-1}$) and chlorophyll to carotenoids ratio of *E. gracilis* cultured under different concentrations of mannitol and xylitol.

	Mannitol		Xylitol	
Concentrations ($g \cdot L^{-1}$)	Total chlorophyll ($mg \cdot L^{-1}$)	Chlorophyll to carotenoids ratio	Total chlorophyll ($mg \cdot L^{-1}$)	Chlorophyll to carotenoids ratio
0	5.72 ± 1.71^{b}	5.36 ± 0.93^{a}	5.72 ± 1.71^{b}	5.36 ± 0.93^{a}
0.1	7.45 ± 1.02^{b}	4.99 ± 0.23^{ab}	6.56 ± 1.53^{b}	4.66 ± 0.62^{a}
0.5	12.17 ± 0.83^{b}	4.50 ± 0.18^{abc}	6.60 ± 0.88^{b}	5.01 ± 0.81^{a}
2	22.66 ± 4.73^{a}	3.52 ± 0.17^{c}	9.28 ± 2.71^{b}	4.99 ± 0.36^{a}
4	26.06 ± 5.01^{a}	3.94 ± 0.25^{bc}	19.03 ± 0.90^{a}	5.46 ± 0.51^{a}

Data (mean ± standard deviation) with the different letters (superscript) in each column showed significant difference from each other ($p < 0.05$), and data with the same letter in each column showed no significant difference from each other ($p > 0.05$).

2.3.3 Quantification of cell morphology

Cell morphology is an important biological indicator of *E. gracilis*, as it can exhibit different cell aspect ratios in response to physical or chemical perturbations, such as light, temperature, pH, and nutrient concentrations [24]. Physiological response of *E. gracilis* cells to mannitol and xylitol was different. The median cell aspect ratio at different concentrations of mannitol and xylitol was shown in Fig. 2-2. In case of mannitol, the cell aspect ratio increased significantly from 1.37 in the control group to 3.08 in the 2 $g \cdot L^{-1}$ treatment group. Cell morphology also changed from spindled to elongated shapes. However, under the exposure of xylitol, cell aspect ratio did not change so much even when xylitol concentration increased to 4 $g \cdot L^{-1}$. The changes in cell morphology might be mainly attributed to the pH decrease during culture with mannitol. *E. gracilis* is known as an acid-tolerant species, with a viable pH range of 2 to 8 [29,40]. In our previous study, the cell aspect ratio was found increased from 2.42 to 2.96 when the external pH was adjusted from 6.5 to 3.8 using dilute hydrochloric acid, which confirmed the above hypothesis. The external pH of the cultures under xylitol treatment was more stable than that under mannitol treatment, and thereby no special changes in cell morphology were observed with xylitol.

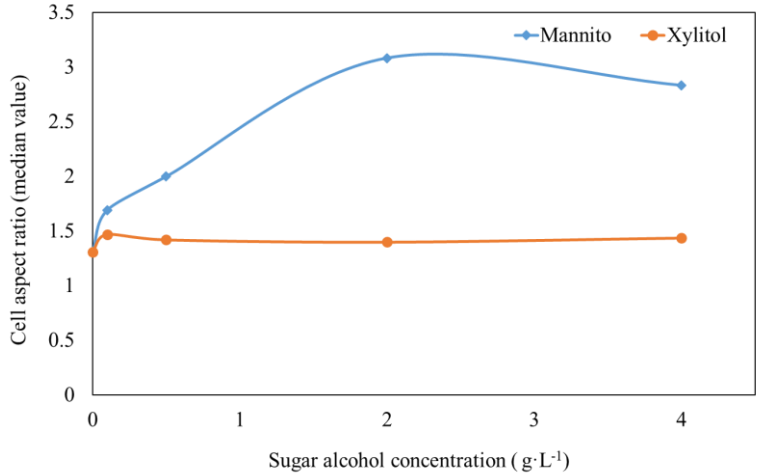

Fig. 2-2. Median aspect ratio of *E. gracilis* cells cultured under different concentrations of mannitol and xylitol.

2.3.4 Detection of cellular components in *E. gracilis* by FT-IR

The FT-IR spectra of the freeze-dried *E. gracilis* cells of the control group, 4 $g \cdot L^{-1}$ mannitol treatment group and 4 $g \cdot L^{-1}$ xylitol treatment group were analyzed, and major metabolites such as proteins, lipids and carbohydrates were well identified. FT-IR spectra in the regions of 1800–1000 cm^{-1} (biomolecular fingerprint region) with high signal-to-noise were normalized, and bands of functional groups from macromolecules including proteins, lipids and carbohydrates were assigned according to Dean et al. [26], Driver et al [27] and Nzayisenga et al. [41]. The bands at 1655 and 1540 cm^{-1} were assigned to νCO stretching of amide I and δN-H stretching of amide II, respectively, which are both related to proteins. The bands at 1736 cm^{-1} and 1078 cm^{-1} ranges were assigned to νCO stretching of lipids and νCOC stretching vibration of carbohydrates, respectively. The main difference between control and sugar alcohols treatment groups was determined in the range of lipids and carbohydrates. Compared with the control group, the spectra bands denoting lipids in both mannitol and xylitol treatment group became more visible at 1736 cm^{-1}, while the peak height of bands denoting carbohydrates at 1078 cm^{-1} decreased.

In Fig. 2-3, relative lipid and carbohydrate content were calculated from the ratio of the lipid (1736 cm^{-1}) and carbohydrate band (1078 cm^{-1}) to the amide I band (1655 cm^{-1}), respectively. To our surprise, a significant increase in relative lipid content was observed with both mannitol and xylitol. Compared with the control, the lipid content in algal cells under 4 $g \cdot L^{-1}$ mannitol and xylitol treatment increased by 1.82 times and 1.49 times, respectively. It might be due these two sugar alcohols provided additional energy and material for biosynthesis of Acetyl-CoA and NADPH, which were important for lipid accumulation in algal cells [42]. However, the trend of carbohydrate was reversed from that of lipid. Carbohydrate content with mannitol and xylitol treatment groups decreased by 32.30% and 22.67%, respectively compared to control group. The promotion effect of mannitol for lipid production was larger than that of xylitol, but the accumulation of carbohydrates was lower accordingly, which was related to the intracellular carbon balance [43]. Carbohydrates and lipid triglycerides are energy stores in microalgae and share a common precursor for synthesis, and therefore they can be converted into each other under different conditions. In general, lipids can be accumulated at nutritional deficiencies such as

nitrogen [44] or phosphorus deficiency [12,45], but at the cost of a reduction in the growth and available biomass. Although different from common approach, these two sugar alcohols were favorable to enhance the lipid yield of *E. gracilis* without diminishing biomass growth.

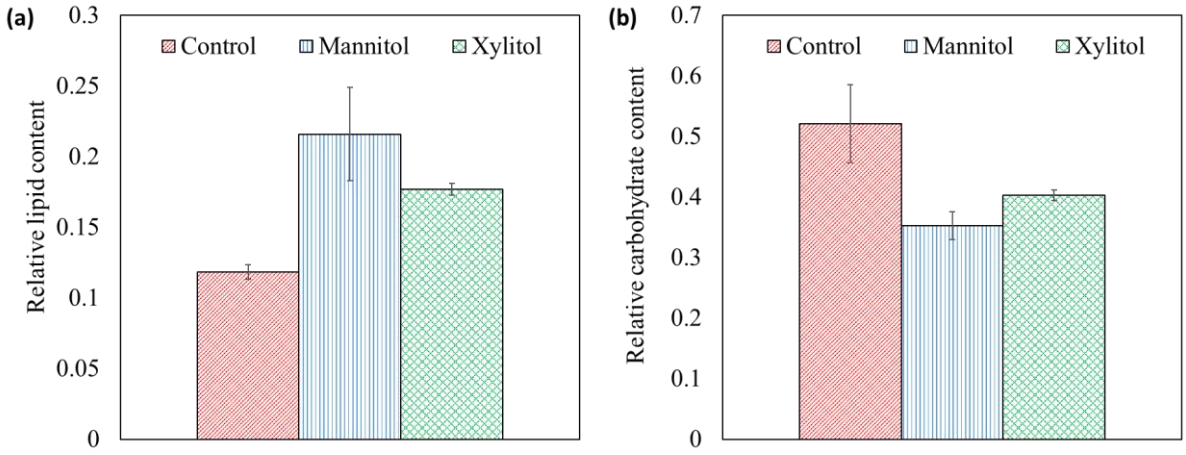

Fig. 2-3. Relative lipid (a) and carbohydrate (b) content of *E. gracilis* cultured under mannitol and xylitol conditions as determined by FT-IR spectroscopy. Error bars represent the standard deviation (n=9).

2.3.5 Differential identification of characteristic metabolites

Many specific bands in the FT-IR spectra are associated with specific metabolites, especially macromolecules. However, evaluating the changes in metabolites based on band intensity or average absorbance could not reflect the complete available information [46]. Therefore, multivariate analysis was used to further compare metabolic fingerprints and observe the discrete trend in metabolites from different culture conditions.

The effect of mannitol to *E. gracilis* metabolism was analyzed by non-supervised PCA as shown in Fig. 2-4(a). The data were resolved into four major components and the cumulative contribution rate R^2X was 0.945. Among them, PC1 accounted for 49.7% of the total variation and PC2 accounted for 35.5%, by which the major of variability was explained. To achieve better visualization of the discriminated sample groups from PCA and further maximize the group separation, the supervised OPLS-DA model was established after orthogonality correction to evaluate the metabolic patterns of *E. gracilis* with or without mannitol treatment. As seen from

Fig. 2-4(b), the parallelism between the control group (solid black circles) and mannitol treatment group (green triangles) was very good and stable, and a sharp separation between these two groups was observed, which revealed that mannitol induced significant biochemical changes in *E. gracilis* cells. OPLS-DA gave a good model (1 predictive + 4 orthogonal) with the cumulative contribution rate $R^2X = 0.981$, $R^2Y = 0.995$ and $Q^2 = 0.983$. The predictive variation explained 45.9% of all variation in the data. To avoid the overfitting of the model, a permutation test with 40 permutations (Fig. 2-4c) was carried out. Generally, the predictive ability of the model would be good when the slope of the two regression lines (R^2 and Q^2) was big and the intercept was small, which suggested that the model was interpreted by more data [47]. In addition, the difference between R^2 and Q^2 in this model was small, reflecting the difference between the data explained by the model and the predicted data was also small, demonstrating that the OPLS-DA model was reliable and predictive [48]. OPLS-DA loading plot as shown in Fig. 2-4(d) was adopted to find the potential biomarkers (potentially different metabolites) between control group and mannitol treatment group by looking at the most positive and negative loadings in the S-line plot. The positive and negative direction of the loading plot denote the variables that are more prominent in the groups located in the positive and negative direction of the scores plot, respectively [49]. As seen from the loading plot of Fig. 2-4(d), compared with the control group, *E. gracilis* cells from the mannitol treatment group contained more prominent spectral absorbance in spectral regions of fatty acids (C=O ester functional groups at 1739 cm^{-1}, and CH_3 and CH_2 bending at 1460 cm^{-1}), amides (N-H bending and C-N stretching vibration from amide II at 1537 cm^{-1}), aromatic compounds (C-N stretching from aromatic amine at 1300 cm^{-1}, and vibrations of aromatic ring at 1180 cm^{-1}), while less prominent spectral absorbance in the regions of carbohydrates (C-O-C stretching at 1155 cm^{-1}, C-O stretching and C-C stretching vibrations at 1111, 1078, and 1045 cm^{-1}, and CH_2 bending at 1363 cm^{-1}), ethers (C-O stretching at 1254 cm^{-1}), carboxylates (COO^- symmetric stretching at 1410 cm^{-1}, and COO^- antisymmetric stretching at 1614 cm^{-1}), as well as the alkene region (C=C stretching at 1672 cm^{-1}). This was consistent with the results shown in Fig. 2-3, which lipids content increased while carbohydrates content decreased under mannitol treatment, but the changes in some other small molecules could also be

unveiled.

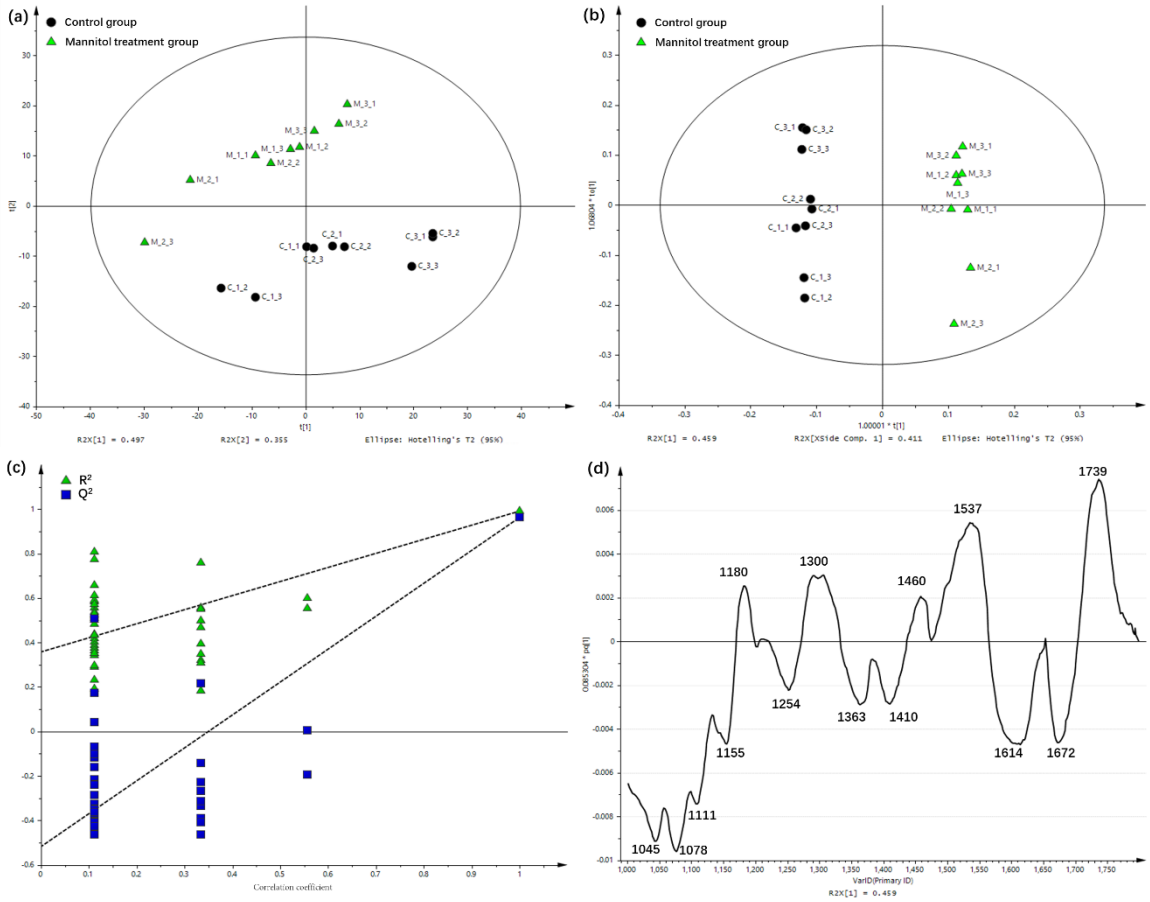

Fig. 2-4. PCA and OPLS-DA scores plots and loading plot based on the FT-IR spectra (1800–1000 cm^{-1}) of *E. gracilis* with or without mannitol treatment (n=9). Solid black circles and green triangles represent control group and mannitol treatment group, respectively. (a): PCA scores plot ($R^2X = 0.945$, Q^2 (cum) = 0.891); (b): OPLS-DA scores plot ($R^2X = 0.981$, $R^2Y=0.995$, Q^2 (cum) = 0.983); (c): permutation test (40 permutations); (d): OPLS-DA loading plot. ($R^2X[1]=0.459$)

PCA analysis between control and xylitol treatment group was also carried out and the results were shown in Fig. 2-5 (a). The data were clearly resolved into 3 major components, and PC1 explained 48.3% of all variation and PC2 explained 41.1%. The cumulative contribution rate R^2X = 0.948, and Q2 = 0.903, indicating that the established PCA model was of good quality. In order to identify the metabolites responsible for the discrimination of control group and xylitol treatment group, OPLS-DA model was carried out to further maximize the group separation. The

model (1 predictive + 2 orthogonal) was good with $R^2X = 0.97$, $R^2Y = 0.985$ and $Q^2 = 0.977$, and permutation test demonstrated its goodness of fit and high predictive capability. As shown in Fig. 2-5(b), mannitol treatment samples clustered with positive scores and control samples clustered with negative scores. Information from other bands was combined to interpret the most positive and negative bands [46]. The loading plot revealed the similar result as mannitol treatment, i.e., xylitol treatment resulted in higher levels of lipids, amides and aromatic compounds than that of the control group, while decreased the content of carbohydrates, ethers, carboxylates and alkenes. In addition to that, slight differences at 1390 cm^{-1} (positive loadings) and 1200 cm^{-1} (negative) were observed, most probably assigned to S=O stretching from sulfates and C-O stretching from phenols or ethers, respectively.

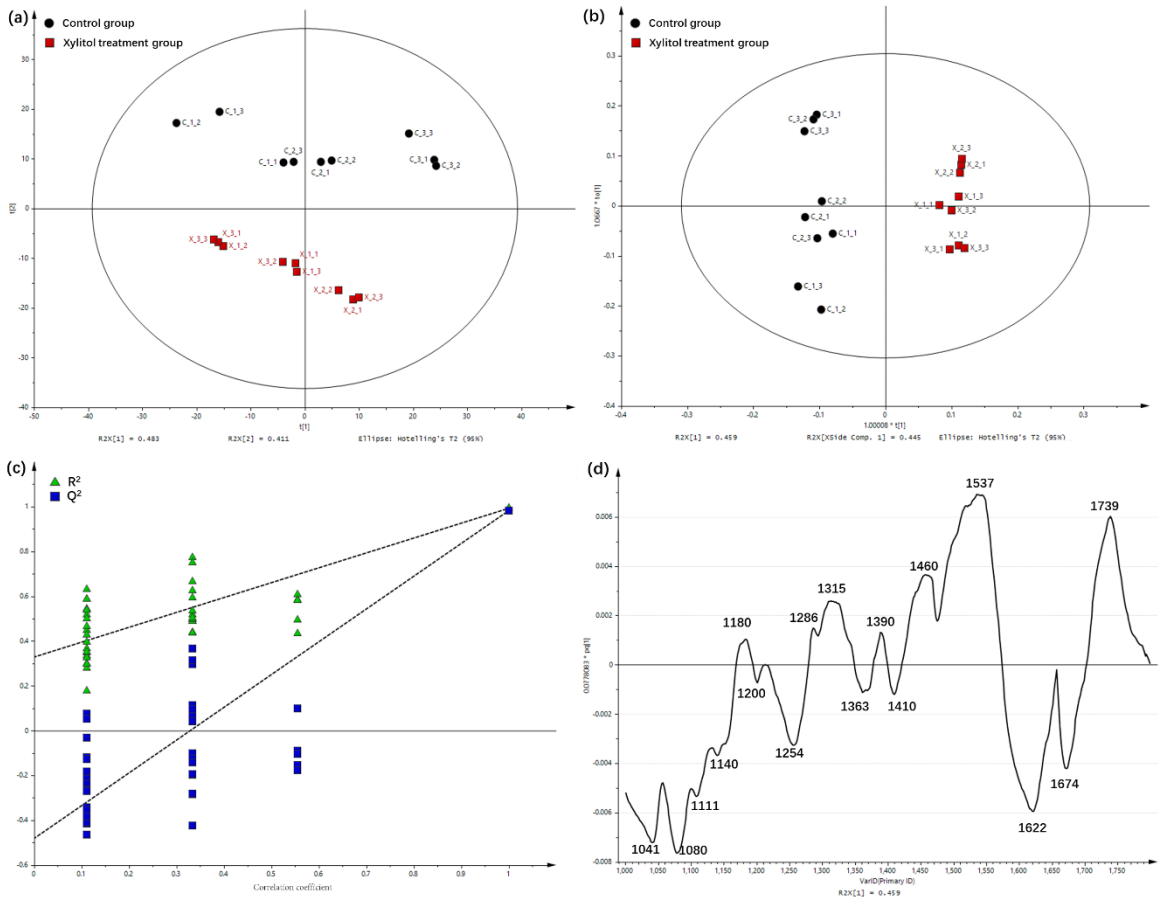

Fig. 2-5. PCA and OPLS-DA scores plots and loading plot based on the FT-IR spectra (1800–1000 cm^{-1}) of *E. gracilis* with or without xylitol treatment (n=9). Solid black circles and red squares represent control group and xylitol treatment group, respectively. (a): PCA scores plot

($R^2X = 0.948$, Q^2 (cum) = 0.903); (b): OPLS-DA scores plot ($R^2X = 0.97$, $R^2Y=0.985$, Q^2 (cum) = 0.977); (c): permutation test (40 permutations); (d): OPLS-DA loading plot ($R^2X[1]=0.459$).

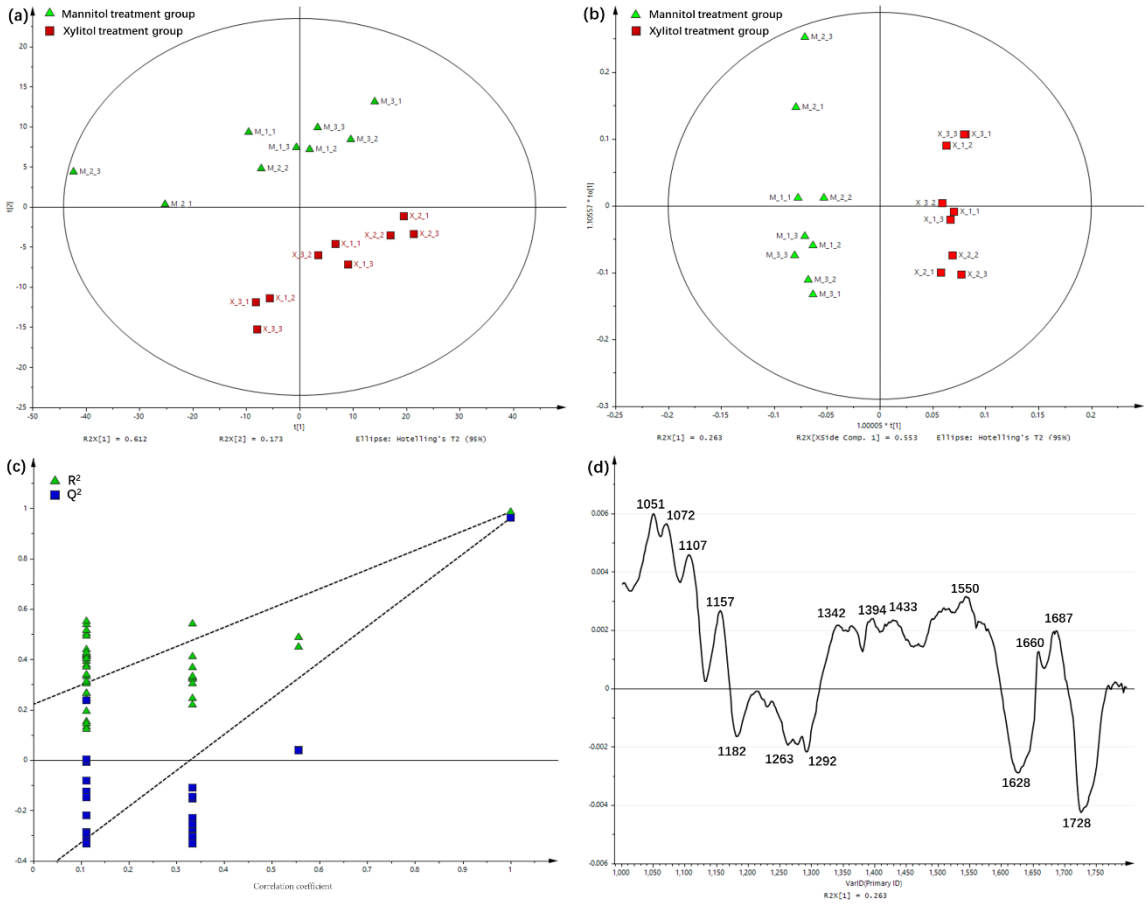

Fig. 2-6. PCA and OPLS-DA scores plots and loading plot based on the FT-IR spectra (1800–1000 cm^{-1}) of *E. gracilis* with mannitol and xylitol treatment (n=9). Green triangles and red squares represent mannitol treatment group and xylitol treatment group, respectively. (a): PCA scores plot ($R^2X = 0.935$, Q^2 (cum) = 0.864); (b): OPLS-DA scores plot ($R^2X = 0.862$, $R^2Y=0.986$, Q^2 (cum) = 0.967); (c): permutation test (40 permutations); (d): OPLS-DA loading plot ($R^2X[1]=0.263$).

The characteristic metabolites between mannitol and xylitol treatment groups were further investigated and compared by multivariate analysis. The obtained unsupervised PCA (Fig. 2-6a) and supervised OPLS-DA (Fig. 2-6b) models were both of good quality. For OPLS-DA, the predictive variation plus two orthogonal explained 86.2% of all variation in the data, and the

permutation test (Fig. 2-6c) confirmed that the model was not overfitting. The corresponding loading plot showed this separation between mannitol and xylitol treatment samples was caused by bands indicative of carbohydrates (1157, 1107, 1072 and 1051 cm^{-1}), sulfides (1433, 1394 and 1342 cm^{-1}) and amides (1687 and 1660 cm^{-1}) on the positive side (more intense towards xylitol treatment group), and bands indicative of lipids (1728 cm^{-1}) and aromatic ethers and esters (1292, 1263 and 1182 cm^{-1}) on the negative side (more intense towards mannitol treatment group).

As a sensitive and high-throughput method, FT-IR combined with multivariate analysis could well reflect the potential differences in metabolites of microalgae cells under different culture conditions and reveal the prominent variables among the metabolites. Both mannitol and xylitol affected the metabolic profiles of *E. gracilis* especially increased the lipid accumulation in the cells. The differences in metabolites treated with mannitol or xylitol were mainly found in the regions of lipids, carbohydrates, sulfides, and aromatic compounds. To determine the specific changes in these metabolites composition and content, analytical techniques that are more precise are still required, but this experiment provides a preliminary understanding on the effect of different sugar alcohols to the metabolite pool of *E. gracilis* cells, which will help further improve the biomass yield and specific metabolites accumulation for industrial application.

2.4 Conclusions

Positive effects on the growth and metabolites biosynthesis of freshwater microalga *E. gracilis* by lignocellulose related sugar alcohols mannitol and xylitol were exhibited in this study. At the optimal dosage of 4 $g \cdot L^{-1}$, mannitol and xylitol increased the biomass yield of algal cells by up to 4.64 and 3.18 times. Increased cell aspect ratio was only observed with mannitol, indicating that the *E. gracilis* had different physiological responses to mannitol and xylitol. Lipid accumulation was promoted by both mannitol and xylitol, revealing that these sugar alcohols from renewable resources have the potential to improve biofuel production by *E. gracilis*.

References

1. Manirafasha, E., Murwanashyaka, T., Ndikubwimana, T., Ahmed, N. R., Liu, J., Lu, Y., Zeng, X., Ling, X., Jing, K. (2018). Enhancement of cell growth and phycocyanin production in

Arthrospira (Spirulina) platensis by metabolic stress and nitrate fed-batch. *Bioresource technology*, *255*, 293-301.

2. Chae, S. R., Hwang, E. J., & Shin, H. S. (2006). Single cell protein production of Euglena gracilis and carbon dioxide fixation in an innovative photo-bioreactor. *Bioresource technology*, *97*(2), 322-329.

3. Priyadarshani, I., & Rath, B. (2012). Commercial and industrial applications of micro algae–A review. *Journal of Algal Biomass Utilization*, *3*(4), 89-100.

4. Yamada, K., Suzuki, H., Takeuchi, T., Kazama, Y., Mitra, S., Abe, T., ... & Iwata, O. (2016). Efficient selective breeding of live oil-rich *Euglena gracilis* with fluorescence-activated cell sorting. *Scientific reports*, *6*, 26327.

5. Likozar, B., & Levec, J. (2014). Effect of process conditions on equilibrium, reaction kinetics and mass transfer for triglyceride transesterification to biodiesel: experimental and modeling based on fatty acid composition. *Fuel Processing Technology*, *122*, 30-41.

6. Rodionova, M. V., Poudyal, R. S., Tiwari, I., Voloshin, R. A., Zharmukhamedov, S. K., Nam, H. G., ... & Allakhverdiev, S. I. (2017). Biofuel production: challenges and opportunities. *International Journal of Hydrogen Energy*, *42*(12), 8450-8461.

7. Song, M., & Pei, H. (2018). The growth and lipid accumulation of *Scenedesmus quadricauda* during batch mixotrophic/heterotrophic cultivation using xylose as a carbon source. *Bioresource technology*, *263*, 525-531.

8. Leite, G. B., Paranjape, K., Abdelaziz, A. E., & Hallenbeck, P. C. (2015). Utilization of biodiesel-derived glycerol or xylose for increased growth and lipid production by indigenous microalgae. *Bioresource technology*, *184*, 123-130.

9. Pittman, J. K., Dean, A. P., & Osundeko, O. (2011). The potential of sustainable algal biofuel production using wastewater resources. *Bioresource technology*, *102*(1), 17-25.

10. Nogami, R., Ushijima, K., Nishida, H., & Wakisaka, M. (2017). Enhancement of Growth and Lipid Production of *Botryococcus braunii* by Steel Slags. *Journal of the Japan Institute of Energy*, *96*(9), 372-375.

11. Zhu, J., & Wakisaka, M. (2018). Growth promotion of *Euglena gracilis* by ferulic acid from

rice bran. *AMB Express*, *8*(1), 1-7.

12. Zhu, J., Hong, D. D., & Wakisaka, M. (2019). Phytic acid extracted from rice bran as a growth promoter for *Euglena gracilis*. *Open Chemistry*, *17*(1), 57-63.
13. Miazek, K., Remacle, C., Richel, A., & Goffin, D. (2014). Effect of lignocellulose related compounds on microalgae growth and product biosynthesis: a review. *Energies*, *7*(7), 4446-4481.
14. Li, P., Miao, X., Li, R., & Zhong, J. (2011). In situ biodiesel production from fast-growing and high oil content *Chlorella pyrenoidosa* in rice straw hydrolysate. *Journal of Biomedicine and Biotechnology*, *2011*.
15. Sibi, G. (2015). Low cost carbon and nitrogen sources for higher microalgal biomass and lipid production using agricultural wastes. *Journal of Environmental Science and Technology*, *8*(3), 113-121.
16. Yang, S., Liu, G., Meng, Y., Wang, P., Zhou, S., & Shang, H. (2014). Utilization of xylose as a carbon source for mixotrophic growth of *Scenedesmus obliquus*. *Bioresource technology*, *172*, 180-185.
17. Leite, G. B., Paranjape, K., & Hallenbeck, P. C. (2016). Breakfast of champions: Fast lipid accumulation by cultures of *Chlorella* and *Scenedesmus* induced by xylose. *Algal Research*, *16*, 338-348.
18. Hassall, K. A. (1958). Xylose as a specific inhibitor of photosynthesis. *Nature*, *181*(4618), 1273-1274.
19. Fernandez, R., Herrero, P., & Moreno, F. (1985). Inhibition and inactivation of glucose-phosphorylating enzymes from *Saccharomyces cerevisiae* by D-xylose. *Microbiology*, *131*(10), 2705-2709.
20. Ghoreishi, S. M., & Shahrestani, R. G. (2009). Innovative strategies for engineering mannitol production. *Trends in food science & technology*, *20*(6-7), 263-270.
21. Osafune, T., Sumida, S., Ehara, T., Ueno, N., Hase, E., & Schiff, J. A. (1990). Lipid (wax) and paramylum as sources of carbon and energy for the early development of proplastids in dark-grown *Euglena gracilis* cells transferred to an inorganic medium. *Microscopy*, *39*(5), 372-

381.

22. Damiani, M. C., Popovich, C. A., Constenla, D., & Leonardi, P. I. (2010). Lipid analysis in *Haematococcus pluvialis* to assess its potential use as a biodiesel feedstock. *Bioresource technology*, *101*(11), 3801-3807.
23. Lichtenthaler, H.K., Wellburn, A.R. (1983). Determinations of total carotenoids and chlorophylls a and b of leaf extracts in different solvents. *Biochemical Society Transactions,* 11(5), 591–592.
24. Li, M., Muñoz, H. E., Goda, K., & Di Carlo, D. (2017). Shape-based separation of microalga *Euglena gracilis* using inertial microfluidics. *Scientific reports*, *7*(1), 1-8.
25. Meng, Y., Yao, C., Xue, S., & Yang, H. (2014). Application of Fourier transform infrared (FT-IR) spectroscopy in determination of microalgal compositions. *Bioresource technology*, *151*, 347-354.
26. Dean, A. P., Sigee, D. C., Estrada, B., & Pittman, J. K. (2010). Using FTIR spectroscopy for rapid determination of lipid accumulation in response to nitrogen limitation in freshwater microalgae. *Bioresource technology*, *101*(12), 4499-4507.
27. Driver, T., Bajhaiya, A. K., Allwood, J. W., Goodacre, R., Pittman, J. K., & Dean, A. P. (2015). Metabolic responses of eukaryotic microalgae to environmental stress limit the ability of FT-IR spectroscopy for species identification. *Algal research*, *11*, 148-155.
28. Piligaev, A. V., Sorokina, K. N., Shashkov, M. V., & Parmon, V. N. (2018). Screening and comparative metabolic profiling of high lipid content microalgae strains for application in wastewater treatment. *Bioresource technology*, *250*, 538-547.
29. Yamane, Y. I., Utsunomiya, T., Watanabe, M., & Sasaki, K. (2001). Biomass production in mixotrophic culture of *Euglena gracilis* under acidic condition and its growth energetics. *Biotechnology Letters*, *23*(15), 1223-1228.
30. Hurlbert, R. E., & Bates, R. C. (1971). Glucose utilization by *Euglena gracilis var. bacillaris* at higher pH. *The Journal of Protozoology*, *18*(2), 298-306.
31. Atta, M., Idris, A., Bukhari, A., & Wahidin, S. (2013). Intensity of blue LED light: a potential stimulus for biomass and lipid content in fresh water microalgae *Chlorella*

vulgaris. *Bioresource technology*, *148*, 373-378.

32. Karsten, U., Barrow, K. D., Nixdorf, O., West, J. A., & King, R. J. (1997). Characterization of mannitol metabolism in the mangrove red alga *Caloglossa leprieurii* (Montagne) J. Agardh. *Planta*, *201*(2), 173-178.
33. Iwamoto, K., Kawanobe, H., Ikawa, T., & Shiraiwa, Y. (2003). Characterization of salt-regulated mannitol-1-phosphate dehydrogenase in the red alga *Caloglossa continua*. *Plant physiology*, *133*(2), 893-900.
34. Yamaguchi, T., Ikawa, T., & NISIZAWA, K. (1969). Pathway of mannitol formation during photosynthesis in brown algae. *Plant and cell physiology*, *10*(2), 425-440.
35. Michel, G., Tonon, T., Scornet, D., Cock, J. M., & Kloareg, B. (2010). Central and storage carbon metabolism of the brown alga *Ectocarpus siliculosus*: insights into the origin and evolution of storage carbohydrates in Eukaryotes. *New Phytologist*, *188*(1), 67-81.
36. Brito, G. G., Sofiatti, V., Brandão, Z. N., Silva, V. B., Silva, F. M., & Silva, D. A. (2011). Non-destructive analysis of photosynthetic pigments in cotton plants. *Acta Scientiarum. Agronomy*, *33*(4), 671-678.
37. Koca, N., Karadeniz, F., & Burdurlu, H. S. (2007). Effect of pH on chlorophyll degradation and colour loss in blanched green peas. *Food Chemistry*, *100*(2), 609-615.
38. Fazeli, M. R., Tofighi, H., Samadi, N., & Jamalifar, H. (2006). Effects of salinity on β-carotene production by *Dunaliella tertiolecta* DCCBC26 isolated from the Urmia salt lake, north of Iran. *Bioresource Technology*, *97*(18), 2453-2456.
39. Kepekçi, R. A., & Saygideger, S. D. (2012). Enhancement of phenolic compound production in *Spirulina platensis* by two-step batch mode cultivation. *Journal of Applied Phycology*, *24*(4), 897-905.
40. Danilov, R. A., & Ekelund, N. G. A. (2001). Effects of pH on the growth rate, motility and photosynthesis in *Euglena gracilis*. *Folia microbiologica*, *46*(6), 549-554.
41. Nzayisenga, J. C., Eriksson, K., & Sellstedt, A. (2018). Mixotrophic and heterotrophic production of lipids and carbohydrates by a locally isolated microalga using wastewater as a growth medium. *Bioresource technology*, *257*, 260-265.

42. Wan, M., Liu, P., Xia, J., Rosenberg, J. N., Oyler, G. A., Betenbaugh, M. J., ... & Qiu, G. (2011). The effect of mixotrophy on microalgal growth, lipid content, and expression levels of three pathway genes in *Chlorella sorokiniana*. *Applied microbiology and biotechnology*, *91*(3), 835-844.

43. Singh, A., Nigam, P. S., & Murphy, J. D. (2011). Mechanism and challenges in commercialisation of algal biofuels. *Bioresource technology*, *102*(1), 26-34.

44. Wang, Y., Rischer, H., Eriksen, N. T., & Wiebe, M. G. (2013). Mixotrophic continuous flow cultivation of *Chlorella protothecoides* for lipids. *Bioresource Technology*, *144*, 608-614.

45. Zhu, J., & Wakisaka, M. (2020). Finding of phytase: Understanding growth promotion mechanism of phytic acid to freshwater microalga *Euglena gracilis*. *Bioresource Technology*, *296*, 122343.

46. Dao, L., Beardall, J., & Heraud, P. (2017). Characterisation of Pb-induced changes and prediction of Pb exposure in microalgae using infrared spectroscopy. *Aquatic Toxicology*, *188*, 33-42.

47. Szymańska, E., Saccenti, E., Smilde, A. K., & Westerhuis, J. A. (2012). Double-check: validation of diagnostic statistics for PLS-DA models in metabolomics studies. *Metabolomics*, *8*(1), 3-16.

48. Bylesjö, M., Rantalainen, M., Cloarec, O., Nicholson, J. K., Holmes, E., & Trygg, J. (2006). OPLS discriminant analysis: combining the strengths of PLS-DA and SIMCA classification. *Journal of Chemometrics: A Journal of the Chemometrics Society*, *20*(8-10), 341-351.

49. Sitole, L., Steffens, F., Krüger, T. P., & Meyer, D. (2014). Mid-ATR-FTIR spectroscopic profiling of HIV/AIDS sera for novel systems diagnostics in global health. *Omics: a journal of integrative biology*, *18*(8), 513-523.

Chapter 3. Application of Lignosulfonate as the Growth Promotor for *Euglena gracilis* to Increase Productivity of Biomass and Lipids

Biomass derived supplements have been recognized as environment-friendly and cost-effective sources of stimulants which can promote growth and valuable metabolites biosynthesis of microalgae. In this research, effect of lignosulfonates (LIGNs) on the growth, cell morphological changes, and valuable products accumulation of microalga *Euglena gracilis* was explored. At the optimal concentration of 5000 $mg \cdot L^{-1}$, LIGNs could promote the growth of *E. gracilis* up to 1.95 folds, and increase the yield of chlorophyll a, chlorophyll b and carotenoids by 3.50, 1.59 and 3.48 times, respectively. Cell morphological changes in aspect ratio and size caused by LIGNs were also observed. Fourier transform infrared spectroscopy measurements followed by multivariate analysis revealed difference in metabolic patterns and prominent metabolites with LIGNs treatment. LIGNs improved the lipid yield since both cell density and lipid content increased, which could contribute to the biofuel production in the future.

3.1 Introduction

The surge in the world population, coupled with the depletion of fossil fuels and the adverse impact of global warming have seriously threatened the environment and production of food and energy on which humankind depends. Microalgae are considered as an adequate sustainable biomass feedstock to overcome these problems [1]. *Euglena gracilis* is one of the most promising freshwater microalga because it can produce a variety of bioactive compounds, such as paramylon, essential amino acids, polyunsaturated fatty acids and vitamins [2]. Thus it has attracted wide interest from various fields such as food, nutraceuticals, pharmaceuticals, food additives, and cosmetics. Apart from this, *E. gracilis* has also been identified as a promising species for biofuel production [3]. However, its productivity is severely restricted by high cost, and has become one of the biggest bottle-necks to meet the vast demand from the market.

A lot of efforts to promote algae growth and biomass accumulation have been reported such as microalgae strain screening, bioreactor development, and nutrients supplementation [4,5]. However, still there is still a gap for the large-scale microalgae cultivation considering the

economic efficiency. Recently, supplementation of additives especially derived from abandoned biomass to microalgae culture has been proposed as cost-effective and efficient strategy to stimulate the algae growth and metabolites accumulation. According to previous reports, 5000 $mg \cdot L^{-1}$ industrial by-product steelmaking slag promoted the growth of *Botryococcus braunii* 1.74 times mainly resulted from iron ions elusion from the slag [6], while 500 $mg \cdot L^{-1}$ ferulic acid extracted from agro-waste rice bran was able to boost the *E. gracilis* growth up to 3.6 times, considered to act like phytohormone in this case [7]. These have attracted a lot of research interest to improve *E. gracilis* growth through efficient recycling of waste biomass from nature.

Lignocellulose is one of the most abundant raw materials in nature, but its utilization rate is relatively low [8], and the current development mainly focused on the use of cellulose, while the utilization of lignin is very limited, as lignin is a cross-linked phenolic polymer which is resistant to degradation and acid- and base-catalyzed hydrolysis [9]. The development of lignocellulosic raw materials inevitably leads to a large amount of lignin being discarded. Especially in the paper industry, a large amount of lignin is removed from wood pulp in the form of lignosulfonates (LIGNs) and becomes the major by-product in sulfite pulping waste liquor [10]. Meanwhile, due to the improper discharge, it has also become the source of significant environmental concerns [11]. In order to solve this problem, making full use of LIGNs is helpful to alleviate the environmental stress and improve the economic benefits of pulping waste liquor. At present, LIGNs are limitedly used in the fields of dispersants, plasticizers in making concrete, humectants, emulsion stabilizers, and sequestrants, etc. [10]. But researchers have keenly discovered the phytohormone-like regulatory role of LIGNs in the cultivation of a variety of higher plants [12-14]. For example, LIGNs could stimulate the growth of beet callus, improve multiplication rate and vigor of a shoot-proliferating poplar cluster, and increase the rooting percentage of holly, ginseng, and poplar shoots [14]. In addition, LIGNs were also found able to promote the growth of some microorganisms, such as fungal mycelium *Pisolithus tinctorius* [15] and *Phlebiopsis gigantea* oidia [16]. Although the positive effects on the vegetative growths, fructification, and the development of the root system were noticed [12,14], there was no report that LIGNs could affect the growth of microalgae. On the other hand, the roles of some common phytohormones in

microalgae cultivation and lipid accumulation have also been confirmed [17,18], but their prices are still high and cheap alternatives are necessary. If LIGNs were able to serve as stimulants for the growth of *E. gracilis*, it will achieve multiple benefits, not only to improve the economic benefits of *E. gracilis* cultivation, but also to reduce the environmental burden caused by pulping liquor.

In this context, the research aimed to investigate the influence of LIGNs on the growth and metabolism of microalgae cells. To better analyze the changes of cell physiology and product biosynthesis of *E. gracilis* in response to LIGNs, parameters such as cell density, photosynthetic pigment content, cell aspect ratio and size, and changes in intracellular macromolecules were evaluated.

3.2 Materials and methods

3.2.1 Algae strain and culture conditions

The axenic freshwater microalga *Euglena gracilis* Klebs (NIES-48) was purchased from National Institute for Environmental Studies, Japan. Cells were maintained in the modified Cramer-Myers (CM) medium for phototrophic cultivation in non-agitated flasks with low light intensity illumination and sub-cultured every 20 days. The composition of CM medium was shown in Table 3-1 [19]. Calcium lignosulfonate (Ca-LIGN; 0.71 USD·g^{-1}, Sigma-Aldrich, USA) stock solution was prepared and sterilized by the vacuum filtration with the pore size of 0.45 μm (Nalgene, Thermo Fisher Scientific, USA). The stock was diluted with fresh CM medium, thus LIGNs solutions with different concentrations were obtained. Then 10 mL of *E. gracilis* cell suspensions at a late logarithmic growth phase were transferred to the 300 mL Erlenmeyer flasks, and 90 mL of LIGNs stock with different concentrations were added to be 100 mL for culture volume of each flask. The final LIGNs concentrations were adjusted to 10, 100, 500, 1000 and 5000 mg·L^{-1}, respectively. All the cultivation was performed at 20 °C. The illumination was provided by white fluorescent lamps and the light intensity was 5000 lx with a 12:12 h light-dark cycle. All cultures are performed in triplicate, and shaken manually at the speed of approximately 180 rpm three times a day to prevent attachment to the bottle wall.

Table 3-1. Composition of the modified CM medium

Nutrients	Concentration ($mg \cdot L^{-1}$)	Trace ingredients	Concentration ($mg \cdot L^{-1}$)
$(NH_4)_2HPO_4$	1000	$FeSO_4 \cdot 7H_2O$	3
KH_2PO_4	1000	$MnCl_2 \cdot 4H_2O$	1.8
$MgSO_4 \cdot 7H_2O$	200	$CoSO_4 \cdot 7H_2O$	1.5
$CaCl_2 \cdot 2H_2O$	20	$ZnSO_4 \cdot 7H_2O$	0.4
		$Na_2MoO_4 \cdot 2H_2O$	0.2
		$CuSO_4 \cdot 5H_2O$	0.02
		Vitamin B_{12}	0.0005
		Thiamine HCl	0.1

3.2.2 Cell growth assessment

Cell density, optical density and dry weight were determined to evaluate the growth of *E. gracilis*. Cell number was counted with the hemocytomter (Thoma, Hirschmann, Germany) and pH of the culture filtrates were determined by pH meter (LAQUA-2103AL, Horiba, Japan). Specific growth rate *SGR* (d^{-1}) and cell doubling time *CDT* (d) were obtained following the Eqs. (1), (2).

$$SGR = (lnN2 - lnN1)/(d2 - d1)) \quad (1)$$

$$CDT = ln2/\mu \quad (2)$$

Where *d1* and *d2* are the start and end time of logarithmic phase, and *N1* and *N2* are the cell density at *d1* and *d2*, respectively.

Optical density of cell suspensions was also measured. Aliquot 4 mL of cell cultures were centrifuged at 5000 rpm. The harvested cells were rinsed with deionized water three times and resuspended to 4 mL to eliminate the effect of LIGNs. The optical density of the cell suspensions was determined at 680nm by the UV-vis spectrophotometer (Genesys 10S, Thermo Fisher Scientific, USA).

The dry weight of cell biomass in each culture group was measured during the stationary growth phase. Aliquots of cell suspension were filtered through the pre-dried filter paper (GC-50, Advantec, Japan), and harvested cells were washed three times to remove the residual LIGNs. Afterwards, the cells deposited on the filter papers were transferred to glass bottles and dried at 80°C for 10 h. Cell dry weight W ($g \cdot L^{-1}$) was calculated according to Eq. (3).

$$W = (M2 - M1)/V \quad (3)$$

Where *M1* and *M2* denote the initial and final weight of the filter paper, respectively. V is the volume of cell suspension.

3.2.3 Calibration of LIGNs concentration

The concentration of LIGNs was measured by spectrophotometry as described by Grigg and Bai [20]. The UV-vis absorption spectra of the culture filtrates with LIGNs showed a distinct characteristic peak at 280 nm which was independent of medium composition but typical for phenolic-hydroxyls of the phenyl propane monomers in LIGNs [21]. To obtain the calibration line, LIGNs solutions with concentrations of 10, 50, 100, 200, and 500 $mg \cdot L^{-1}$ in CM medium were prepared, and their absorbance at 280 nm was recorded. The standard calibration curve (R^2 = 0.9994) of LIGNs was established by data fitting, and the exact concentration ($mg \cdot L^{-1}$) can be calculated in accordance with Eq. (4).

$$C(LIGNs) = 147.64 Abs_{280} - 4.8383 \quad (4)$$

Where Abs_{280} is the absorbance of the solution at 280 nm. NOTE: The LIGNs has to be diluted to no more than 500 $mg \cdot L^{-1}$ to obtain a linear relationship between concentration and absorbance at 280 nm.

3.2.4 Observation of cell morphology

Cell aspect ratio and size of *E. gracilis* were important parameters to evaluate its physiological state, as it will exhibit different cell morphologies (spindled, elongated, and spherical shapes) in response to changes in the external environment [2,22]. Images of more than 150 cells for each sample were recorded by Image Plus 2.2S (Motic, Japan). Cell aspect ratio and cell projection area (approximated as cell size) were measured by particle analysis using the open source software ImageJ [23].

3.2.5 Photosynthetic pigment analysis

Photosynthetic pigment content was analyzed using the method given by Lichtenthaler and Wellburn [24]. Aliquot 5 mL of the cell cultures was filtrated, and the harvested cells were ground until they were completely crushed. Afterwards, the pigments were repeatedly extracted with 80% acetone. The ground homogenate was further filtered to remove impurities, and the volume of the filtrate was made to 10 mL with a volumetric flask. Photosynthetic pigments content were measured by spectrophotometry in accordance with Eqs. (5)-(7). In order to better compare the photosynthesis and physiological state of algal cells in different treatment groups, chlorophyll a/b ratio, and chlorophyll a/carotenoids ratio were also calculated.

$$Chl_a = 12.21Abs_{663} - 2.81Abs_{646} \quad (5)$$

$$Chl_b = 20.13Abs_{646} - 5.03Abs_{663} \quad (6)$$

$$C_{x+c} = (1000Abs_{470} - 3.27Chl_a - 104Chl_b)/229 \quad (7)$$

Chl_a, Chl_b, and C_{x+c} denote the chlorophyll a, chlorophyll b, and carotenoids content, and Abs_{470}, Abs_{646}, and Abs_{663} denote the absorbance at the wavelength of 470, 646, and 663 nm, respectively.

3.2.6 Analysis of cell composition by FT-IR spectroscopy

To better investigate the effects of LIGNs to the metabolism of *E. gracilis* cells, FT-IR analysis was employed to analyze the biochemical composition of algal cells in different treatment groups according to the following modified method [25]. Algae cells were collected by centrifugation at 6000 rpm for 10 min, and rinsed with Milli-Q (Millipore) water to eliminate the influence of LIGNs and medium composition on the spectrum. The rinsed cells were snap-frozen and dried at -50 °C under a vacuum overnight. Afterwards, the cell samples were ground together with KBr in a ratio of 0.2-1% (w/w) until the cell composition was evenly dispersed. Then they were pressed into thin sheets and FT-IR spectrometer (Nicolet iZ10, Thermo Fisher Scientific, USA) was employed to analyze the samples. The absorbance spectrum was acquired from 32 scans at 1800-1000 cm^{-1}, which contained the majority of the spectral information, and recorded by OMINIC software (Thermo Fisher Scientific, US). KBr spectrum was collected as the background, and each sample was analyzed in 9 replicates. All the acquired spectra of samples

were baseline and atmospheric corrected in accordance with the automatic correction algorithms. To interpret the differences in samples thickness, spectra were normalized to amide I band at 1655 cm^{-1}. Relative contents of lipids and carbohydrates were calculated from the peak height ratios of lipid/amide I and carbohydrate/amide I, respectively [26].

3.2.7 Multivariate data analysis

The difference in the external culture environment will cause myriad changes in the biosynthesis of metabolites within the cells. For rapid comparison of the metabolic fingerprints of cells cultured with and without LIGNs and observe discrete trends in their metabolites, multivariate analysis was employed to further analyze the FT-IR spectra. Normalized FTIR spectra in the regions of 1800-1000 cm^{-1} were analyzed by SIMCA-P software (version 13.0, Umetrics, Sweden). Principal components analysis (PCA) was employed as a non-supervised model to quickly compare the metabolic patterns of cells before and after LIGNs treatment, and the difference between these two groups were visualized and clustered in the score plot. Moreover, the supervised orthogonal partial least squares discriminant analysis (OPLS-DA) with Pareto scaling were also performed, to sharpen the separation between the observation groups, and indicate which peaks/bands from the characteristic metabolites are the sources of greatest variance within the data,

3.2.8 Statistical analysis

The growth and pigment analyses were performed in triplicate and the data were shown as mean ± standard deviation. For FT-IR analysis, each sample was analyzed in 9 replicates. The statistical difference in the growth and metabolites of different samples was analyzed by one-way analysis of variance (ANOVA), and post-hoc Fisher's Least Significant Difference (LSD) test was performed for pairwise comparisons using the SPSS software (version 16.0, IBM, USA), and the confidence interval was 95%.

3.3 Results and discussion

3.3.1 Effect of LIGNs on the growth profiles of *E. gracilis*

Growth promotion effect of LIGNs on *E. gracilis* was observed in this research. As shown

in Fig. 3-1 (a), the cell density was significantly promoted in the LIGNs treatment group with a concentration-dependent manner. Cell density of each group reached it maximum value on the 23rd day, indicating that the cell growth became stable at the end of the logarithmic phase. Cell density under 5000 mg·L^{-1} LIGNs showed a good growth promotion effect of 1.95-fold higher than that of the control group.

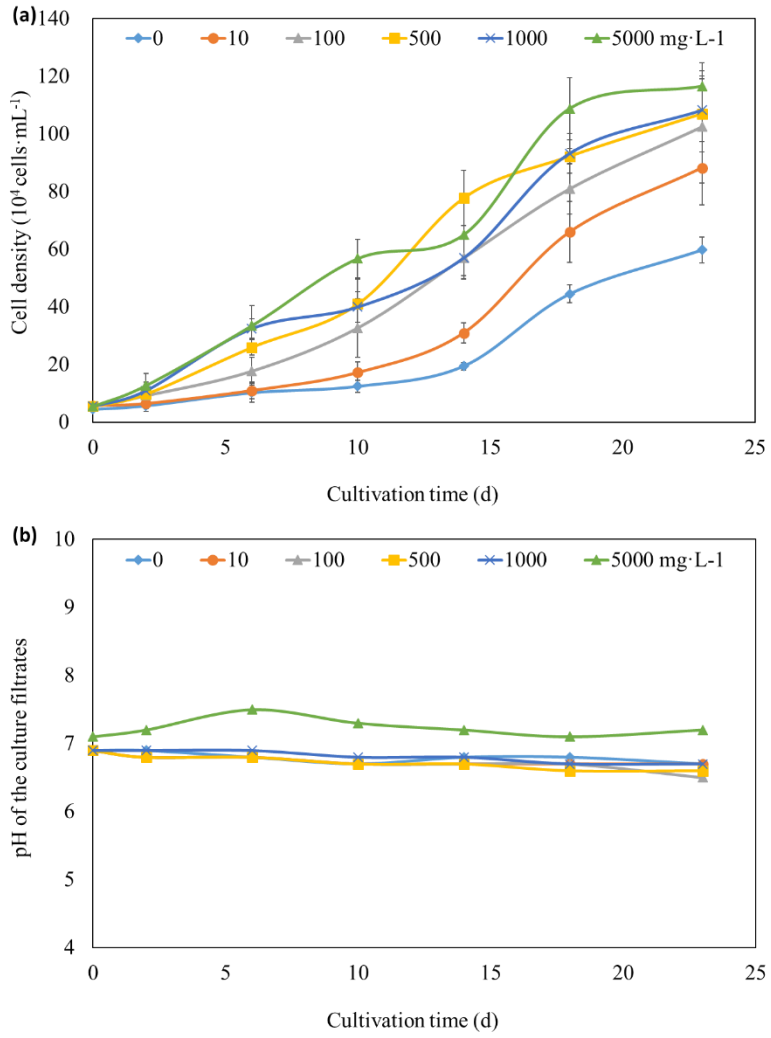

Fig. 3-1. Growth profiles of *E. gracilis* under different concentrations of LIGNs. (a): growth curves of *E. gracilis* under LIGNs treatment; (b): pH of the culture filtrates under LIGNs treatment.

Other growth profiles including specific growth rate (SGR), cell doubling time (CDT), and

biomass yield (BY) under different concentrations of LIGNs were summarized in Table 3-2, which were consistent with cell density results. The addition of 5000 mg·L^{-1} LIGNs significantly increased the SGR and shortened the CDT of *E. gracilis*. The BY also increased from 0.45 mg·L^{-1} of the control group to 0.77 mg·L^{-1} at 5000 mg·L^{-1} LIGNs ($p < 0.05$). LIGNs exhibited a dose-dependent promotion effect on the growth of *E. gracilis*. However, the difference in the growth of higher concentrations (500, 1000 and 5000 mg·L^{-1}) of LIGNs treatment groups was not statistically significant ($p > 0.05$), which might be mainly attributed to the shading effect of LIGNs [27]. LIGNs became brownish yellow in the solution, and darker with the increase of concentrations. High concentrations of LIGNs in the media would hinder the light utilization, and part of the promotion effect of the LIGNs could be slightly diminished by the shading effect. Nonetheless, the treatment with 5000 mg·L^{-1} LIGNs still achieved the highest biomass yield of *E. gracilis*.

Table 3-2. Growth parameters (SGR, CDT and BY) of algae cells cultured under different concentrations of LIGNs.

Dosages (mg·L^{-1})	SGR (d^{-1})	CDT (d)	BY (g·L^{-1})
0	0.113 ± 0.007^{b}	6.17 ± 0.36^{a}	0.45 ± 0.02^{b}
10	0.119 ± 0.012^{ab}	5.88 ± 0.58^{ab}	0.47 ± 0.10^{b}
100	0.127 ± 0.016^{ab}	5.53 ± 0.76^{ab}	0.59 ± 0.05^{ab}
500	0.129 ± 0.010^{a}	5.39 ± 0.45^{b}	0.59 ± 0.11^{ab}
1000	0.130 ± 0.011^{a}	5.37 ± 0.47^{b}	0.64 ± 0.21^{ab}
5000	0.133 ± 0.009^{a}	5.23 ± 0.40^{b}	0.77 ± 0.13^{a}

Data were expressed as mean ± standard deviation, and the same superscript in each column do not differ significantly ($p > 0.05$).

Fig. 3-1(b) reflected pH variation of the cultures throughout the growth. The lower concentrations of LIGNs had little effect on the initial pH of the cultures. When LIGNs

concentration increased to 5000 mg·L^{-1}, the initial pH of the cultures increased from 6.9 of the control group to 7.1, and rose to 7.5 on day 6 of the culture. This might be due to LIGNs chelating some metal ions (such as calcium, magnesium, iron, zinc, etc.) at the beginning, which thanks to the reticular structure of the LIGNs, resulting in the release of hydroxide anions in the solution and increase of pH [28]. However, the pH decreased as the culture progressed. This was due to the rapid proliferation of algae cells in 5000 mg·L^{-1} LIGNs treatment group causing the reduction of ammonium and increase in carbon dioxide [29].

This is the first report that LIGNs can be used as a growth regulator for freshwater microalgae. However, the significant decrease in the concentration of LIGNs during the growth of *E. gracilis* was not observed, which suggested that LIGNS were not consumed as the carbon source by *E. gracilis* in large quantities. It is reasonable because LIGNs are complex phenolic polymers which are less susceptible to degradation due to a lot of aryl-aryl bonds and the high redox potential [9]. In addition, it was found that the promotion effect of LIGNs had nothing to do with mineral nutrition, because additional supplemental calcium did not promote its growth in the case of sufficient calcium ions in the media.

Nevertheless, growth of *E. gracilis* was still notably promoted by LIGNs, which was consistent with the previous results observed in higher plant cells [12,14] and some microorganisms [15,16]. Growth stimulation mechanism of LIGNs for *E. gracilis* was mainly related to the regulation of endogenous phytohormone concentration [12,13,30]. LIGNs were able to cause the temporary inductive increase in the endogenous indole-3-acetic acid (IAA) in the poplar shoots [31,32]. Moreover, LIGNs could function as auxin protectors to favor growth promotion due to the phenolic nature [14]. Because these phenol structures are also substrates for auxin oxidase, and they can prevent the degradation of auxin through a competitive mechanism. On the other hand, Savy et al. [30] found water soluble lignin could improve the development of plants and seeds by influencing gibberellin-mediated physiological mechanisms. Growth promotion of *E. gracilis* could be related to phytohormone-like effect as previously reported with higher plants because of similarity with microalgae in cellular response.

3.3.2 Effect of LIGNs on the cell morphology

The perturbations of external environment will influence cell morphologies of E. gracilis, since the cells lack rigid cellulose walls and the pellicle is flexible [7]. Especially when the accumulation of intracellular macromolecules such as carbohydrates or lipids increases, the cells will turn to a bigger size. In this study, the quantitative comparison of cell morphology was carried out through cell aspect ratio and cell size (projection area), and the results were shown in Fig. 3-2. The horizontal lines represented the median values, and 50% of the algal cells in different shapes were comprised within the box. The cell aspect ratio increased and more spindled and elongated cells were observed in the lower concentrations (100, 500 and 1000 $mg \cdot L^{-1}$) of LIGNs treatment groups. However, cell aspect ratio returned to the level of control group at a higher concentration (5000 $mg \cdot L^{-1}$) of LIGNs. This was because the color of the media became darker as the LIGNs concentration increased, while illumination is an important factor influencing cell morphology [2,22]. In addition, LIGNs also increased the cell size of *E. gracilis* in a dose-dependent manner, and it might be related to the phytohormone-like effect of LIGNs. Noble et al. [33] found various plant hormones such as IAA and GA could stimulate the cell elongation and enlargement of *E. gracilis*, which was consistent with the findings in cell morphology (Fig. 3-2). The same phenomenon was observed in *Scenedesmus* sp. and *Chlorella sorokiniana* [34]. The treatment of the two auxins, naphthylacetic acid (NAA) and indole-3-butyric acid (IBA), significantly increased average diameter of *C. sorokiniana* cells and the aspect ratio of *Scenedesmus* sp., which was accompanied by an increase in lipid content in the cells of these two species. Wijffels and Barbosa has reported that the ideal microalgae for biofuel production will have the large-sized cells [35]. Therefore, further analysis of cellular components in *E. gracilis* was necessary for better understanding the changes in cell morphologies.

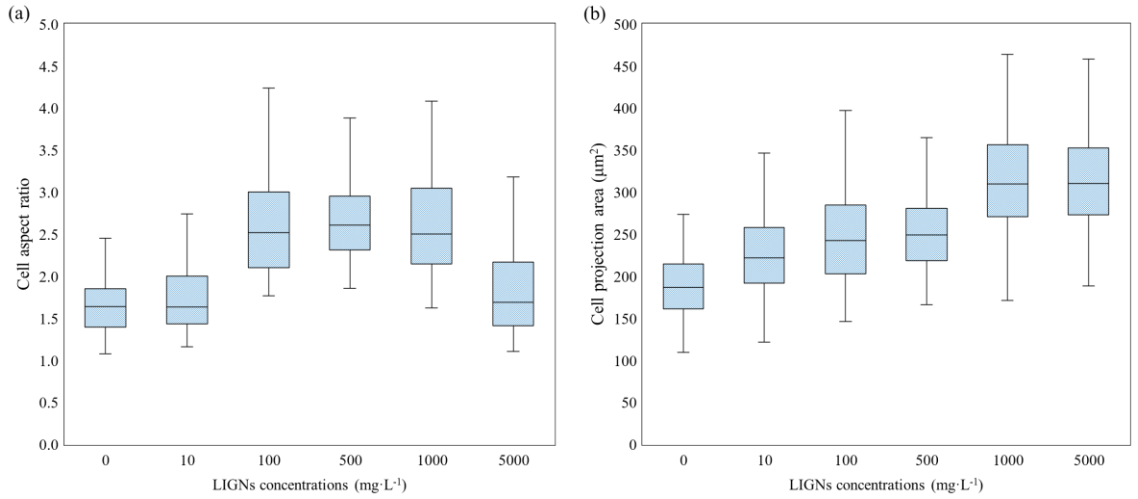

Fig. 3-2. Boxplot of cell aspect ratios and sizes (projection areas) of *E. gracilis* under LIGNs treatment. The lower and upper boundary of the boxes represent the 1st (25%) and 3rd quartile (75%) for the data distribution. The horizontal line represents the median value (50%), whereas the whiskers indicate the minimum and maximum values. Cell volume for observation in each group (cells): N_0=150, N_{10}=152, N_{100}=162, N_{500}=156, N_{1000}=168, N_{5000}=163. (a): cell aspect ratio; (b): cell projection area (μm^2).

3.3.3 Effect of LIGNs on the photosynthetic pigment of *E. gracilis*

Photosynthetic pigment yield and content in microalgae cells under different treatment groups were summarized in Fig.3-3. The chlorophyll a, chlorophyll b and carotenoids yield increased with the concentration of LIGNs, corresponding to the changes in dry weight of cellular biomass. At the optimal concentration of 5000 $mg \cdot L^{-1}$ LIGNs, chlorophyll a, chlorophyll b and carotenoids yield were increased by 3.50, 1.59 and 3.48 folds, respectively. However, the changes of photosynthetic pigment content in response to LIGNs treatment were different. The content of chlorophyll a (Fig. 3-3a) and carotenoids (Fig. 3-3c) in dry biomass was increased significantly, while the change of chlorophyll b content (Fig. 3-3d) was not notable.

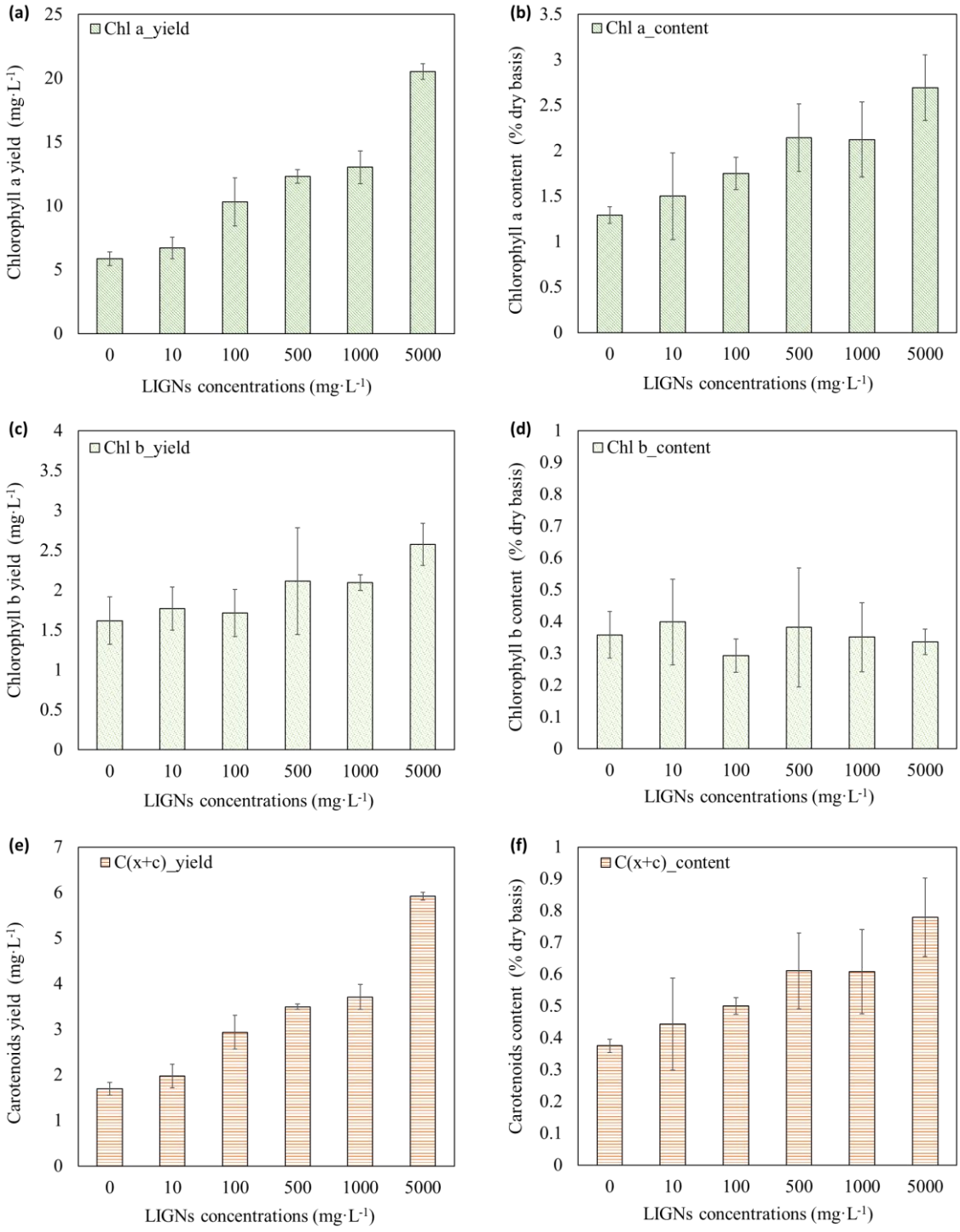

Fig. 3-3. Pigments yield and content of *E. gracilis* under different concentrations of LIGNs. (a): chlorophyll a yield (mg·L^{-1}); (b): chlorophyll a content (%dry basis); (c): chlorophyll b yield (mg·L^{-1}); (d): chlorophyll b content (%dry basis); (e): carotenoids yield (mg·L^{-1}); (f): carotenoids content (%dry basis).

Similar phenomena were also observed in higher plants. The treatment of LIGNs-humate increased the chlorophyll content in *Zea mays* L. and played a positive role in the photosynthetic process, which was closely related to the increase of phenolic compounds in the tissues such as protocatechuic acid, caffeic acid, and ferulic acid [13]. As previously mentioned, the action of LIGNs on the growth and physiology of plant cells was that of a specific hormone type, and consistent results have been found in the treatment of microalgae with various phytohormone related substances [17,36,37]. It was reported that auxin precursors and analogs could increase chlorophyll and carotenoids content in *Chlorella pyrenoidosa* by an average of 213–273% and 164–258% [38], which was consistent with this research, and further corroborated that LIGNs displayed a phytohormone-like activity for *E. gracilis* cells.

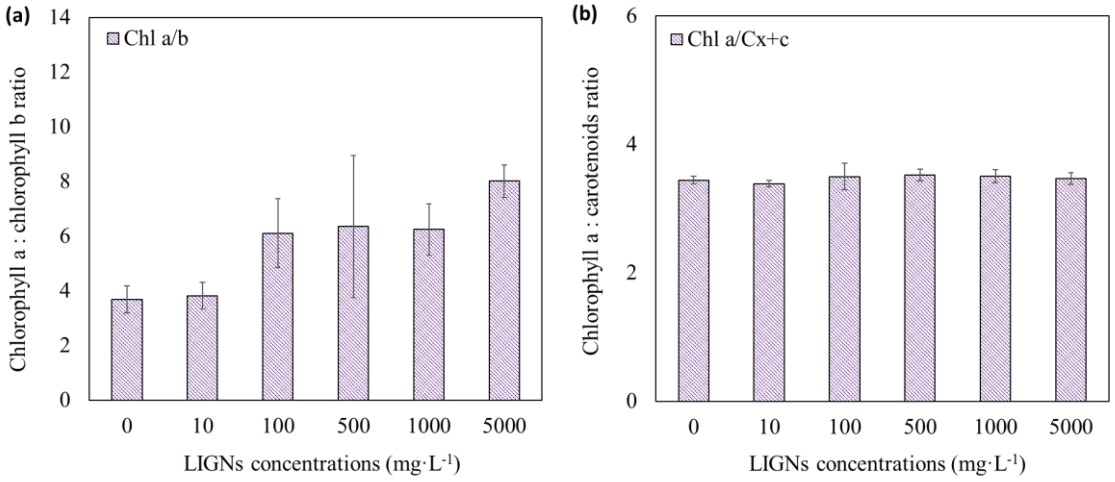

Fig. 3-4. The chlorophyll a/b ratio, and the chlorophyll a/carotenoids ratio in *E. gracilis* under different concentrations of LIGNs. (a): chlorophyll a to chlorophyll ratio; (b): chlorophyll a to carotenoids.

The effects of LIGNs on the chlorophyll a/b ratio, and chlorophyll a/carotenoids ratio were also analyzed (Fig. 3-4). The chlorophyll a/b ratio was positively correlated with LIGNs concentrations, indicating that LIGNs could improve the light-capturing ability of *E. gracilis* [39]. Generally, the ratio of chlorophyll a to carotenoids is a good indicator of the physiological state

of algal cells, and value around 3-4 was favorable to the growth [40]. A decrease in the chlorophyll a/carotenoids ratio usually indicates a poor physiological state of the cells such as cell senescence and stress [41]. Here the LIGNs treatment did not decrease the ratio of chlorophyll a to carotenoids and the values were within a reasonable range, indicating that *E. gracilis* in all culture groups were in a good physiological state.

3.3.4 Estimation of cell biochemical composition by FT-IR

FT-IR spectroscopy was employed to analyze the biochemical composition of *E. gracilis* cells with or without LIGNs treatment (5000 mg·L^{-1}), and the spectra at the range of 1800-1000 cm^{-1} were obtained. Bands from the spectra were assigned to specific molecules according to the previously described literature [42], and macromolecular components (proteins, lipids, carbohydrates, and phosphorylated molecules) were well identified. The two bands at 1655 and 1540 cm^{-1} were attributed to υ(C=O) stretching of amide I, and δ(N-H) bending of amide II from proteins; the band at 1260 cm^{-1} was attributed to υ_{as}(P=O) stretching from phosphodiester backbone of phosphorylated molecules (DNA and RNA); the two bands of 1738 cm^{-1} and 1080 cm^{-1} were of particular interest, and assigned to υ(C=O) stretching of fatty acids and υ(C-O-C) stretching vibration of carbohydrates, respectively.

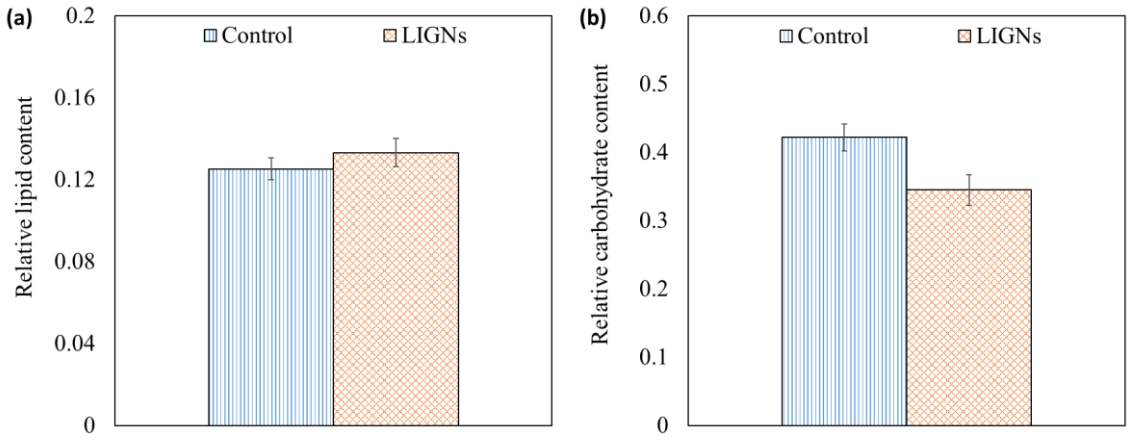

Fig. 3-5. The relative contents of lipid and carbohydrate in *E. gracilis* under control and 5000 mg·L^{-1} LIGNs treatment as determined by FT-IR spectroscopy (nine replicates). (a): relative lipid content; (b): relative carbohydrate content.

Compared with the control group, the LIGNs treated spectrum showed higher absorbance for the bands related to lipids, while the absorbance for the bands associated with carbohydrates decreased. To better reflect the changes in the content of cellular components, the relative content of lipids and carbohydrates were calculated. As illustrated in Fig. 3-5, 5000 $mg \cdot L^{-1}$ LIGNs treatment slightly increased the relative lipid content by 6.3%. Lipid yield would also be greatly improved (2.07-fold) since LIGNs did not sacrifice the lipids content and increased the cell density. This was consistent with the previous report that LIGNs induced the increase in the lipid concentration and yield of oleaginous yeast *Rhodosporidium toruloides* by 44.9% and 15.7%, respectively [43]. Similar results were also observed in phytohormone-treated microalgae cells (Table 3-3). Most of these phytohormones, such as IAA, IBA GA, NAA, kinetin, zeatin, 1-triacontanol, and abscisic acid (ABA), could significantly promoted the accumulation of intracellular lipids while increasing the biomass production [35,44,45,46]. On the contrary, the relative content of carbohydrates presented exactly opposed trends, and decreased under the treatment of LIGNs, implying a competing interaction with lipids. Carbohydrates are one of the major energy stores in microalgae cells and common synthetic precursor (triacylglycerols) were shared with lipids. Thus, they can be converted into each other in response to metabolic changes. It is reported that these phytohormone-like activities of LIGNs on cell metabolism are due to the biological actions of phenolic compounds. Allelopathic properties of some monomers from LIGNs (such as vanillic acid, protocatechuic acid, and ferulic acid, etc.) have been discovered. The interaction between these phenolics and some plant hormones determines different biosynthetic pathways and flow of carbon to metabolites [13]. As described by previous reports [35,45,47], with the increasing auxins concentrations, the carbohydrate content in the algal cells gradually decreased while lipid content increased. It was consistent with the metabolic changes caused by LIGNs (Fig. 3-5). Generally, environment cues that induce lipogenesis are, for the most part, identical to the ones inducing carotenoids accumulation [48]. Consistently, the treatment of LIGNs to *E. gracilis* increased both carotenoids and lipids content. Unlike conventional methods (nitrogen and phosphorus deficiency), it would not diminish the growth and available biomass, which was favorable to enhance the lipid and carotenoids yiled in *E. gracilis* biomass production.

Table 3-3. Comparison with the effect of phytohormone on microalgal growth, morphology and metabolism.

Species	Elicitor	Impact on growth	Impact on morphology	Impact on metabolism	Ref.
Scenedesmus sp. and *Chlorella sorokiniana*	NAA and IBA	59.3%-76.6% increase	Significantly increased average diameter of *C. sorokiniana* cells and the aspect ratio of *Scenedesmus sp*.	Carbohydrate content declined while lipid content was greatly increased	[35]
Chlamydomonas reinhardtii	IAA, GA, kinetin, 1-triacontanol, and ABA	54%-69% increase	Marked increase of cell size in all five phytohormone tested groups	Protein content increased but starch content did not show any difference; Lipid production was improved when phytohormones were added during the early exponential growth phase.	[44]
Phaeodactylum tricornutum	2,4-dichlorophenoxyacetic	60% increase	Larger oil bodies were	Protein and carbohydrate	[45]

	acid and ABA		observed.	content were downregulated, while lipid accumulation was greatly upregulated.	
Acutodesmus obliquus	kinetin, zeatin	50%-60.7% increase	N.D.	Lipid content and productivity were greatly increased; Carbohydrate productivity was also found to be increased with zeatin supplementation.	[46]
Monoraphidium sp.	Melatonin	No significant influence.	N.D.	Lipid accumulation was increased, while protein and carbohydrate content was decreased.	[47]

N.D. Not detected.

3.3.5 Discrimination of characteristic metabolites by multivariate analysis

Multivariate analysis was operated to further analyze the FT-IR spectra and discriminate the characteristic metabolites from different culture conditions, and these metabolic profiles were shown in Fig. 3-6. Firstly, the effect of LIGNs to the metabolic fingerprint of *E. gracilis* was

analyzed by PCA analysis which was a non-supervised model. Five major components were resolved, and the cumulative contribution rate R^2X was 94.7% (PC-1 accounting for 59.6% and PC-2 accounting for 16%). However, there was no complete separation between control and LIGNs treated samples in the PCA analysis. Thus, the supervised OPLS-DA was employed after the orthogonal-correction, which could maximize the discrimination between samples from different groups. As shown in Fig. 3-6(b), it was clear that the parallelism between these two groups in OPLS-DA model was good and the separation was sharp, revealing that the metabolic patterns of algae cells with LIGNs treatment has been differentiated. The OPLS-DA model gave one predictive component and three orthogonal with $R^2X = 0.932$, and the predictive component explained 34.9% of the total variation in the datasets of *E. gracilis*. To guard against model overfitting and assess its validity, cross-validation with 200 permutations (Fig. 3-6c) was carried out and showed a much more reliable Q^2 than R^2. Moreover, Q^2 value of the original data was larger than those obtained from the randomly permuted data, and y-intercepts of Q^2 were negative, suggesting the model was reliable and predicative [49].

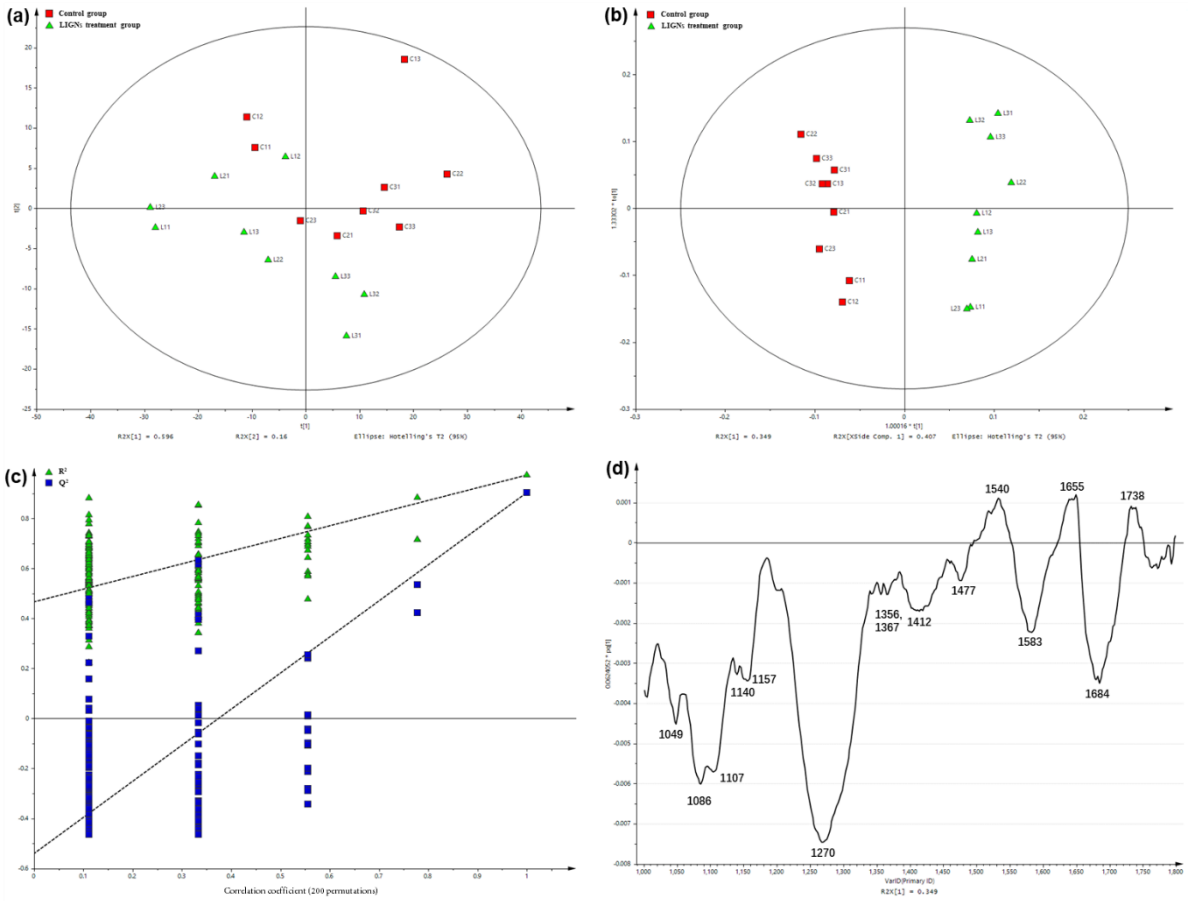

Fig. 3-6. Multivariate analysis of FT-IR spectra collected from different treatment groups of *E. gracilis* (nine replicates). (a): PCA score plot ($R^2X = 0.947$, $Q^2 = 0.848$); (b): OPLS-DA score plot ($R^2X = 0.932$, $R^2Y = 0.968$ $Q^2 = 0.94$); (c): permutation test of 200 iterations; (d): OPLS-DA loading plot. ($R^2X[1] = 0.349$)

Potential biomarkers in the control and LIGNs treated samples were analyzed. As shown in Fig. 3-6(d). The positive loadings represent the variables (bands) more prominent in the positive direction of the OPLS-DA score plot (here refer to LIGNs samples), and vice versa for the negative loadings [50]. In comparison with control samples, algae cells with LIGNs treatment had more prominent spectral absorbance (positive side) in the regions of lipids (C=O stretching of esters at 1738 cm^{-1}) and proteins (C=O stretching of amide I at 1655 cm^{-1}, and N–H bending of amide II at 1540 cm^{-1}), while less prominent absorbance (negative side) in the regions of carbohydrates (C-H bending at 1367 cm^{-1}, C-O-C stretching at 1157 cm^{-1}, C-O and C-C stretching

vibrations at 1140, 1107, 1086, and 1049 cm^{-1}), carboxylates (C=O stretching of carbonyl group at 1684 cm^{-1}, COO^- symmetric stretching at 1583, 1412, and 1356 cm^{-1}), aromatic ethers (C-O stretching at 1270 cm^{-1}), and alkane regions (C-H bending of methyl group and methylene group at 1477 cm^{-1}). The loading plot revealed the effect of LIGNs on the metabolic patterns of microalgae cells, and identified the prominent variables among these metabolites. The results that lipid content increased whereas carbohydrate content declined with LIGNs treatment, were consistent with the previous quantitative comparison. This technology provided a preliminary understanding of the effects of LIGNS to the metabolic patterns of *E. gracilis*, which could contribute to further improving specific metabolites biosynthesis in *E. gracilis* for large-scale industrial application.

3.4 Conclusions

Phytohormone-like positive effects of LIGNs on the growth and metabolites accumulation of *E. gracilis* were discovered for the first time. LIGNs at the optimal concentration of 5000 $mg \cdot L^{-1}$ promoted the cell growth 1.95-fold. Increase in cell aspect ratio (except 5000 $mg \cdot L^{-1}$ due to the dark brown color) and cell size were also observed with LIGNs treatment. Metabolic patterns of *E. gracilis* were changed by LIGNs and the yield of valuable metabolites such as chlorophyll, carotenoids and lipids were improved. LIGNs as a by-product of pulping process has the potential to greatly improve the biomass yield of *E. gracilis*.

References

[1] Franchino, M., Tigini, V., Varese, G. C., Sartor, R. M., & Bona, F. (2016). Microalgae treatment removes nutrients and reduces ecotoxicity of diluted piggery digestate. *Science of the Total Environment*, *569*, 40-45.

[2] Li, M., Muñoz, H. E., Goda, K., & Di Carlo, D. (2017). Shape-based separation of microalga *Euglena gracilis* using inertial microfluidics. *Scientific reports*, *7*(1), 1-8.

[3] Nagappan, S., Devendran, S., Tsai, P. C., Dahms, H. U., & Ponnusamy, V. K. (2019). Potential of two-stage cultivation in microalgae biofuel production. *Fuel*, *252*, 339-349.

[4] Chae, S. R., Hwang, E. J., & Shin, H. S. (2006). Single cell protein production of E*uglena gracilis* and carbon dioxide fixation in an innovative photo-bioreactor. *Bioresource*

technology, *97*(2), 322-329.

[5] Zhu, J., & Wakisaka, M. (2020). Effect of two lignocellulose related sugar alcohols on the growth and metabolites biosynthesis of *Euglena gracilis*. *Bioresource Technology*, *303*, 122950.

[6] Nogami, R., Ushijima, K., Nishida, H., & Wakisaka, M. (2017). Enhancement of Growth and Lipid Production of *Botryococcus braunii* by Steel Slags. *Journal of the Japan Institute of Energy*, *96*(9), 372-375.

[7] Zhu, J., & Wakisaka, M. (2018). Growth promotion of Euglena gracilis by ferulic acid from rice bran. *AMB Express*, *8*(1), 1-7.

[8] Yao, D., Dong, S., Wang, P., Chen, T., Wang, J., Yue, Z. B., & Wang, Y. (2017). Robustness of *Clostridium saccharoperbutylacetonicum* for acetone-butanol-ethanol production: Effects of lignocellulosic sugars and inhibitors. *Fuel*, *208*, 549-557.

[9] Guo, D., Wu, S., Lyu, G., & Guo, H. (2017). Effect of molecular weight on the pyrolysis characteristics of alkali lignin. *Fuel*, *193*, 45-53.

[10] Aro, T., & Fatehi, P. (2017). Production and application of lignosulfonates and sulfonated lignin. *ChemSusChem*, *10*(9), 1861-1877.

[11] Zhang, S. J., Yu, H. Q., & Wu, L. X. (2004). Degradation of calcium lignosulfonate using gamma-ray irradiation. *Chemosphere*, *57*(9), 1181-1187.

[12] Kevers, C., Soteras, G., Baccou, J. C., & Gaspar, T. (1999). Lignosulfonates: Novel promoting additives for plant tissue cultures. *In Vitro Cellular & Developmental Biology-Plant*, *35*(5), 413-416.

[13] Ertani, A., Francioso, O., Tugnoli, V., Righi, V., & Nardi, S. (2011). Effect of commercial lignosulfonate-humate on *Zea mays* L. metabolism. *Journal of agricultural and food chemistry*, *59*(22), 11940-11948.

[14] Docquier, S., Kevers, C., Lambe, P., Gaspar, T., & Dommes, J. (2007). Beneficial use of lignosulfonates in in vitro plant cultures: stimulation of growth, of multiplication and of rooting. *Plant cell, tissue and organ culture*, *90*(3), 285-291.

[15] Niemi, K., Kevers, C., & Häggman, H. (2005). Lignosulfonate promotes the interaction

between Scots pine and an ectomycorrhizal fungus *Pisolithus tinctoriusin* vitro. *Plant and soil*, *271*(1-2), 243-249.

[16] Dumas, M. T. (2011). Stimulatory effect of ammonium lignosulfonate on germination and growth of *Phlebiopsis gigantea* spores. *Forest Pathology*, *41*(3), 189-192.

[17] Tate, J. J., Gutierrez-Wing, M. T., Rusch, K. A., & Benton, M. G. (2013). The effects of plant growth substances and mixed cultures on growth and metabolite production of green algae *Chlorella* sp.: a review. *Journal of plant growth regulation*, *32*(2), 417-428.

[18] Lin, B., Ahmed, F., Du, H., Li, Z., Yan, Y., Huang, Y., ... & Meng, C. (2018). Plant growth regulators promote lipid and carotenoid accumulation in *Chlorella vulgaris*. *Journal of Applied Phycology*, *30*(3), 1549-1561.

[19] Cramer, M., & Myers, J. (1952). Growth and photosynthetic characteristics of *Euglena gracilis*. *Archiv für Mikrobiologie*, *17*(1-4), 384-402.

[20] Grigg, R. B., & Bai, B. (2004). Calcium lignosulfonate adsorption and desorption on Berea sandstone. *Journal of colloid and interface science*, *279*(1), 36-45.

[21] Li, H., Liu, H., Fu, S., & Zhan, H. (2011). Surface hydrophobicity modification of cellulose fibers by layer-by-layer self-asssembly of lignosulfonates. *BioResources*, *6*(2), 1681-1695.

[22] Murray, J. M. (1981). Control of cell shape by calcium in the *Euglenophyceae*. *Journal of cell science*, *49*(1), 99-117.

[23] Zhu, J., & Wakisaka, M. (2020). Finding of phytase: Understanding growth promotion mechanism of phytic acid to freshwater microalga *Euglena gracilis*. *Bioresource Technology*, *296*, 122343.

[24] Lichtenthaler, H.K., Wellburn, A.R. (1983). Determinations of total carotenoids and chlorophylls a and b of leaf extracts in different solvents. *Biochemical Society Transactions,* 11(5), 591–592.

[25] Dean, A. P., Sigee, D. C., Estrada, B., & Pittman, J. K. (2010). Using FTIR spectroscopy for rapid determination of lipid accumulation in response to nitrogen limitation in freshwater microalgae. *Bioresource technology*, *101*(12), 4499-4507.

[26] Meng, Y., Yao, C., Xue, S., & Yang, H. (2014). Application of Fourier transform infrared

(FT-IR) spectroscopy in determination of microalgal compositions. *Bioresource technology*, *151*, 347-354.

[27] Schwab, F., Bucheli, T. D., Lukhele, L. P., Magrez, A., Nowack, B., Sigg, L., & Knauer, K. (2011). Are carbon nanotube effects on green algae caused by shading and agglomeration?. *Environmental science & technology*, *45*(14), 6136-6144.

[28] Khvan, A. M., & Abduazimov, K. A. (1990). Interaction of lignosulfonate with certain metal ions. *Chemistry of Natural Compounds*, *26*(5), 575-577.

[29] Yamane, Y. I., Utsunomiya, T., Watanabe, M., & Sasaki, K. (2001). Biomass production in mixotrophic culture of *Euglena gracilis* under acidic condition and its growth energetics. *Biotechnology Letters*, *23*(15), 1223-1228.

[30] Savy, D., Canellas, L., Vinci, G., Cozzolino, V., & Piccolo, A. (2017). Humic-like water-soluble lignins from giant reed (*Arundo donax* L.) display hormone-like activity on plant growth. *Journal of Plant Growth Regulation*, *36*(4), 995-1001.

[31] Hausman, J. F., Kevers, C., & Gaspar, T. (1995). Auxin-polyamine interaction in the control of the rooting inductive phase of poplar shoots in vitro. *Plant Science*, *110*(1), 63-71.

[32] Gaspar, T., Kevers, C., Penel, C., Greppin, H., Reid, D. M., & Thorpe, T. A. (1996). Plant hormones and plant growth regulators in plant tissue culture. *In vitro Cellular & Developmental Biology-Plant*, *32*(4), 272-289.

[33] Noble, A., Kisiala, A., Galer, A., Clysdale, D., & Emery, R. N. (2014). *Euglena gracilis (Euglenophyceae)* produces abscisic acid and cytokinins and responds to their exogenous application singly and in combination with other growth regulators. *European journal of phycology*, *49*(2), 244-254.

[34] Yu, Z., Song, M., Pei, H., Jiang, L., Hou, Q., Nie, C., & Zhang, L. (2017). The effects of combined agricultural phytohormones on the growth, carbon partitioning and cell morphology of two screened algae. *Bioresource technology*, *239*, 87-96.

[35] Wijffels, R. H., & Barbosa, M. J. (2010). An outlook on microalgal biofuels. *Science*, *329*(5993), 796-799.

[36] Lu, Y., & Xu, J. (2015). Phytohormones in microalgae: a new opportunity for microalgal

biotechnology?. *Trends in plant science*, *20*(5), 273-282.

[37] Han, X., Zeng, H., Bartocci, P., Fantozzi, F., & Yan, Y. (2018). Phytohormones and effects on growth and metabolites of microalgae: a review. *Fermentation*, *4*(2), 25.

[38] Czerpak, R., Bajguz, A., Białecka, B., Wierzchołowska, L. E., & Wolańska, M. M. (1994). Effect of auxin precursors and chemical analogues on the growth and chemical composition in *Chlorella pyrenoidosa* Chick. *Acta Societatis Botanicorum Poloniae*, *63*(3-4), 279-286.

[39] Dale, M. P., & Causton, D. R. (1992). Use of the chlorophyll a/b ratio as a bioassay for the light environment of a plant. *Functional Ecology*, 190-196.

[40] Orosa, M., Franqueira, D., Cid, A., & Abalde, J. J. B. T. (2005). Analysis and enhancement of astaxanthin accumulation in *Haematococcus pluvialis*. *Bioresource Technology*, *96*(3), 373-378.

[41] Saha, S. K., Moane, S., & Murray, P. (2013). Effect of macro-and micro-nutrient limitation on superoxide dismutase activities and carotenoid levels in microalga *Dunaliella salina* CCAP 19/18. *Bioresource technology*, *147*, 23-28.

[42] James, G. O., Hocart, C. H., Hillier, W., Chen, H., Kordbacheh, F., Price, G. D., & Djordjevic, M. A. (2011). Fatty acid profiling of *Chlamydomonas reinhardtii* under nitrogen deprivation. *Bioresource technology*, *102*(3), 3343-3351.

[43] Xu, J., Du, W., Zhao, X., & Liu, D. (2016). Renewable microbial lipid production from Oleaginous Yeast: some surfactants greatly improved lipid production of *Rhodosporidium toruloides*. *World Journal of Microbiology and Biotechnology*, *32*(7), 107.

[44] Park, W. K., Yoo, G., Moon, M., Kim, C. W., Choi, Y. E., & Yang, J. W. (2013). Phytohormone supplementation significantly increases growth of *Chlamydomonas reinhardtii* cultivated for biodiesel production. *Applied biochemistry and biotechnology*, *171*(5), 1128-1142.

[45] Zhang, H., Yin, W., Ma, D., Liu, X., Xu, K., & Liu, J. (2020). Phytohormone supplementation significantly increases fatty acid content of *Phaeodactylum tricornutum* in two-phase culture. *Journal of Applied Phycology*, 1-11.

[46] Renuka, N., Guldhe, A., Singh, P., Ansari, F. A., Rawat, I., & Bux, F. (2017). Evaluating the

potential of cytokinins for biomass and lipid enhancement in microalga *Acutodesmus obliquus* under nitrogen stress. *Energy Conversion and Management*, *140*, 14-23.

[47] Zhao, Y., Li, D., Xu, J. W., Zhao, P., Li, T., Ma, H., & Yu, X. (2018). Melatonin enhances lipid production in *Monoraphidium* sp. QLY-1 under nitrogen deficiency conditions via a multi-level mechanism. *Bioresource technology*, *259*, 46-53.

[48] Varela, J. C., Pereira, H., Vila, M., & León, R. (2015). Production of carotenoids by microalgae: achievements and challenges. *Photosynthesis research*, *125*(3), 423-436.

[49] Cao, M., Zhao, L., Chen, H., Xue, W., & Lin, D. (2012). NMR-based metabolomic analysis of human bladder cancer. *Analytical Sciences*, *28*(5), 451-456.

[50] Sitole, L., Steffens, F., Krüger, T. P., & Meyer, D. (2014). Mid-ATR-FTIR spectroscopic profiling of HIV/AIDS sera for novel systems diagnostics in global health. *Omics: a journal of integrative biology*, *18*(8), 513-523.

Chapter 4. Effect of phenolic acids from the basic structures of lignin on the growth and metabolism of *Euglena gracilis*.

Abstract: A novel and cost-effective approach to improving lipid productivity without sacrificing microalgae growth was established. Syringic acid (SA) and *p*-coumaric acid (*p*-CA) are two major lignin hydrolysates, widely distributed in the wastewater from downstream industries of lignin. In this study, their potential in regulating the growth and the metabolites biosynthesis of freshwater microalgae *Euglena gracilis* was investigated. The results revealed that the cell growth was increased by 1.63 and 1.93 times at the optimal dosage of 0.5 $g \cdot L^{-1}$ SA and 0.3 $g \cdot L^{-1}$ *p*-CA, respectively. Cell morphology also varied under the two phenolic acids, reflecting the changes in cellular physiological status. Moreover, increased chlorophyll a content was only observed under *p*-CA treatment, indicating the influence of these compounds on photosynthesis were different. Fourier-transform infrared spectroscopy analysis followed by multivariate analysis revealed that the lipid biosynthesis was improved under both phenolic acids, which were favorable to the biofuel production.

Keywords: *Euglena gracilis*; syringic acid; *p*-coumaric acid; lipid; multivariate analysis

4.1 Introduction

Microalgae are photosynthetic microorganisms growing in various aquatic habitats, such as freshwater, marine and sediments, and their photosynthetic efficiency is much higher than that of terrestrial plants [1]. By virtue of occupying no arable lands, fast growth cycle, high output per unit of area, and good adaptability to extreme environments, microalgae have been identified as adequate feedstock for the mitigation of resource and energy crisis and sustainable economic growth [2]. *Euglena gracilis* is one of the most commercially successful freshwater microalgae, as it is a rich source of valuable products such as amino acids, paramylon, carotenoids, ascorbic acid, α-tocopherol and polyunsaturated fatty acids. Thus its potentials in food, feed, nutraceuticals, pharmaceuticals, and cosmetics industries have been highly exploited [3]. Meanwhile, considerable interests in *E. gracilis* as a novel and renewable feedstock for biofuel and biodiesel production have been aroused due to its high lipid biosynthesis efficiency and positive

environment impact [4]. However, there are still many bottlenecks of the commercialization that require to overcome in the large-scale promotion of *E. gracilis* based biofuels. At present, high energy consumption and high production costs are still the main constraints on the development of microalgae biofuels [5]. Thus, developing new technologies and selecting proper culturing conditions to increase the biomass and lipid yield has become an urgent topic.

In general, nutrient starvation and stress is considered as a valid strategy to increase the lipid productivity of microalgae cells, since the carbon flux will shift to the biosynthesis of neutral lipids (mainly triacylglycerols) under adverse culture conditions [6]. However, the ensuing loss of growth due to nutrient deficiency will hinder the feasibility of this strategy for biofuel production, because the decrease in cell growth will reduce the total productivity of lipids [7]. On the other hand, the supplementation of exogenous carbon sources in microalgae cultivation will also favor the lipid biosynthesis since it can increase the carbon supply thus elevate the availability of pyruvates. Although this method realizes the simultaneous production of microalgae biomass and lipids, the supply of a large amount of organic carbon sources will inevitably cause a marked increase in cost, and is not conducive to large-scale outdoor cultivation since it is prone to cause the eutrophication and bacterial contamination in water bodies [8]. Another efficient approach to increasing lipid productivity of microalgae without the sacrifice of cell growth is to introduce phytohormones during the growth process. Phytohormones are chemical messengers which coordinate plant cell growth and development, including embryogenesis, regulation of organ size, pathogen defense, stress tolerance and reproductive development, and their regulatory effects on growth and metabolism have also been observed within microalgae [9]. For example, Park et al. discovered indole-3-acetic acid (IAA), gibberellic acid, kinetin, 1-triacontanol, and abscisic acid were able to remarkably promote the growth and biofuel production of *Chlamydomonas reinhardtii* [10]. However, the high cost of commercial phytohormones is still a limiting factor for large-scale promotion.

The production of microalgae biomass and biofuels by recycling active ingredients from abandoned biomass has been proposed as a novel, eco-friendly and cost-effective method. According to previous report [11], the application of wastewater from the monosodium glutamate

factory to cultivate *Spirulina subsalsa* significantly promoted the accumulation of algal biomass and increased the lipid production, thereby saving costs in the wastewater treatment and creating economic benefits from the production of algal biomass. In addition, lignosulfonate, the major by-product of pulping waste liquor, has also been found able to enhance the biomass yield and lipid accumulation of *E. gracilis*, possibly through its phenolic monomers [12]. These phenolic substances are widely distributed in the waste stream of downstream industries such as petroleum refining, petrochemical, coking, pulp, pharmaceutical, tanning, etc., and have become one of the main environmental burdens, posing a great threat to human health and aquatic ecosystem [13]. But on the other hand, it has also been reported that some phenolic substances such as ferulic acid, vanillic acid and protocatechuic acid have allelopathic effects, and can work as defensive compounds in certain plants to resist a variety of abiotic stresses [14]. If the phenolic substances in these waste streams can be applied to the cultivation of microalgae and the production of biofuels, it can meet the dual demands of microalgae biomass production and positive impact on the environment. In previous reports, Pinto et al. discovered that two phenol-resistant microalgae, *Ankistrodesmus braunii* and *Scenedesmus quadricauda*, could be employed to treat the wastewater of olive oil plant and 50% of low-molecular-weight phenolics were removed [15]. Similarly, *Haematococcus pluvialis* has also been reported to be able to convert these exogenous phenylpropanoids into a series of vanilla-flavored products, which further demonstrates that some microalgae can utilize and degrade these phenolic compounds [16]. However, up till now, there have been few studies on the effect of phenolic substances on the biochemical synthesis of microalgae, especially on lipid synthesis. Therefore, it is necessary to evaluate the influence of these phenolic compounds on the growth and biochemical composition of *E. gracilis*, which will not only help to better deal with the treatment of phenolic wastewater but also lead to the commercially successful microalgae cultivation for biofuel production. Syringic acid (SA) and *p*-coumaric acid (*p*-CA) are the two major phenolic substances in wastewater from downstream industries of lignin, which have a variety of physiological activities, such as antioxidant, antibacterial, anti-tumor and anti-diabetic [14,17]. However, there is little research on the effects of SA and *p*-CA on the growth and biochemical synthesis of *E. gracilis*. Therefore, this study

aimed to evaluate the effects of SA and *p*-CA, as the predominant phenolic derivatives in waste streams, on the physiological and biochemical parameters of *E. gracilis*.

In this research, the changes in cell density, dry biomass weight, cell morphology, and carbon allocation of macromolecular pools of *E. gracilis* under two phenolic acid treatments were investigated, and the potential and feasibility of SA and *p*-CA in microalgae and lipid production were evaluated. In addition, the changes in the metabolic patterns of microalgae were investigated by Fourier transform infrared spectroscopy and multivariate analysis, providing a basis for understanding the accumulation of high-value added bioproducts.

4.2 Materials and methods

4.2.1 Microalga and culture conditions

The strain of *Euglena gracilis* Klebs (NIES-48) was provided by the National Institute for Environmental Studies of Japan. The algal cells were aseptically sub-cultured in CM medium with a cycle of one month for further use [18]. The stock solutions of SA and *p*-CA were prepared using fresh CM medium based on their solubility, and the sterilization was operated by the sterile single-use vacuum filter with a 0.45 μm pore size (Nalgene, Thermo Fisher Scientific, US). For cell inoculation, the algal cells at the exponential growth phase with the volume of 10 mL were transferred into the Erlenmeyer flask with fresh medium, and different proportions of phenolic acid stock solutions were diluted and mixed, making up the final culture volume to 100 mL. Concentrations of SA and *p*-CA treatment groups were set at 0, 0.05, 0.1, 0.3 and 0.5 $g \cdot L^{-1}$. Microalgae experimental groups were cultured at 25 ºC, and illuminated at the light intensity of 5000 lx with a light/dark cycle of 12h L/12h D, using the cool-white fluorescent lamps. The cultivation for each treatment was operated in triplicate, and shaken manually three times per day to avoid the attachment of cells to the bottle walls.

4.2.2 Cell growth parameters

Cell growth parameters including cell density and optical density were periodically measured. Cell density was counted under the optical microscope with a Thoma hemocytometer (Hirschmann, Germany). For optical density, 4 mL of cell suspension was withdrawn and centrifuged at 8000 rpm for 5 min to remove the supernatant. The cell pellets were rinsed with

distilled water to eliminate the effect of media compositions, and re-suspended with distilled water to 4 mL for optical density determination at 680 nm. In addition to the periodical measurement of cell density, cell biomass yield was also determined at the end of cultivation by cell dry weight. The harvested cells after rinsing were transferred to pre-weighed glass bottles and then dried at 105 ºC for 2 h, and the dry weight was obtained by calculating the weight difference of the glass bottles with and without the algal cells.

4.2.3 Variation of pH and conductivity during the cultivation

The pH and electricity conductivity (EC) of the media were important indicators reflecting some of the key changes in status of cell physiology and metabolism. To ascertain the variation in pH and EC, 1 mL of cell suspension was centrifuged at 8000 rpm for 5 min, and the supernatant was taken for pH and EC analyses. The pH was ascertained by compact pH meter (LAQUAtwin B-712, Horiba, Japan), and the EC was determined by the pocket electrical conductivity meter (LAQUAtwin EC-33, Horiba, Japan).

4.2.4 Quantification of changes in cell morphology

E. gracilis cells could changes their morphologies (spherical, elongated and spindled shapes) due to the lack of rigid cellulose walls, in response to the changes of a cascade of factors such as biological clock, cell cycle, photosynthesis, respiration and external environment conditions [19]. To quantify the morphological variation of *E. gracilis* cells resulted from different treatments, images of 150 cells for each group were recorded by the Motic Image Plus 2.2S software (Shimadzu, Japan) under the microscope, and aspect ratio (ratio of the maximum to the minimum Feret diameter) was determined by the particle shape analysis through ImageJ v1.8.0 (Java based open source software).

4.2.5 Photosynthetic pigment analysis

Photosynthetic pigment content was detected according to the modified method of Lichtenthaler and Wellburn [20]. The algal cells were harvested by the filtration of 10 mL of cell suspension through the filter paper with a pore diameter of 0.45 μm. After rinsing with distilled water to remove the remained salts, the cells were transferred to the mortar and 80% (v/v) acetone was added as the solvent. The mixture was ground with glass sands until the pigments were

completely extracted. The homogenate was filtered again, and the extract was combined to a volumetric flask and diluted to 10 mL using 80% (v/v) acetone. The amounts of chlorophyll a (Chl_a), chlorophyll b (Chl_b) and carotenoids (C_{x+c}) were determined by the absorbances (Abs) at the wavelength of 470, 645, and 663 nm with a UV-vis spectrophotometer, in accordance with the Eqs. (1-3). The ratio of chlorophyll a to chlorphyll b, and the ratio of chlorophyll a to carotenoids were also calculated to evaluate the photosynthetic properties of *E. gracilis* cells.

$$Chl_a = 12.21Abs_{663} - 2.81Abs_{646} \quad (1)$$

$$Chl_b = 20.13Abs_{646} - 5.03Abs_{663} \quad (2)$$

$$C_{x+c} = (1000Abs_{470} - 3.27Chl_a - 104Chl_b)/229 \quad (3)$$

4.2.6 Cell composition analyzed by FT-IR analysis

Fourier Transform Infrared (FT-IR) spectroscopy, as an emerging and robust approach, was employed to analyze the changes in major macromolecule pools within the cells. Samples preparation process was following the previous reports with slight modification [21,22]. Microalgal cells were harvested by centrifugation at the speed of 5000 rpm for 15 min, and then rinsed with distilled water for 5 times until the media composition was completely removed. The obtained cells were quickly frozen using the liquild nitrogen, and then immediately transferred to the vacuum freeze dryer (EYELA, FDU-1200, Japan). After drying at -50 ºC for 24 h, the samples were ground with potassium bromide (KBr) at a weight ratio of 1:100, until the cells were completely broken and evenly dispersed in the Kbr powder. The mixture was pressed in to thin pellets by the hand-press for FT-IR analysis. FT-IR spectra of samples at the range of 4000-400 cm^{-1} were acquired with 32 scans at a spectral resolution of 4 cm^{-1} by FT-IR spectroscopy (iZ10, Thermo Fisher Scientific, US). Each sample was analyzed in triplicate and a total of 9 replicate spectra were obtained for each treatment (n=9). Spectrum of Kbr was collected as the background, and all the spectra were baseline and atmosphere corrected using the algorithms of OMNIC software (Thermo Fisher Scientific, US). To simplify the spectral information, the spectra were narrowed to the fingerprint region of 1800-1000 cm^{-1} which contained the key bands of macromolecules. Normalization to the amide I band at 1657 cm^{-1} was achieved to eliminate the difference of deposit thickness. To further analyze the changes in cell composition with different

treatments, relative content of carbohydrate and lipid were calculated by the peak height ratios of carbohydrate/amide I and lipid/amide I, respectively [21,22,23].

4.2.7 Differentiation of metabolites by multivariate analysis

The normalized spectra were imported into SMICA-P software (ver.13, Umetrics, Sweden) for principle component analysis (PCA) and orthogonal partial least squares discriminant analysis (OPLS-DA). PCA is a common method for data simplification and exploratory analysis of high dimensional data sets. Since different phenolic acid treatments would lead to a cascade of changes in metabolites bio-synthesis, PCA was employed to further discriminate the subtle differences in metabolic patterns. Furthermore, supervised orthogonal partial least squares discriminant analysis (OPLS-DA) was also operated for the rapid comparison of metabolic fingerprints and observation of discrete trends between different samples.

4.2.8 Statistical analysis

The data were processed by statistical analysis software SPSS (ver.16, IBM, USA) and finally expressed in mean ± standard deviation (SD). One-way analysis of variance (ANOVA) combined with post hoc Dunnett's test were used to analyze the differences in the parameters between different treatment groups at a significance level of 95%.

4.3 Results and discussion

4.3.1 Growth promotion of E. gracilis by SA and p-CA

Positive effects of SA and *p*-CA on the growth of *E. gracilis* cells were both observed, and the cell density was notably increased by these two phenolic acids in concentration dependent manners. The results were illustrated in Fig. 4-1. For SA treatment, cell density at the optimal dosage of 0.5 $g \cdot L^{-1}$ was increased by 1.63 folds, indicating the SA could be utilized as an effective growth promotor for *E. gracilis*. Result of *p*-CA treatment was similar to that of SA, and cell density at 0.3 $g \cdot L^{-1}$ *p*-CA treatment was increased by 1.93 folds over the control. The promotion effect weakened when the *p*-CA concentration continued to increase to 0.5 $g \cdot L^{-1}$, but the cell density was still much higher than that of the control. The optical density result was consistent with the cell density, suggesting that the dosage used for microalgae cultivation was crucial to the promotion effect. Dry cell weight were further analyzed and the results were illustrated in Fig. 4-

2. At the optimal dosage of 0.5 g·L^{-1} SA and 0.3 g·L^{-1} *p*-CA, the biomass yield was enhanced by 1.70 and 1.69 times over the control, respectively.

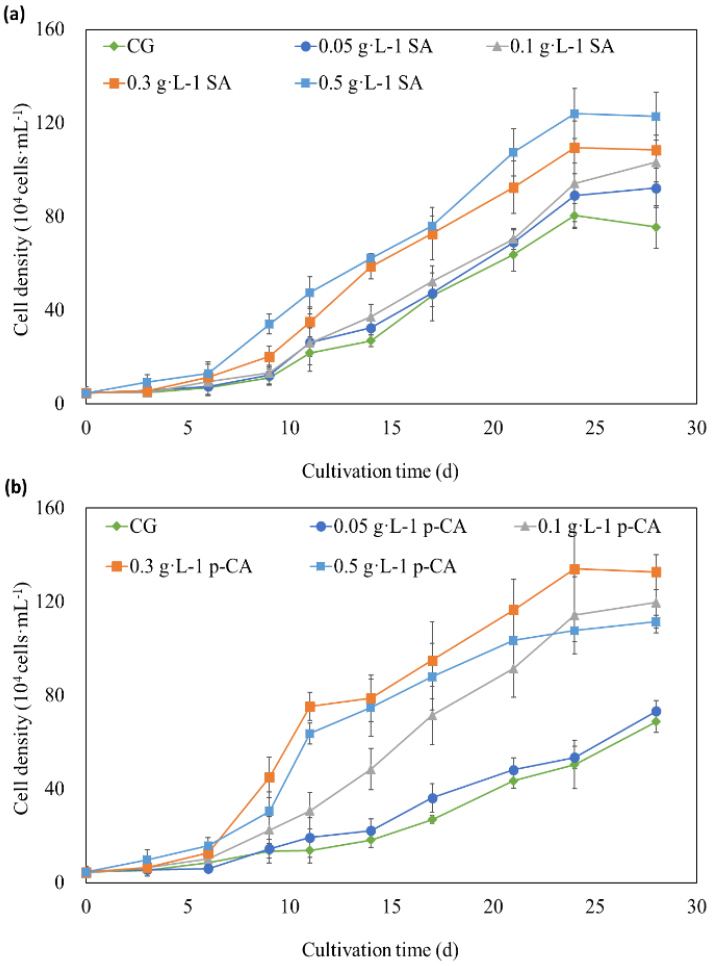

Fig. 4-1. Growth curves of microalgal cells cultured under different concentrations of SA and *p*-CA. Error bars represent the SD, and CG denotes the control group. (a): growth curves under SA treatments; (b): growth curves under *p*-CA treatments.

Effects of *E. gracilis* growth on the pH and EC of the media were investigated as well. SA and *p*-CA both resulted in a decline in the initial pH of the media, and at the concentration of 0.5 g·L^{-1} SA and *p*-CA, pH dropped from 6.9 of the control group to 6.5. In addition, accompanied by the rapid proliferation of cells, pH of the media also decreased during the cultivation, which mainly due to the increase of carbonate and bicarbonate ions (carbon dioxide). The decrements of pH in higher concentrations (0.3 and 0.5 g·L^{-1}) of SA and *p*-CA treatment groups were larger than that in the control group, indirectly demonstrated the algal growth in these groups was

improved. The EC reflected the concentration of dissolved ions in the media, and it was observed that the EC of the media also decreased over time, which was mainly due to the absorption of nutrients ions by the algae cells. However, the treatments of phenolic acids with different concentrations appeared to have no marked effects on the EC of the media.

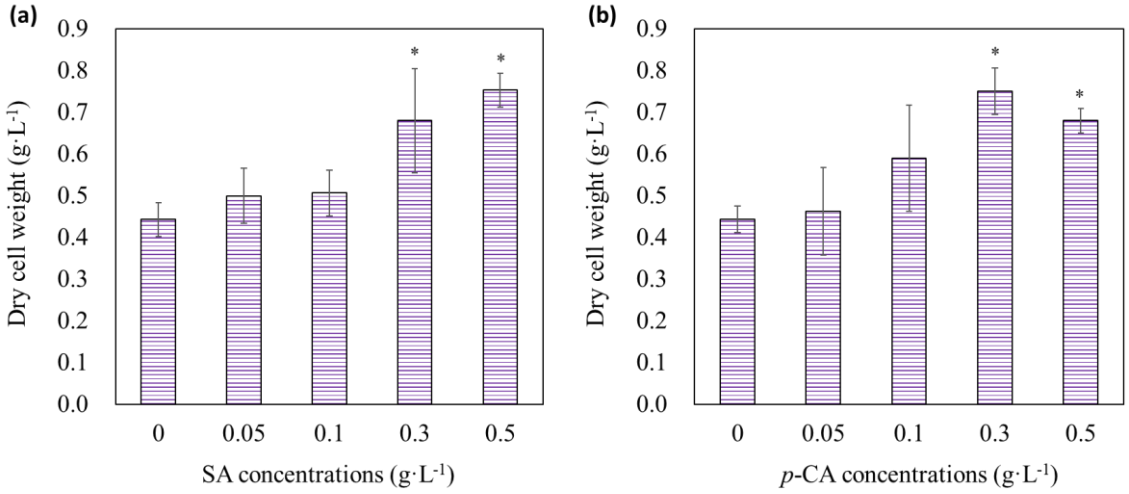

Fig. 4-2. Dry biomass of algal cells treated under different concentrations of SA and *p*-CA. Error bars represent the SD with three replicates, and the asterisk represents a significant difference between the treatment and control group. (a): dry biomass under SA; (b): dry biomass under *p*-CA.

This is the first report that SA and *p*-CA can be utilized as the elicitors for *E. gracilis* growth. In the previous research [24,25], a cascade of shikimate pathway produced phenols were considered as inhibitors for microalgae growth. Nakai et al. investigated the inhibitory effects and inducement modes of 11 plant-produced phenols on the growth of algae, including SA and *p*-CA used in this experiment [25]. The result revealed that SA had an extremely significant inhibitory effect on the blue-green algae *Microcystis aeruginosa*, but it was not observed with *p*-CA. This was mainly due to the difference in the structure of these two phenolic acids, makes SA more prone to auto-oxidation than *p*-CA. However, no adverse effects of SA and *p*-CA on the growth of *E. gracilis* were observed in this study. On the contrary, both treatments showed extremely high growth promotion effects, which was mainly due to the difference in algae species. In addition, the optimal pH environment for *M. aeruginosa* is alkaline [26], and phenolic acids may be affected in this condition and generate some toxic substances such as quinones, while *E. gracilis*

has a wider survival pH range (4.0-8.0), able to adjust the internal pH of the cells to adapt to a variety of environments [27]. Thus, the species of algae are vital to the utilization of phenols, and different microalgae have different tolerances to the same phenolic substances. The growth promotion effect of SA and *p*-CA on the growth of *E. gracilis* might be mainly attributed to the physiological roles similar to phytohormones, which affected the growth, survival and reproduction of algae cells by affecting their endogenous plant hormone levels such as auxin, cytokinin, and gibberellin. It was reported that phenylpropanoids were able to affect the biosynthesis of L-tryptophan and its conversion to IAA [28], which is a type of auxin that can regulate the microalgal growth. In addition, the metabolic evidence for the auxin-phenols balance has been demonstrated by some studies, and the regulation of endogenous auxin levels by phenolic compounds is in a concentration-dependent manner [29,30]. At low concentrations, these phenolic compounds can synergize auxin, and protect the IAA from decarboxylation through a competitive mechanism, but at high concentrations, they will become the co-factors for IAA degradation [29]. This maybe the reason why the promotion effect weakened as the concentration of *p*-CA increased. Moreover, in higher plants, phenolic substances also have a positive impact on the gibberellin-mediated physiological mechanism and cytokinin synthesis, which indirectly influences the growth of plants. The growth regulatory effect of SA and *p*-CA on higher plants have also been widely discovered [31]. Since the cellular response of microalgae is similar to that of higher plants, growth promotion effects of *E. gracilis* by SA and *p*-CA are supposed to be closely related to the regulation of endogenous phytohormones levels, which still requires further biological evidence.

4.3.2 Morphological variation under SA and p-CA treatments

The cell morphology of *E. gracilis* is an important indicator reflecting the cellular physiological status, since it can exhibit various cell morphologies when exposed to different external environments, including spherical, spindled and elongated shapes [19]. Therefore, the cell morphologies treated with different concentrations of phenolic acids were quantified by the cell aspect ratio, and the results were illustrated in Fig. 4-3. The aspect ratio of the cells in the control group without any treatment was in the range of 1.1-2.7, which was between spherical

and spindled shapes. But as the concentration of SA increased, more elongated cells appeared. The median value of the cell aspect ratio rose from 1.8 of the control to 2.2 of 0.3 $g \cdot L^{-1}$ SA treatment group, and 25% of the cells had an aspect ratio in the range of 2.6 to 3.7 which was much larger than that of the control group. However, inconsistent with the trend of cell growth, when the concentration of SA increased to 0.5 $g \cdot L^{-1}$, the cell aspect ratio started to decrease. This might be related to the darkening of the media under SA treatments, which hindered the photosynthesis of the cells, resulting in a lower cell aspect ratio [32]. Similar changes in cell morphology were found under *p*-CA treatment, and more elongated cells were observed in 0.3 $g \cdot L^{-1}$ treatment group. Although the cell aspect ratio also declined in 0.5 $g \cdot L^{-1}$ p-CA treatment, this was consistent with the growth trend of *p*-CA treatment. In view of the fact that the color of the medium did not change under *p*-CA treatment, the decrease in cell aspect ratio at 0.5 $g \cdot L^{-1}$ might be due to the weakening of the growth promotion effect. In general, *E. gracilis* cells under stress will exhibit spherical shapes with a reduced cell viability, while cells at more active physiological status tend to be elongated shapes which is more conducive to the cell swimming, and their photosynthesis and respiration are more active [19,32]. In view of this, it is necessary to further characterize the intracellular photosynthetic pigments of *E. gracilis*. The notable increase in cell aspect ratio under both SA and *p*-CA treatments indicated that cell viability were greatly enhanced under these two phenolic acids, which was consistent with the improvement in cell growth.

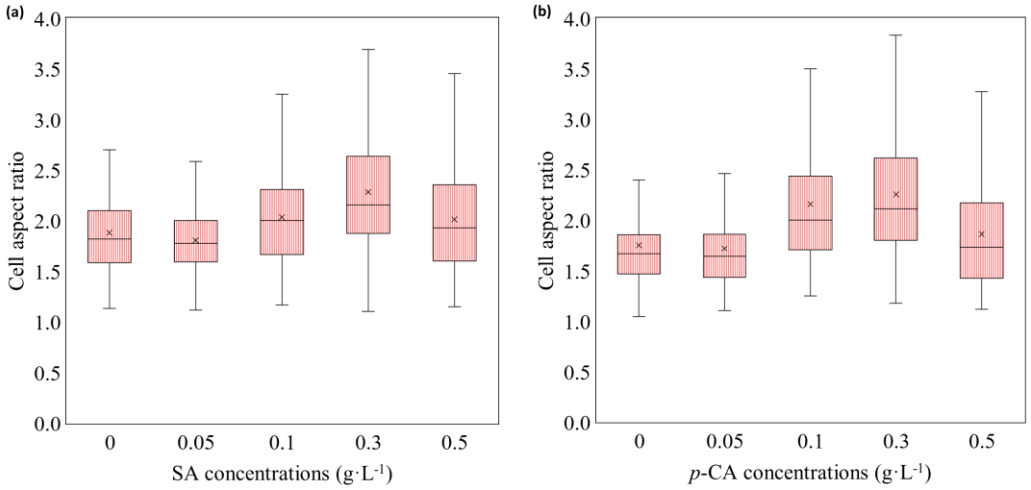

Fig. 4-3. Boxplots of cell aspect ratio of *E. gracilis* cultured under different concentrations of

SA and *p*-CA. (a): cell aspect ratio under SA treatments; (b): cell aspect ratio under *p*-CA treatments. The upper and lower boundaries of the box-shaped bars represent the third quartile (75%) and the first quartile (25%) of the cell aspect ratio distribution interval, and the horizontal line in the middle of the box represents the median value; The whiskers represent the maximum and minimum values (excluding outliers), and the asterisk represents the mean value.

4.3.3 Impact on photosynthetic pigments content

The changes in the yield and ratio of photosynthetic pigments under different concentrations of SA and *p*-CA were further analyzed, and the results were shown in Fig. 4-4. The yield of Chlorophyll a was increased with SA concentration, and the highest yield was achieved under the treatment of 0.3 $g \cdot L^{-1}$ SA. However, when the concentration of SA increased to 0.5 $g \cdot L^{-1}$, the production of chlorophyll a decreased, showing a variation trend similar to the cell morphology. In addition, the yield of chlorophyll b and carotenoids also increased notably, indicating that SA has a promotion effect on the accumulation of photosynthetic pigments. To further understand the changes in photosynthesis capacity and physiological state of algal cells under phenolic acid treatment, the ratio of chlorophyll a to chlorophyll b, and the ratio of chlorophyll a to carotenoids were analyzed. The former could reflect the capacities of light capture and dark adaptation of the algae cells, and the latter could reflect the physiological status of the cells [33]. The Fig. 4-4(b) illustrated that the ratio of chlorophyll a to chlorophyll b continued to decrease as the SA concentration increased, indicating the increase in the ratio of photosystem II to photosystem I [34]. The increase of chlorophyll b relative to chlorophyll a also implied that the wavelength range of light absorption by chloroplasts increased, which usually occurred in shade-adapted plants [34]. Therefore, the decrease in the ratio of chlorophyll a to chlorophyll b was mainly due to the shading effect of SA, which is a manifestation of the dark adaptation of algal cells. In addition, the decrease in the ratio of chlorophyll a to carotenoids was only observed at 0.5 $g \cdot L^{-1}$ SA treatment, and it was mainly caused by the decrease in chlorophyll a content.

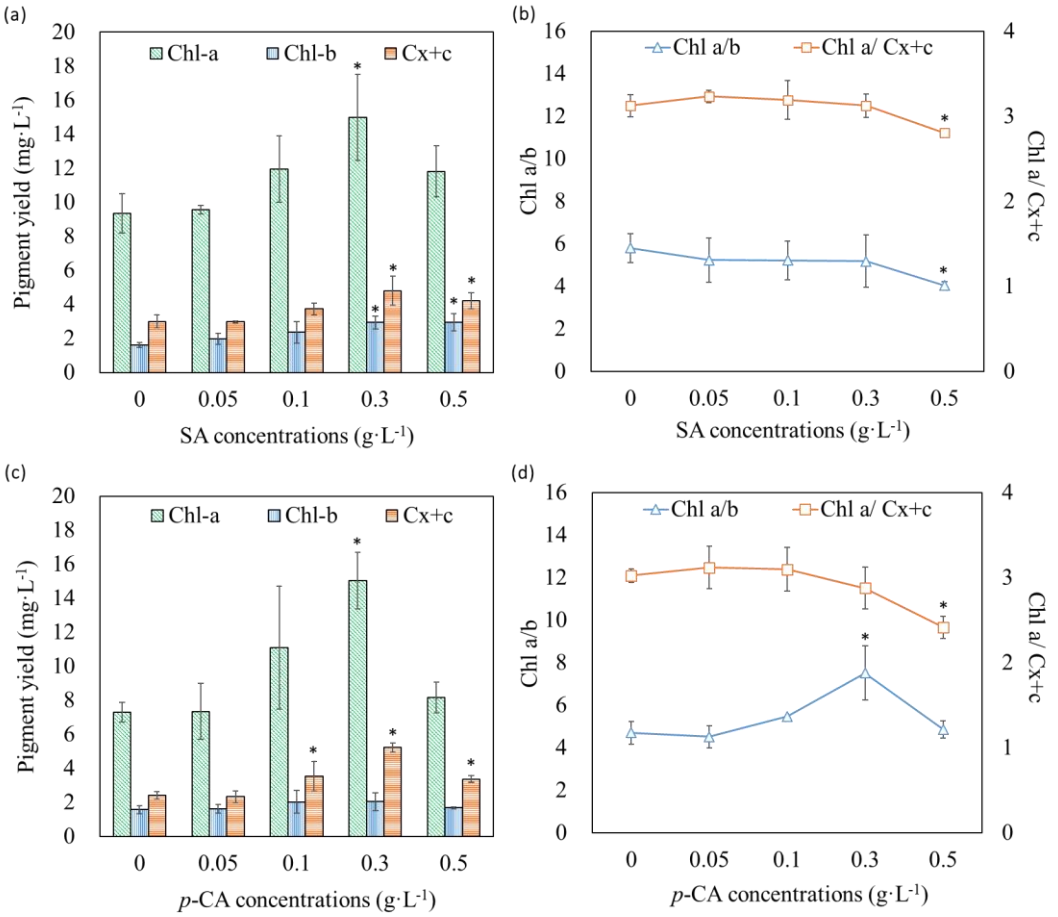

Fig. 4-4. Pigment yield and ratios under different concentrations of SA and *p*-CA. (a), (c): Pigment yield under SA and *p*-CA treatments, respectively; (b), (d): pigment ratios (ratio of chlorophyll a to chlorophyll b; ratio of chlorophyll a to carotenoids) under SA and *p*-CA treatments, respectively. Error bars represent the SD with three replicates, and the asterisk represents a significant difference between the treatment and control group.

The yield of photosynthetic pigments were also remarkably improved by the treatment of *p*-CA. At the optimal dosage of 0.3 $g \cdot L^{-1}$, the yields of chlorophyll a, chlorophyll b and carotenoids were increased by 2.06, 1.31, and 2.16 folds over the control group, respectively. Unlike the SA treatment, the ratio of chlorophyll a to chlorophyll b increased with the *p*-CA concentration, indicating an enhanced capacity of light utilization. As *p*-CA concentration increased to 0.5 $g \cdot L^{-1}$, the ratio returned to the normal level in the control group, which was consistent with the changes in the algal growth under *p*-CA treatment. On the contrary, the ratio of chlorophyll a to carotenoids

decreased notably, which was mainly due to the increase in carotenoids content. In general, chlorophylls are the primary electron donors in the electron transport chain, while carotenoids are the auxiliary pigment which can protect the photosynthetic apparatus by energy dissipation through non-photochemical quenching [35]. Furthermore, the biosynthesis of carotenoids in microalgae cells has identical environmental clues to the inducement of synthesis of triacylglycerols [36], which implies the application potential of phenolic compounds in the accumulation of lipids and carotenoids. Therefore, it is necessary to further analyze the changes in the macromolecules pools in microalgae cells.

4.3.4 Relative content of carbohydrate and lipid

The biochemical composition of *E. gracilis* cells under the treatment of phenolic acids were analyzed by the FT-IR spectroscopy. According to previous reports and literature [21,22,23], major macromolecules, including carbohydrates, lipids, proteins and phosphorylated molecules were well identified in the "fingerprint region" ($1800cm^{-1}$-$1000cm^{-1}$) of the FT-IR spectra. As seen from the spectra, the SA and *p*-CA treated samples had higher absorbance at the band (1734 cm^{-1}) associated with the υ(C=O) stretching vibration of fatty acids over the control samples, while the two phenolic acids exhibited different influences on the band (1078 cm^{-1}) related to the υ(COC) vibration of polysaccharides, which indicated the difference in the biosynthesis of major macromolecules in *E. gracilis* by SA and *p*-CA.

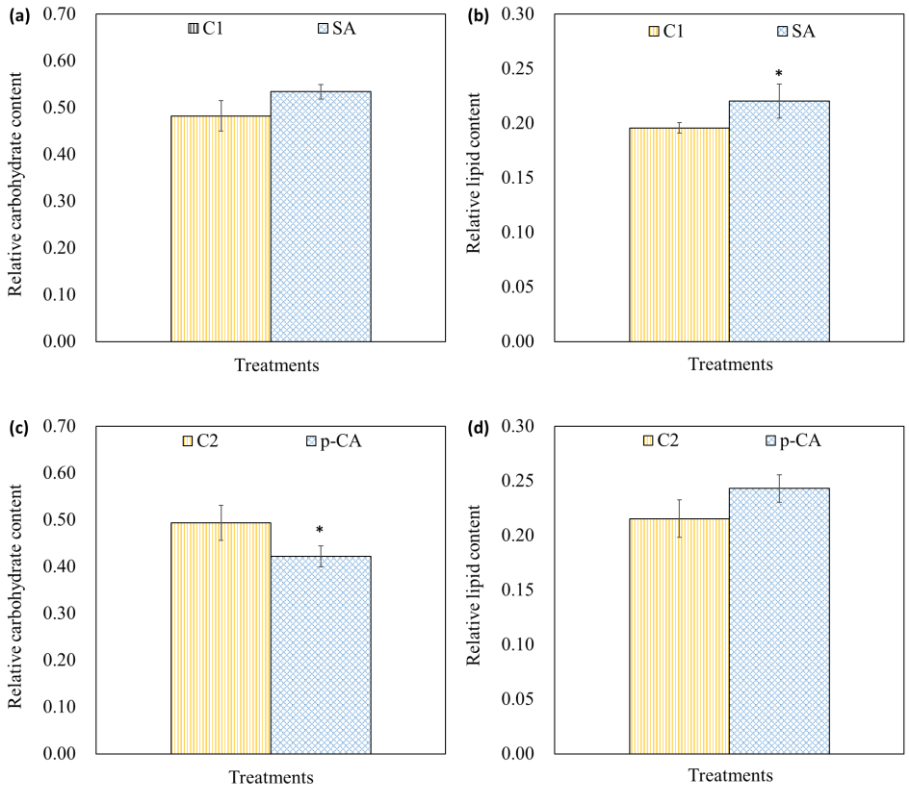

Fig. 4-5. Relative content of carbohydrate and lipid at the optimal dosage of SA and *p*-CA. C1 and C2 are the control group for each independent experiment, and the optimal dosages for SA and *p*-CA are 0.5 $g \cdot L^{-1}$ and 0.3 $g \cdot L^{-1}$, respectively. Error bars represent the SD with nine replicates, and the asterisk represents a significant difference between the treatment and control group.

To understand the specific changes in the cellular biochemical composition under the exposure of phenolic acids, the relative content of carbohydrate and lipid were further compared, and the results were shown in Fig. 4-5. Compared with the control group, the intracellular carbohydrate and lipid content at 0.5 $g \cdot L^{-1}$ SA increased by 10.75% and 12.58%, respectively. Since the cell density also increased remarkably under the SA treatment, it suggested that the final production of carbohydrate and lipid in *E. gracilis* would be greatly enhanced. Similar result was also observed in the previous research. Tam et al. reported that ferulic acid extracted from rice bran could simultaneously increase the accumulation of carbohydrate and lipid in *Nannochloropsis oculata*, but at the expense of protein content [37]. SA might have a similar role

as ferulic acid in the regulation of metabolites in *E. gracilis*, which could contribute to the production of high value-added metabolites. Different from the influence of SA, *p*-CA at the optimal concentration of 0.3 $g \cdot L^{-1}$ significantly decreased the carbohydrate content by 14.46%, but increased the accumulation of intracellular lipids by 12.83%. It is reasonable because carbohydrate and lipid, as both energy stores in microalgae cells, share the same precursors such as pyruvate and triacylglycerol, and can be converted into each other in response to different external environments [6]. Based on the different results obtained from SA and *p*-CA, it can be inferred that different phenolic compounds determine different biosynthetic pathways and the flow of carbon to metabolites in microalgae cells, but it is consistent that both SA and *p*-CA treatments can significantly increase the lipid production of *E. gracilis* cells. Unlike the traditional methods that promote lipid biosynthesis through nitrogen starvation and abiotic stress, SA and *p*-CA treatments will not sacrifice microalgae growth, and the accumulation of biomass and lipids can be achieved simultaneously, which will favor the large-scale commercial production of biofuels from *E. gracilis*.

4.3.5 Multivariate analysis

The FT-IR spectra were further analyzed by unsupervised PCA and supervised OPLS-DA models to obtain complete available information about the metabolic patterns of *E. gracilis* cells before and after different phenolic acid treatments. First, the spectra of algae cells under SA treatment was characterized, and the PCA scores plot was shown in Fig. 4-6(a). The distribution of datasets from the control and SA-treated samples was very concentrated, suggesting that the difference was not well distinguished [38]. To better visualize the differentiation of datasets between samples, the metabolic profiles of the control and SA treatment groups were evaluated through a supervised OPLS-DA model. The two groups were clearly separated in the OPLS-DA scores plot with good parallelism, indicating that SA induced significant biochemical changes in the physiological metabolism of *E. gracilis*. One major component and four orthogonal components were resolved from the model, and the cumulative contribution rate R^2X was 0.996. The loading plot of the major predictive component (explained 46.4% of the total variation) was employed to determine the characteristic metabolites under different treatments. Generally, the

treatment group located in the positive direction of the scores plot has more prominent metabolites assigned by these bands with positive loadings (in the loading plot), and vice versa [39]. Therefore, Fig. 4-6(c) illustrated that the protein content was more prominent in the control group, since the band at 1651cm^{-1} was located in the negative direction of the loading plot, where this band was associated with the υ(C=O) vibration from the amide I of the proteins. The content of many other metabolites including lipids (1757 cm^{-1}), carboxylates (1408 cm^{-1}), phosphorylated molecules (1252 cm^{-1}) and carbohydrates (1155, 1109, 1080 and 1051 cm^{-1}) were more prominent in the SA-treated samples. This result was consistent with the previous quantification of carbohydrate and lipid content (Fig. 4-5), indicating the reliability of the models.

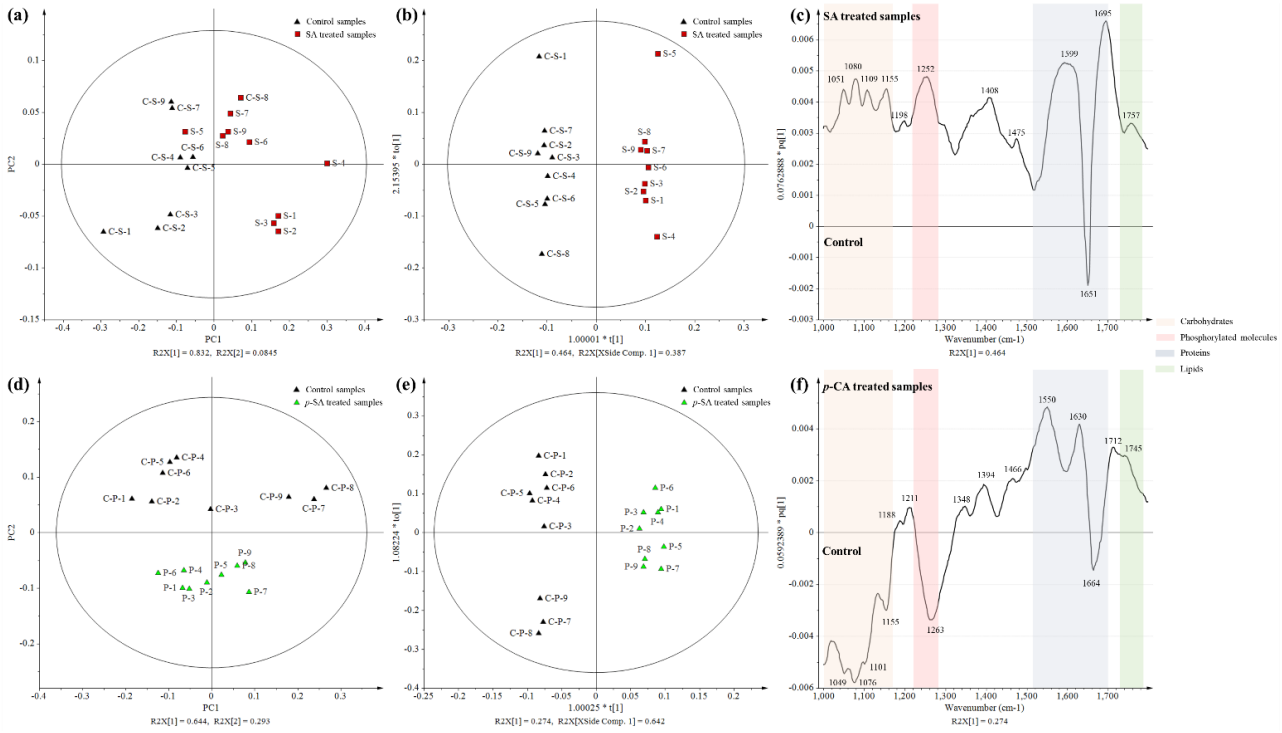

Fig. 4-6. PCA and OPLS-DA scores plots (left and middle) and loading plots (right) of the *E. gracilis* cell samples with different treatments. (a): PCA scores plot of samples with and without SA treatment ($R^2X = 0.969$, $Q^2(cum) = 0.942$); (b): OPLS-DA scores plot of samples with and without SA treatment ($R^2X = 0.996$, $R^2Y = 0.991$, $Q^2(cum) = 0.972$); (c): OPLS-DA loading plot of samples with and without SA treatment ($R^2X1 = 0.464$); (d): PCA scores plot of samples with and without *p*-CA treatment ($R^2X = 0.973$, $Q^2(cum) = 0.955$); (e): OPLS-DA scores plot of samples with and without *p*-CA treatment ($R^2X = 0.948$, $R^2Y = 0.983$, $Q^2(cum) = 0.962$); (f):

OPLS-DA loading plot of samples with and without *p*-CA treatment ($R^2X1 = 0.274$). In the OPLS-DA loading plot, the bands in light orange, red, grey and green regions were associated with carbohydrates, phosphorylated molecules, proteins and lipids, respectively. The bands with the positive loadings indicate the content of assigned metabolites are higher in the group with positive scores, and vice versa.

The PCA and OPLS-DA models were also established for the differentiation of metabolic patterns from algae cell samples with and without *p*-CA treatments. As seen from Fig. 4-6(d), the control and *p*-CA treatment groups were clearly separated in the PCA scores plot, and PC1 and PC2 accounted for 64.4% and 29.3% of the total variation, respectively. The separation between these two groups were mainly in the PC2 direction. The characteristic metabolites of *p*-CA treatment were further analyzed, and the scores plot and loading plot of OPLS-DA were obtained. A total of one predictive component and two orthogonal components were resolved from the data. The cumulative contribution rate R^2X was 0.948, and Q^2 was 0.962, indicating that the OPLS-DA model was predictable. To avoid overfitting of the models, permutation test with 20 permutations were operated and the result showed the OPLS-DA model was of a good quality. As illustrated in the loading plot, *p*-CA treated samples had more prominent spectral absorbance in the regions of lipids (C=O stretching vibration at 1745 cm^{-1}, and CH_3 and CH_2 bending at 1460 cm^{-1}), carboxylates (COO^- antisymmetric stretching at 1630 cm^{-1}), amide II (N-H bending and C-N stretching vibration at 1550 cm^{-1}), sulfate (S=O stretching at 1394 and 1348 cm^{-1}) and ethers (C-O stretching at 1211cm^{-1}), while less prominent spectral absorbance in the regions of amide I (C=O vibration at 1664 cm^{-1}), phosphorylated molecules (PO_2^- asymmetric vibration at 1263 cm^{-1}) and carbohydrates (C-O-C of glycosidic bonds and C-OH side groups at 1155, 1101, 1076 and 1049 cm^{-1}). This was consistent with the previous results shown in Fig. 4-5(c) and (d). The *p*-CA treatment increased the accumulation of intracellular lipids in *E. gracilis*, but diminished the carbohydrate content. FT-IR spectroscopy combined with multivariate analysis not only reflects the variation trend of biological macromolecules, but also reveals the perturbations of other metabolites including some small molecules. Although the determination of specific changes in these metabolites still requires precise analytical techniques, it provides effective evidence for the

rapid evaluation of changes in microalgae metabolism profiles under different phenolic acid treatments, and provides the guidance for the accumulation of high-value-added metabolites in microalgae and biofuel production.

4.4 Conclusion

Supplementation of SA and *p*-CA simultaneously enhanced the biomass and lipid production of *E. gracilis*. At optimum exogenous supply, 0.5 $g \cdot L^{-1}$ SA and 0.3 $g \cdot L^{-1}$ *p*-CA increased the lipid yield by 91.30% and 90.88%, respectively. In addition, morphological variation together with the increase in photosynthetic pigments yield were also observed under phenols treatment. Further research on the utilization of wastewater rich in other phenols to microalgal cultivation will be necessary, for the purpose of relieving the stress of aquatic environments and increasing the production of microalgal biomass and lipids for biofuels.

Reference

[1] Vassilev, S. V., & Vassileva, C. G. (2016). Composition, properties and challenges of algae biomass for biofuel application: an overview. *Fuel*, *181*, 1-33.

[2] Manirafasha, E., Murwanashyaka, T., Ndikubwimana, T., Ahmed, N. R., Liu, J., Lu, Y., ... & Jing, K. (2018). Enhancement of cell growth and phycocyanin production in *Arthrospira (Spirulina) platensis* by metabolic stress and nitrate fed-batch. *Bioresource technology*, *255*, 293-301.

[3] Kottuparambil, S., Thankamony, R. L., & Agusti, S. (2019). Euglena as a potential natural source of value-added metabolites. A review. *Algal Research*, *37*, 154-159.

[4] Khan, M. I., Shin, J. H., & Kim, J. D. (2018). The promising future of microalgae: current status, challenges, and optimization of a sustainable and renewable industry for biofuels, feed, and other products. *Microbial cell factories*, *17*(1), 36.

[5] Su, Y., Song, K., Zhang, P., Su, Y., Cheng, J., & Chen, X. (2017). Progress of microalgae biofuel's commercialization. *Renewable and Sustainable Energy Reviews*, *74*, 402-411.

[6] Sun, H., Ren, Y., Mao, X., Li, X., Zhang, H., Lao, Y., & Chen, F. (2020). Harnessing C/N balance of *Chromochloris zofingiensis* to overcome the potential conflict in microalgal production. *Communications Biology*, *3*(1), 1-13.

[7] Tan, K. W. M., & Lee, Y. K. (2016). The dilemma for lipid productivity in green microalgae: importance of substrate provision in improving oil yield without sacrificing growth. *Biotechnology for biofuels*, *9*(1), 1-14.

[8] Yamane, Y. I., Utsunomiya, T., Watanabe, M., & Sasaki, K. (2001). Biomass production in mixotrophic culture of *Euglena gracilis* under acidic condition and its growth energetics. Biotechnology Letters, 23(15), 1223-1228.

[9] Tarakhovskaya, E. R., Maslov, Y. I., & Shishova, M. F. (2007). Phytohormones in algae. *Russian Journal of Plant Physiology*, *54*(2), 163-170.

[10] Park, W. K., Yoo, G., Moon, M., Kim, C. W., Choi, Y. E., & Yang, J. W. (2013). Phytohormone supplementation significantly increases growth of *Chlamydomonas reinhardtii* cultivated for biodiesel production. *Applied biochemistry and biotechnology*, *171*(5), 1128-1142.

[11] Jiang, L., Pei, H., Hu, W., Ji, Y., Han, L., & Ma, G. (2015). The feasibility of using complex wastewater from a monosodium glutamate factory to cultivate *Spirulina subsalsa* and accumulate biochemical composition. *Bioresource technology*, *180*, 304-310.

[12] Zhu, J., & Wakisaka, M. Application of lignosulfonate as the growth promotor for freshwater microalga *Euglena gracilis* to increase productivity of biomass and lipids. *Fuel*, *283*, 118920.

[13] Tišler, T., & Zagorc-Končan, J. (1997). Comparative assessment of toxicity of phenol, formaldehyde, and industrial wastewater to aquatic organisms. *Water, Air, and Soil Pollution*, *97*(3-4), 315-322.

[14] Esakkimuthu, S., Krishnamurthy, V., Wang, S., Hu, X., Swaminathan, K., & Abomohra, A. E. F. (2020). Application of p-coumaric acid for extraordinary lipid production in *Tetradesmus obliquus*: A sustainable approach towards enhanced biodiesel production. *Renewable Energy*. 2020;157: 368-376.

[15] Pinto, G., Pollio, A., Previtera, L., Stanzione, M., & Temussi, F. (2003). Removal of low molecular weight phenols from olive oil mill wastewater using microalgae. *Biotechnology Letters*, *25*(19), 1657-1659.

[16] Tripathi, U., Rao, S. R., & Ravishankar, G. A. (2002). Biotransformation of phenylpropanoid

compounds to vanilla flavor metabolites in cultures of *Haematococcus pluvialis*. *Process Biochemistry*, *38*(3), 419-426.

[17] Srinivasulu, C., Ramgopal, M., Ramanjaneyulu, G., Anuradha, C. M., & Kumar, C. S. (2018). Syringic acid (SA)–a review of its occurrence, biosynthesis, pharmacological and industrial importance. *Biomedicine & Pharmacotherapy*, *108*, 547-557.

[18] Cramer, M., & Myers, J. (1952). Growth and photosynthetic characteristics of *Euglena gracilis*. *Archiv für Mikrobiologie*, *17*(1-4), 384-402.

[19] Li, M., Muñoz, H. E., Goda, K., & Di Carlo, D. (2017). Shape-based separation of microalga *Euglena gracilis* using inertial microfluidics. *Scientific reports*, *7*(1), 1-8.

[20] Lichtenthaler, H.K., Wellburn, A.R. (1983). Determinations of total carotenoids and chlorophylls a and b of leaf extracts in different solvents. *Biochemical Society Transactions,* 11(5), 591–592.

[21] Dean, A. P., Sigee, D. C., Estrada, B., & Pittman, J. K. (2010). Using FTIR spectroscopy for rapid determination of lipid accumulation in response to nitrogen limitation in freshwater microalgae. *Bioresource technology*, *101*(12), 4499-4507.

[22] Meng, Y., Yao, C., Xue, S., & Yang, H. (2014). Application of Fourier transform infrared (FT-IR) spectroscopy in determination of microalgal compositions. *Bioresource technology*, *151*, 347-354.

[23] Driver, T., Bajhaiya, A. K., Allwood, J. W., Goodacre, R., Pittman, J. K., & Dean, A. P. (2015). Metabolic responses of eukaryotic microalgae to environmental stress limit the ability of FT-IR spectroscopy for species identification. *Algal research*, *11*, 148-155.

[24] Della Greca, M., Monaco, P., Pollio, A., & Previtera, L. (1992). Structure-activity relationships of phenylpropanoids as growth inhibitors of the green alga *Selenastrum capricornutum*. *Phytochemistry*, *31*(12), 4119-4123.

[25] Nakai, S., Inoue, Y., & Hosomi, M. (2001). Algal growth inhibition effects and inducement modes by plant-producing phenols. *Water Research*, *35*(7), 1855-1859.

[26] Yang, J., Tang, H., Zhang, X., Zhu, X., Huang, Y., & Yang, Z. (2018). High temperature and pH favor *Microcystis aeruginosa* to outcompete *Scenedesmus obliquus*. *Environmental*

Science and Pollution Research, *25*(5), 4794-4802.

[27] Lane, A. E., & Burris, J. E. (1981). Effects of environmental pH on the internal pH of *Chlorella pyrenoidosa*, *Scenedesmus quadricauda*, and *Euglena mutabilis*. *Plant physiology*, *68*(2), 439-442.

[28] Kefeli, V., & Kutáček, M. (1979). Effects of phenolic compounds on auxin biosynthesis and vice versa. In *Regulation of Secondary Product and Plant Hormone Metabolism* (pp. 13-23). Pergamon..

[29] Larson, L. J. (1989). Effect of phenolic acids on growth of *Chlorella pyrenoidosa*. *Hydrobiologia*, *183*(3), 217-222.

[30] De Klerk, G. J., Guan, H., Huisman, P., & Marinova, S. (2011). Effects of phenolic compounds on adventitious root formation and oxidative decarboxylation of applied indoleacetic acid in Malus 'Jork 9'. *Plant Growth Regulation*, *63*(2), 175-185.

[31] Krogmeier, M. J., & Bremner, J. M. (1989). Effects of phenolic acids on seed germination and seedling growth in soil. *Biology and fertility of soils*, *8*(2), 116-122.

[32] Lonergan, T. A. (1983). Regulation of cell shape in *Euglena gracilis*: I. involvement of the biological clock, respiration, photosynthesis, and cytoskeleton. *Plant physiology*, *71*(4), 719-730.

[33] Kepekçi, R. A., & Saygideger, S. D. (2012). Enhancement of phenolic compound production in *Spirulina platensis* by two-step batch mode cultivation. *Journal of Applied Phycology*, *24*(4), 897-905.

[34] Kitajima, K., & Hogan, K. P. (2003). Increases of chlorophyll a/b ratios during acclimation of tropical woody seedlings to nitrogen limitation and high light. *Plant, Cell & Environment*, *26*(6), 857-865.

[35] Gorman, D. S., & Levine, R. P. (1965). Cytochrome f and plastocyanin: their sequence in the photosynthetic electron transport chain of *Chlamydomonas reinhardi*. *Proceedings of the National Academy of Sciences of the United States of America*, *54*(6), 1665..

[36] Varela, J. C., Pereira, H., Vila, M., & León, R. (2015). Production of carotenoids by microalgae: achievements and challenges. *Photosynthesis research*, *125*(3), 423-436.

[37] Tam, L. T., Ha, N. C., Zhu, J. Y., Wakisaka, M., & Hong, D. D. (2020). Ferulic acid extracted from rice bran as a growth promoter for the microalga *Nannochloropsis oculata*. *Journal of Applied Phycology*, 1-9.

[38] Liu, Z. X., You, S., Tang, B. P., Wang, B., Sheng, S., Wu, F. A., & Wang, J. (2019). Inositol as a new enhancer for improving lipid production and accumulation in *Schizochytrium* sp. SR21. *Environmental Science and Pollution Research*, *26*(35), 35497-35508.

[39] Sitole, L., Steffens, F., Krüger, T. P., & Meyer, D. (2014). Mid-ATR-FTIR spectroscopic profiling of HIV/AIDS sera for novel systems diagnostics in global health. *Omics: a journal of integrative biology*, *18*(8), 513-523.

Chapter 5. Enhancement of biomass yield and lipid accumulation of freshwater microalga *Euglena gracilis* by phenolic aldehydes from basic structures of lignin

Introducing biomass-derived additives into microalgae cultivation to increase its yield has been regarded as a more cost-effective and environment-friendly method compared with gene-editing and nutrients supplementation. In this research, feasibility of three major phenolic compounds from lignin's basic structures (guaiacyl-, hydroxyphenyl- and syringyl- types) for freshwater microalga *Euglena gracilis* cultivation was evaluated. The results indicated that trans-4-hydroxy-3-methoxycinnamic acid (HMA), 4-hydroxybenzaldehyde (HBA), and syringaldehyde (SRA) could all promote microalgae growth in a phytohormone-like role, and the highest promotion effect was achieved under HMA treatment. HMA at 0.5 $g \cdot L^{-1}$ enhanced the cell biomass yield by 2.30 times, while HBA and SRA at the concentration of 0.1 $g \cdot L^{-1}$ increased the yield by 1.30 and 1.21 times, respectively. In addition, increased carotenoids and lipid biosynthesis were also observed under the treatments of phenolic compounds, which would contribute to the microalgae biofuel production, since the growth and lipid accumulation of *E. gracilis* were simultaneously enhanced.

5.1 Introduction

Facing a cascade of problems such as the depletion of fossil fuels, surge in world population, intensification of greenhouse effect, and deterioration of environment, people have been devoting extensive attempts to finding alternative sources of biofuels and food to meet the growing demands [1]. Nowadays, microalgae, regarded as the cell factories for various natural products (such as lipids, proteins, carbohydrates, pigments, enzymes) have attracted great interest worldwide due to the fast growth cycle, high biomass yield and positive environment impact [2]. *Euglena gracilis* is one of the most widely and successfully cultivated commercial microalgae, and it has been applied across food, feed, pharmaceuticals, and cosmetics industries, due to its success in outdoor mass cultivation and harvesting, as well as the rich content of high value added products [3]. Moreover, owing to the advantages of high lipid productivity, no occupation of farm

lands and no competition with food production, the potential of microalgae in biofuel production has also been exploited [4]. However, the high cost associated with the culture process, as well as existing productivity constraints, are projected to hamper the growth of *E. gracilis* market. Therefore, exploring novel cultivation methods that are efficient and cost-effective has become a top priority to overcome the bottleneck of microalgae commercialization.

Generally, nitrogen starvation and stress are conventional approaches to increasing the lipid accumulation of microalgae [1,5]. However, they are often not conducive to the growth of microalgae, which is a potential conflict in its production [6]. Therefore, increasing the lipid content without sacrificing cell growth is vital for the development of microalgal biofuel industry. Supplementation of phytohormones and/or carbon sources during growth are another strategies to increase lipid accumulation. Phytohormone is the stress signaling molecule, which can interfere with enzymes involved in lipid synthesis and inhibit their competitive pathways, while organic carbon sources can be directly assimilated in metabolic pathways, increasing the supply of carbon flux and precursors for lipid synthesis [1,7]. However, commercial phytohormones will greatly increase the cost of cultivation, and the amount of organic carbon sources used for microalgae culture tends to be relatively large, which will easily cause eutrophication and bacterial contamination of water bodies [8].

A cost-effective and environmentally friendly method for enhancing the yield of microalgal biomass and valuable metabolites through additives from waste biomass has been proposed. In previous reports, Nogami et al. [9] found that 0.5 $g \cdot L^{-1}$ industrial waste steel-making slags improved the microalgal growth and lipid yield of *Botryococcus braunii* by 1.74 and 2.61 times, respectively. In addition, studies showed that the hydrolysate of agro-waste rice straw as the medium of *Chlorella pyrenoidosa* could significantly increase the biomass concentration and lipid content, which could contribute to the biodiesel production [10]. Lignin is also a potential alternative, since it is one of the most abundant raw materials on earth, exceeded only by cellulose, and its current availability is very low. Furthermore, it is an important source of bioactive phenolic substances, and mainly composed of three basic monolignols which was oxidatively coupled (as building blocks), including guaiacyl (G), *p*-hydroxyphenyl (H), and syringyl (S) alcohols [11]. In

the previous research, it was observed that lignosulfonate, the major byproduct of the pulping liquid, could act as the growth stimulant for *E. gracilis* and increase its lipid production, and it might play the role similar to phytohormones through these phenolic monomers [12]. It has already been sporadically reported that several phenolic compounds such as vanillic acid and protocatechuic acid have allelopathic properties and can exist as response and defense substances in plants against various abiotic stresses [13]. Moreover, Esakkimuthu et al. [1] discovered that 1 mM *p*-coumaric acid (from H-type lignin hydrolysate) was able to improve the biomass yield and lipid production of *Tetradesmus obliquus* by 1.34 and 2.45 times, respectively, of which the effect was comparable to phytohormones jasmonic acid and salicylic acid. Therefore, it seems promising to search for growth stimulants of microalgae from lignin hydrolysates, since it will satisfy the dual demands, not only massively increase biomass production at a lower cost, improving the commercial value of microalgae, but also make full use of phenolic substances in the waste streams from the textile, pulp, leather and petrochemical industries, reducing environmental pollution.

For the moment, the role of lignin related phenolic derivatives in the growth of microalgae is still poorly understood, and there is also a lack of discussion on the relationship between different structures of phenolic compounds and their effects. To make up for this, three major types of phenolic compounds from the downstream byproducts of lignin hydrolysis, trans-4-hydroxy-3-methoxycinnamic acid (HMA: G-type), 4-hydroxybenzaldehyde (HBA: H-type), and syringaldehyde (SRA: S-type) were selected in this research, and their effects on microalgal growth and lipid content were investigated. The parameters including cell density, biomass yield, cellular morphology, photosynthetic pigments and macromolecules content were also evaluated. Moreover, the possible impacts of structural differences of phenolic compounds on the growth of microalgae were discussed.

5.2 Materials and methods

5.2.1 Phenolic compounds from basic structures of lignin

Trans-4-hydroxy-3-methoxycinnamic acid (HMA), 4-hydroxybenzaldehyde (HBA), and syringaldehyde (SRA) were mainly from guaiacyl- (G-type), hydroxyphenyl- (H-type), and

syringyl- (S-type) lignins, respectively. These phenolic compounds were purchased from Fujifilm Wako Pure Chemical Corporation, Japan. Prepared 500 mL of stock solution for later use. To avoid the composition variation of the stock solution caused by high temperature of autoclaving, it was sterilized by vacuum filtration device of which the pore diameter was 0.45 μm (Nalgene, Thermo Fisher Scientific, USA).

5.2.2 Microalga and culture conditions

Euglena gracilis Klebs (NIES-48) strain was obtained from the National Institute for Environmental Studies, Japan. Microalgal cells were cultured in modified Cramer-Myers (CM) medium for autotrophic cultivation [14]. The temperature was maintained at 25 ºC. Flask culture process in this experiment was according to the previous reports [15,16], to simulate the natural growth conditions, no extra air-aeration was provided since the air in the Erlenmeyer flask was sufficient and each flask was fitted with a breathable rubber plug. For experiment, 10 mL of active cells at log phase were inoculated into fresh medium and mixed with different proportions of phenolic compound stock solutions, making the final culture volume of 100 mL in the Erlenmeyer flasks. The concentrations of the three phenolic compounds were 0, 0.05, 0.1, 0.3, 0.5, and 1 $g \cdot L^{-1}$. The illumination (light/dark cycle: 12/12 h) was provided by cool-white fluorescent lamps and light intensity was 5000 lx. All groups were shaken twice a day to avoid massive accumulation of algal cells on the flask wall. The cultures were operated in triplicate and experiment for each phenolic compound has an independent control group.

5.2.3 Cell growth parameters

Cell growth was evaluated by the parameters such as cell density, optical density of cell re-suspensions and cell dry weight. Cell density was periodically counted by hemocytomter (Thoma, Hirschmann, Germany) under optical microscope (BA210, Motic, Japan). Correspondingly, the optical density at 680 nm of cell re-suspensions were also determined. Aliquots 4 mL of cell suspensions were centrifuged at the speed of 5000 rpm for 5 minutes. The supernatant was collected for pH determination, and cell pellets were rinsed with deionized water to eliminate the influence of media and additives. Cells were re-suspended to 4 mL and the optical density at 680 was determined by the UV–vis spectrophotometer (Genesys 10S, Thermo Fisher Scientific, USA).

Microalgal cells were harvested at the end of the culture for dry weight analysis. Aliquots 20 mL of cell suspensions were centrifuged at the speed of 5000 rpm for 15 minutes, and washed with distilled water three times. The rinsed cells were then transferred to the pre-dried and weighed glass bottles, and dried at 105 ºC for 2 h. The dry weight of cell biomass was obtained by calculating the difference between the initial and final weight of the glass bottle.

5.2.4 Analysis of morphological changes

The cell morphology of *E. gracilis* is an important parameter reflecting cell physiology and metabolism under different culture conditions. Morphologies of 120 algal cells were randomly observed under the optical microscope (BA210, Motic, Japan), and recorded by the software Motic Image Plus 2.2S. Quantification of cell morphology was achieved by particle-shape analysis with the software ImageJ (National Institutes of Health, US). To evaluate the changes in morphologies under different treatments, cell aspect ratio was calculated by the ratio of cell length to width according to Eq. (1), and cell size was approximated by the projection area. Feret's diameter, MinFeret, and projection area were all recorded through the automatic algorithm of ImageJ.

$$Cell\ \ aspect\ \ ratio = Feret's\ \ diameter/MinFeret \quad (1)$$

Where the Feret's diameter is the longest distance between any two points along the selection boundary, and MinFeret is the minimum caliper diameter, representing cell length and width, respectively.

5.2.5 Analysis of photosynthetic pigments

Photosynthetic pigments content was measured following the previous report [17]. Ten milliliter of cell suspensions were filtrated and rinsed with distilled water three times. Hereafter the cells were ground together with glass sands and 80%(v/v) acetone solutions, till the pigments were completely transferred to the solvents. The extract homogenate were filtrated again to remove the insolubles. The filtrates were combined and made to 10 mL using acetone solutions, and the absorbances of the extract at 470, 646, and 663 nm were determined by the UV–vis spectrophotometer. The content of photosynthetic pigments ($mg \cdot L^{-1}$) were measured according to the following Eqs. (2)- (4).

$$C_a = 12.21Abs_{663} - 2.81Abs_{646} \quad (2)$$

$$C_b = 20.13Abs_{646} - 5.03Abs_{663} \quad (3)$$

$$C_{x+c} = (1000Abs_{470} - 3.27Chl_a - 104Chl_b)/229 \quad (4)$$

Where C_a, C_b, and C_{x+c} denote chlorophyll a, chlorophyll b, and carotenoids content, and Abs_{470}, Abs_{646}, and Abs_{663} denote their absorbances at 470, 646, and 663 nm, respectively.

5.2.6 Analysis of changes in biochemical composition

Fourier-transform infrared (FT-IR) spectroscopy analysis, a high-throughput and sensitive technique, was employed for better comparisons of the changes in cellular components under different treatments. Relative content of carbohydrates and lipids was analyzed by FT-IR analysis, requiring only a small amount of cell biomass, and without any complicated cell extraction process [18]. The detailed process was according to the modified method given by Meng et al. [19]. Aliquots 15 mL of cell suspensions were centrifuged at 5000 rpm for 10 min to remove the media, and the cell pellets were rinsed with de-ionized water five times to eliminate the effect of reversed salts and other media components. Afterwards the harvested cell biomass was snap-frozen using liquid nitrogen and dried at -50 ºC under vacuum for 24 h. For FT-IR analysis, lyophilized cells were ground together with KBr at a ratio of 0.5-2%. The obtained fine flour-like powder was pressed into thin sheets by a manual press. The FT-IR spectra of cell samples were obtained from the FT-IR spectrometer (Nicolet iZ10, Thermo Fisher Scientific, USA), and spectrum of KBr was set as the background. FT-IR analysis of each group was repeated three times, and a total of 9 repeated analyses were performed for each treatment (in triplicate). The absorbance spectrum in the regions of 4000-400 cm^{-1} was acquired with 32 scans co-added and averaged, and the spectral resolution was 4 cm^{-1}. The spectra were resorted to baseline and atmospheric correction using the automatic algorithms of OMINIC software (Thermo Fisher Scientific, US), and narrowed to the fingerprint regions of 1800-1000 cm^{-1} which contained key bands providing information about the cellular biochemical composition [18]. To minimize the influence of inhomogeneous thickness of sample sheets, the spectra were normalized to amide I at 1657 cm^{-1} (as the internal reference peak). Relative content of lipids and carbohydrates were estimated by calculating the peak height ratios of lipid/amide I and carbohydrate/amide I bands,

respectively.

5.2.7 Principle component analysis

Principle component analysis (PCA) was also employed to analyze the discrete trends in the metabolic fingerprint of microalgal cells under the treatments of different phenolic compounds. Normalized FT-IR spectra were imported into the software SIMCA-P (v.13.0, Umetrics, Sweden) and PCA model was established to compare the metabolic difference between the algal cells with and without phenols treatment.

5.2.8 Statistical analysis

All analyses were operated in triplicate. The data were processed by SPSS (v.16, IBM, USA) and expressed in mean plus/minus one standard deviation. One-way analysis of variance (ANOVA) followed by post hoc Dunnett's test were performed to analyze the difference in growth and metabolism parameters between the control group and the target treatment groups with a 95% confidence level.

5.3 Results and discussion

5.3.1 Growth promotion of *E. gracilis* with different phenolic compounds

The regulatory effects on growth of *E. gracilis* were observed under the treatments of three phenolic substances, and this dose response phenomenon was similar to the hormesis effect, i.e., it promoted growth at lower concentrations but exhibited significant inhibitory effect at high concentrations. The result was shown in Fig. 5-1. Among them, HMA had the most obvious growth promotion effect on *E. gracili*s and showed a concentration-dependent manner. The maximum growth promotion effect was achieved under 0.5 $g \cdot L^{-1}$ HMA treatment, with the cell density increased by 1.60 times over the control group, consistent with the result of optical density at 680 nm. However, in the case of direct exposure to 1 $g \cdot L^{-1}$ of HMA, growth of *E. gracilis* was completely inhibited, indicating that HMA is acutely toxic to *E. gracilis* at very high concentrations (over 0.5 $g \cdot L^{-1}$). Different from HMA treatment, *E. gracilis* cells were very sensitive to HBA and SRA treatments. When the concentration increased to 0.3 $g \cdot L^{-1}$, its growth was completely inhibited. However, the treatment of lower dosages (0.05 and 0.1 $g \cdot L^{-1}$) of HBA and SRA showed notable growth promotion effect on algae. Dry weight of cell biomass as shown

in Fig. 5-2 was consistent with the results of cell density. The maximum promotion effect was achieved at 0.5 $g \cdot L^{-1}$ HMA, and the biomass yield of *E. gracilis* was increased by 2.30 times over the control group. Although the promotion effect was lower than that of HMA, HBA and SRA at concentration of 0.1 $g \cdot L^{-1}$ still significantly increased the biomass production by 1.30 and 1.21 times, respectively.

All the three phenolic compounds caused decline in the initial pH of the medium (as shown in Fig. 5-1b, d, f), among which HMA was the most obvious due to the nature of phenolic acid. The pH of the medium dropped from 6.9 to 5.0 when HMA concentration increased to 1 $g \cdot L^{-1}$, while it only decreased to 6.6 under the same concentration of HBA and SRA treatments (weakly acidic due to the alpha-hydrogen from the aldehyde group). In addition, the pH of 0.5 $g \cdot L^{-1}$ HMA treatment group dropped sharply from 6.2 to 4.6 during the cultivation, which was mainly due to the intense consumption of ammonium salts and the production of carbon dioxide in the medium, resulting from the rapid proliferation of *E. gracilis* cells [8,12]. More importantly, this phenomenon of pH drop induced by HMA was beneficial to outdoor cultivation of *E. gracilis*, since bacterial contamination was not prone to occur under such a low pH [8].

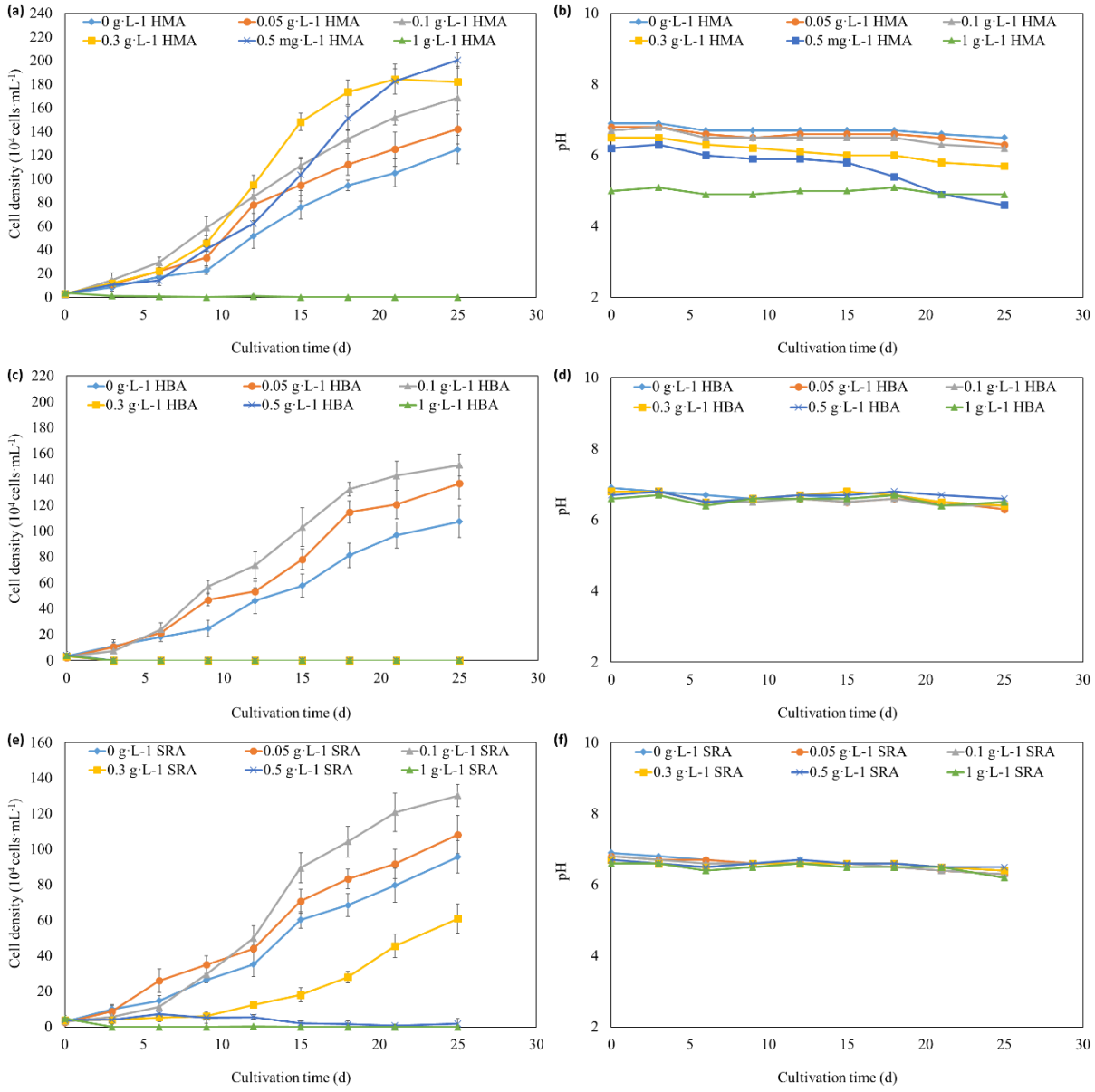

Fig. 5-1. Growth profiles of *E. gracilis* in response to different dosages of HMA, HBA and SRA. Error bar represents the standard deviation of three replicates. (a), (c), (e): growth curves of algae cells under the treatments of HMA, HBA and SRA, respectively; (b), (d), (f): pH variation of the media under the treatments of HMA, HBA and SRA, respectively.

This is the first report on the application of HMA, HBA and SRA to *E. gracilis* culture, and significant growth promotion effects have been observed in all three phenolic compounds. In previous reports, effects of phenolic compounds on microalgae growth were controversial. Nakai et al. [20] reported that a cascade of shikimate pathway-produced phenolic acids (caffeic acid,

protocatechuic acid, gallic acid, sinapic acid, and syringic acid) showed inhibitory effects on growth of cyanobacteria *Microcystis aeruginosa*, but meanwhile, growth stimulation effects of *p*-hydroxybenzoic acid, vanillic acid, syringic acid and *p*-coumaric acid on some green algae were also observed [1,21,22]. For example, *p*-coumaric acid could increase the biomass yield of *Tetradesmus obliquus* by 34.1%. In this research, HMA, HBA and SRA could stimulate the growth of *E. gracilis* at low concentrations, but inhibit the growth at high concentrations. Based on the aforementioned previous research and the results in this study, it can be inferred that different species of microalgae have different tolerances to exposure of phenolic compounds, and the dosage used for the specified microalgae cultivation is also crucial. This research demonstrated that *E. gracilis* is a promising alga to utilize the downstream phenolic compounds from lignins. This was mainly due to its wide pH range and the features of both animal and plant. The former enables it to adapt to the acidic pH of phenols, while the latter enables it not only to grow autotrophically through photosynthesis, but also to assimilate nutrients through phagocytosis.

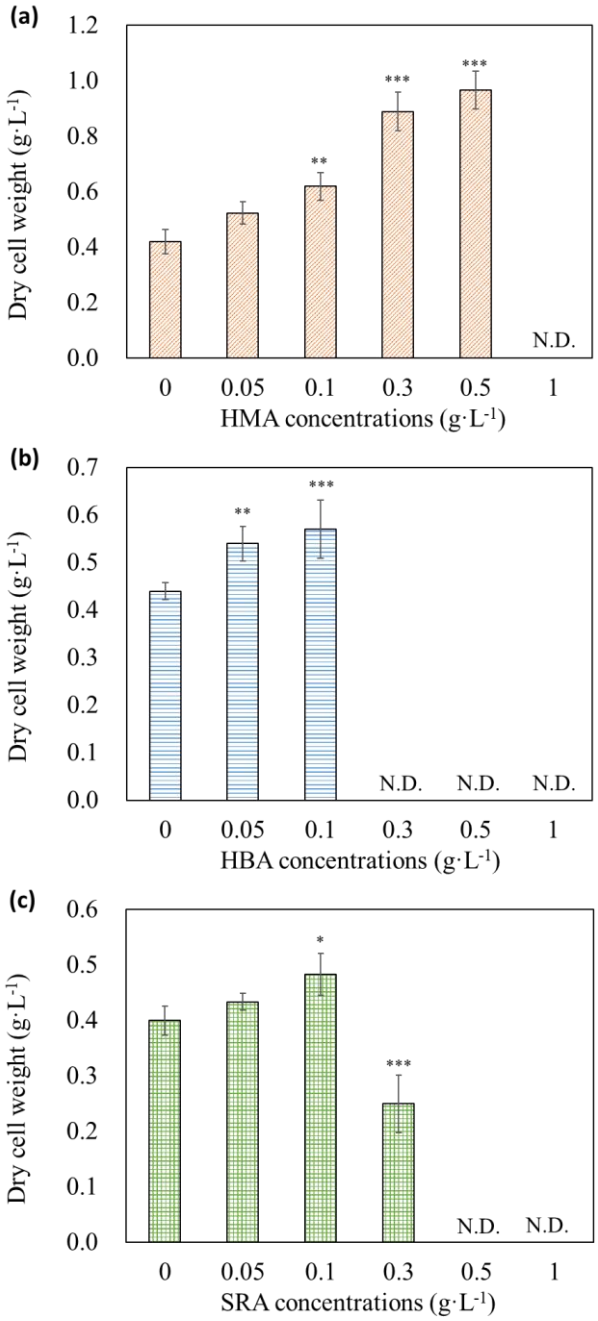

Fig. 5-2. Dry biomass yield of algae cells under the treatments of HMA, HBA and SRA. (a): dry weight under HMA treatment; (b): dry weight under HBA treatment; (c): dry weight under SRA treatment. N.D. denotes not determined due to very low biomass; the asterisk indicates the significance of the difference from the control group, and *, ** and *** denote significance at the 95%, 99%, and 99.9% levels, respectively.

The role of HMA, HBA and SRA in growth regulation of *E. gracilis* was similar as

phytohormones. In previous reports, the exogenous supply of 45 μM jasmonic acid (jasmonate class of plant hormone) resulted in a 51% increase in the growth of *Chlorella vulgaris*, while higher concentrations led to growth retardation [23]. In addition, salicylic acid (phenolic phytohormone, *o*-hydroxybenzoic acid) at low concentrations significantly increased the biomass of *Haematococcus pluvialis*, but at high concentrations it decreased chlorophyll content and bleached the cells [24]. Consistent results were also observed in all three phenols, and bleaching and apoptosis of cells occurred in high concentration treatment group as well. The stimulation effect of these phenolic compounds on microalgae was mainly attributed to the regulation of endogenous phytohormones levels. Some cases have shown that phenylpropanoid compounds are able to affect the biosynthesis of L-tryptophan and the conversion to indole-3-acetic acid (IAA), thereby interfering with plant growth and development [25]. Phenolic compounds at low concentrations appear to act as auxin synergist to reduce the auxin degradation by auxin oxidase through a competitive mechanism, but at high concentrations they tend to be cofactors in the degradation of IAA [21,22]. Moreover, they are also able to indirectly influence the number of cytokinin (CK) synthesis sites and the gibberellin (GA)-mediated physiological mechanism [26], which maybe a reason for further improvement of *E. gracilis* growth. The difference in the effectiveness of three phenolic compounds could be related to the formation of quinones. HBA and SRA as aromatic aldehydes were more prone to be oxidized into quinones than HMA which was confirmed by the changes in UV-vis spectra, and these oxidation products have been shown to cause the degradation of CKs because they are the preferred electron acceptors in the reactions catalyzed by CK dehydrogenase [27]. Moreover, the formation of quinones is often accompanied by the production of reactive oxygen species, which will be adverse to the algae growth. Therefore, compared with HBA and SRA, the more stable HMA was supposed to have far superior growth promotion effects and less toxicity on *E. gracilis*. The discovery from this research could provide some inspiration for screening more stable and excellent growth elicitors.

5.3.2 Influence on cell morphology

The cell morphology of *E. gracilis* is an important indicator reflecting the physiological

status of algae cells. Under different conditions, *E. gracilis* cells will show different morphologies, including sub-spherical, spindled and elongated types. Its shape is closely correlated to biological clock, photosynthesis, respiration, metabolic modes and external environmental factors [28]. In this study, the effects of three phenols on the cell morphology were evaluated by the changes in cell aspect ratio and size, and the results were illustrated in Fig. 5-3. The cell aspect ratio in all treatment groups ranged from 1 to 6, consistent with the previous reports [28,29]. For HMA treatment, the cell aspect ratio distribution showed an increasing trend with the increase of HMA concentration, and the median cell aspect ratio increased from 2.36 of the control group to 3.51 of the 0.5 $g \cdot L^{-1}$ treatment group, indicating that more elongated cells appeared. Correspondingly, the cell size also increased by 23.81%. Similar results were also observed under HBA and SRA treatments, although the increments were smaller than that under HMA treatment. In addition, when the dosage of SRA increased to 0.3 $g \cdot L^{-1}$, cell aspect ratio and size also dropped along with the emergence of the inhibitory effect, which was consistent with the previous report that *E. gracilis* would show a bigger and rounder cell morphology due to the cellular stress response and the accumulation of paramylon [28].

The regulation effects of phenols on the microalgal cell morphology were similar to those of some phytohormones. Park et al. [30] discovered that five different phytohormones (IAA, GA, kinetin, 1-triacontanol, and abscisic acid) caused the marked increase in cell size of *Chlamydomonas reinhardtii*, because many daughter cells were retained in the single cell before cell division. For *E. gracilis*, *the* cells generally reproduced through longitudinal binary fission, and the stimulation of phenols on mitosis before the cell release might be the reason for the increase in cell aspect ratio. Similar morphological variation of *E. gracilis* cells was also observed under the treatment of exogenous IAA and GA [31], which further supported our results. In addition, the combined treatment of indole-3-butyric acid and GA would also increase the cellular diameter of *Chlorella sorokiniana*, and trigger an increase in the aspect ratio of *Scenedesmus* sp. cells. More importantly, the changes in morphology of the two microalgae implied the alteration of cellular patterns, and an increase in intracellular lipid accumulation was observed [32]. Generally, the ideal biofuel-producing microalgae cells will have a large size [33], thus, the

enlargement of cell size of *E. gracilis* may increase its potential for biofuel production, which still requires further analyses.

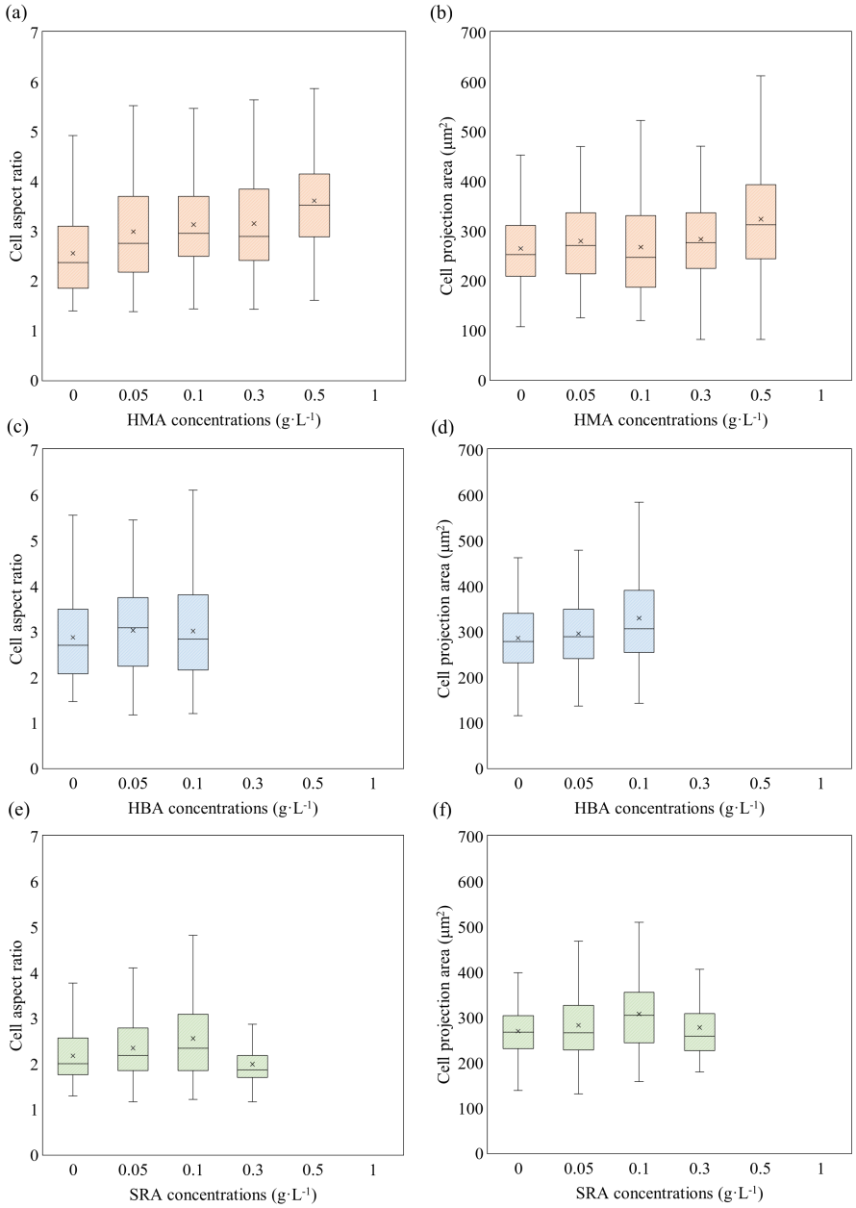

Fig. 5-3. Box plots of cell aspect ratio and projection area of *E. gracilis* under the treatment of phenolic compounds. (a): cell aspect ratio under HMA; (b): cell projection area under HMA; (c): cell aspect ratio under HBA; (d): cell projection area under HBA; (e): cell aspect ratio under SRA; (f): cell projection area under SRA. The horizontal line represents the median, and the asterisk indicates the mean. The interquartile range box represents the middle 50% of the data, and the whiskers indicate the ranges for the bottom 25% and the top 25% of the data values,

excluding outliers.

5.3.3 Influence on photosynthetic pigment composition and content

Photosynthetic pigments play vital roles in photosynthesis and carbon dioxide fixation, thus the content and yield of chlorophyll a, chlorophyll b, and carotenoids under different concentrations of phenols treatments were determined and the results were shown in Fig. 5-4. Consistent with the cell growth results, the three phenolic compounds significantly increased the photosynthetic pigments yield at low concentrations. When exposed to the optimal concentrations of HMA, HBA and SRA (0.5 $g \cdot L^{-1}$ for HMA, and 0.1 $g \cdot L^{-1}$ for HBA and SRA), the production of chlorophyll a increased by 3.08, 1.17 and 1.43 times, respectively. Correspondingly, the carotenoids yield under the treatment of phenols has also been significantly improved. To further analyze the influence of phenolic compounds on the pigments content within the cells, the proportion of photosynthetic pigments in unit dry biomass was compared as illustrated in Fig. 5-4b, d, e. Both HMA and SRA significantly increased the intracellular chlorophyll a content, but the change was not significant under HBA treatment. Moreover, the treatment of these phenols also decreased the chlorophyll b content in *E. gracilis*, leading to a rise in the ratio of chlorophyll a to chlorophyll b, which indicated an increase in the light-capturing capacity of algal cells [34]. Similar results have also been reported in rice *Oryza sativa* L., and pretreatment with salicylic acid could significantly increase the chlorophyll a content and improve photosynthesis, whereas protocatechuic acid greatly decreased the chlorophyll b content [35]. These phenolic substances have been demonstrated to be able to improve membrane perturbation of plant cells, and subsequently produce a cascade of physiological effects, including improving the cell-water relationships, photosynthesis and respiration rates [13]. Furthermore, the positive effects of three phenols on carotenoids content were also observed. HMA greatly increased the carotenoids content in *E. gracilis* (P <0.01), and equivalent trends were observed under HBA and SRA treatments, but the increment was not significant (P >0.05). Carotenoids are crucial for the stability and functionality of the photosynthetic apparatus, and for the most part, the environment cues that induce carotenogensis in algae are identical to the ones which will induce the biosynthesis of neutral lipids. Therefore, it is necessary to further analyze the changes in cellular

components of microalgae.

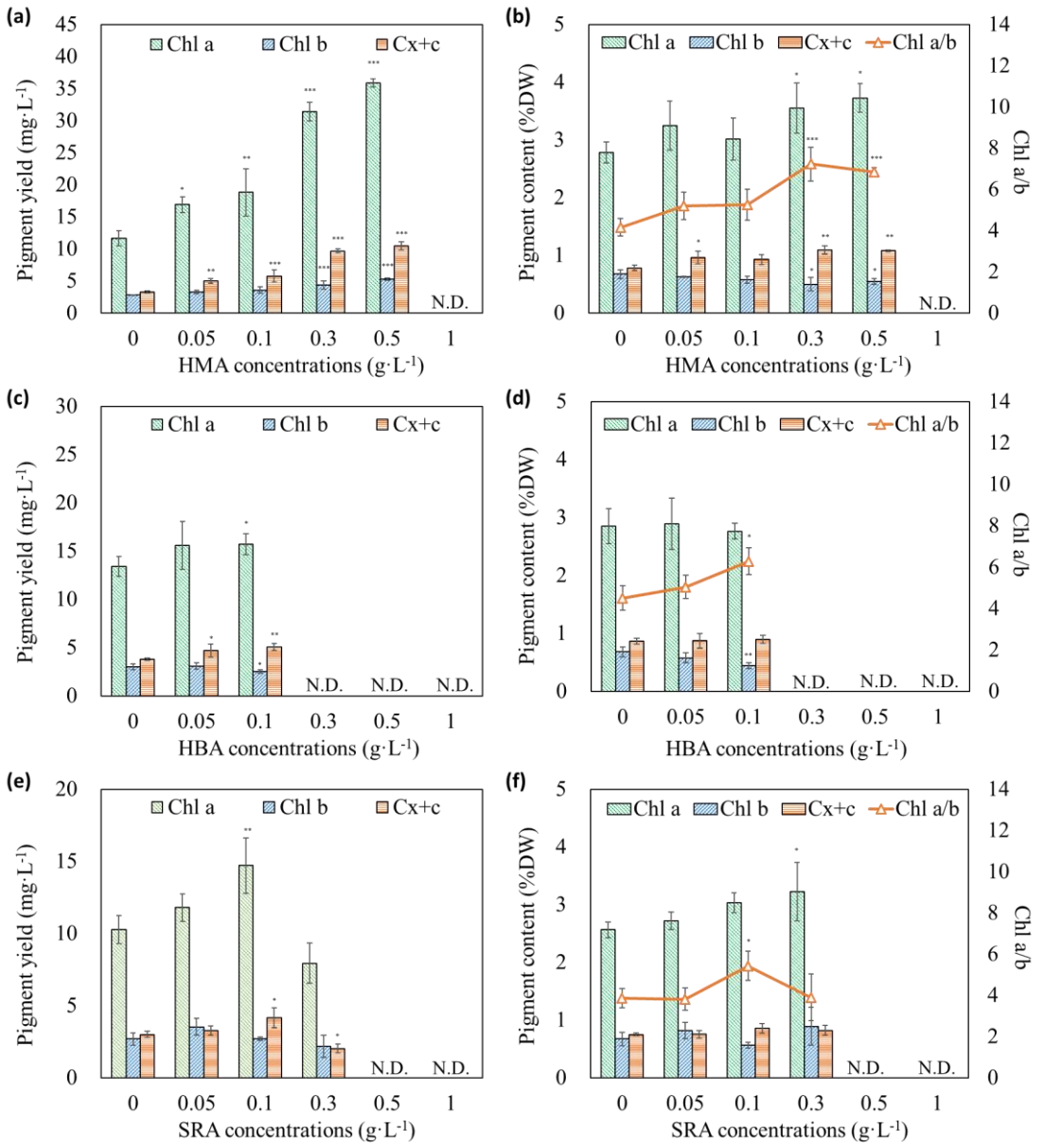

Fig. 5-4. Photosynthetic pigments yield and content in *E. gracilis* under different concentrations of HMA, HBA and SRA. (a), (c), (e): pigment yield under HMA, HBA and SRA treatments, respectively; (b), (d), (f): intracellular pigment content and ratio of chlorophyll a to chlorophyll b under HMA, HBA and SRA treatments, respectively; N.D. represents not determined due to very low biomass; the asterisk indicates the significance of the difference from the control group, and *, ** and *** denote significance at the 95%, 99%, and 99.9%

levels, respectively.

5.3.4 Influence on cell biochemical composition

The growth promotion effects of three phenolic compounds on *E. gracilis* has been confirmed. To further explore their potential in the field of biofuels, the changes in cell biochemical composition under different phenols treatments were analyzed through FT-IR analysis. Chemical bonds within the functional groups of biochemical molecules have unique vibration properties, thus relative content of these macromolecules can be effectively determined by FT-IR analysis [18]. The spectra of *E. gracilis* cell samples treated with different phenols were obtained with high signal-to-noise ratios, and the bands assigned to functional groups from the major macromolecules could be clearly identified in the fingerprint regions of 1800-1000 cm^{-1}. The bands at 1657 cm^{-1} and 1451 cm^{-1} are assigned to amide I and amide II, respectively, which are related to the protein content. The phosphorylated molecules content corresponds to the band at 1263 cm^{-1}, which is mainly attributed to the stretching of $\nu_{as}(PO_2^-)$. The band at 1738 cm^{-1} is assigned to the ν_s (C=O) stretching from lipids, and the band at 1080 cm^{-1} comes from the ν (C-O-C) stretching of glycosidic bonds of carbohydrates.

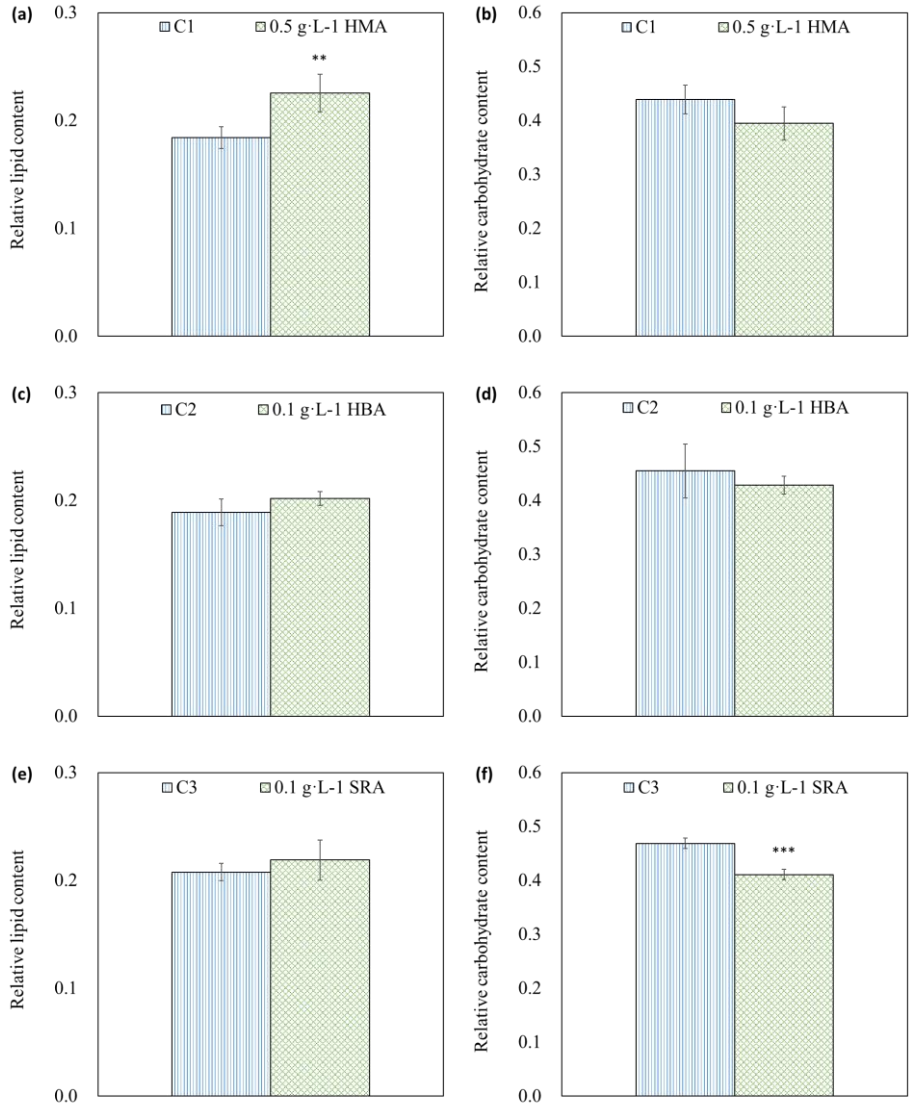

Fig. 5-5. Relative content of lipid and carbohydrate under the optimal dosage of phenols (0.5 g·L^{-1} for HMA, and 0.1 g·L^{-1} for HBA and SRA). (a), (c), (e): relative lipid content under HMA, HBA and SRA treatments, respectively; (b), (d), (f): relative carbohydrate content under HMA, HBA and SRA treatments, respectively; C1, C2, and C3 represent the independent control group for each phenol experiment. The asterisk indicates the significance of the difference from the control group, and *, ** and *** denote significance at the 95%, 99%, and 99.9% levels, respectively.

For further comparison of the changes in metabolic patterns and carbon assimilation, relative content of carbohydrate and lipid was analyzed based on the previous research [36,37]. The results

were shown in Fig. 5-5. The treatments of all three phenolic compounds resulted in an increase in the lipid accumulation of the cells. Lipid content under 0.5 $g \cdot L^{-1}$ HMA treatment increased by 22.51% over the control. In the 0.1 $g \cdot L^{-1}$ HBA and SRA treatment groups, the trend of enhanced lipid biosynthesis was also observed, which increased by 6.81% and 5.39%, respectively. This was consistent with the increase in intracellular carotenoids content, since synthesis of lipids and carotenoids shared acetyl-CoA (acetyl coenzyme A) and pyruvate as common precursors [6,38]. Furthermore, with the significant increase in algae cell density without sacrificing lipid accumulation, the lipid yield under these phenols treatments would also be greatly enhanced. The lipid yield in 0.5 $g \cdot L^{-1}$ HMA treatment group would increase by 2.82 times over the control. This was consistent with the previous report of [1] that 1 mM exogenous *p*-coumaric acid could increase the lipid production of *Tetradesmus obliquus* by 2.45 times compared with the control group, which was comparable to the effects of phytohormones jasmonic acid and salicylic acid. Li et al. [39] also reported that four benzoic acid derivatives promoted the lipid production of marine fungus *Schizochytrium limacinum*, and the biochemical mechanism was discovered related to glycolysis, pentose phosphate pathway and lipid synthesis pathway (polyketide synthase and fatty acid synthase). These phenolic compounds might play the similar role to determine a different biosynthesis and flow of carbon to metabolites by interacting with several phytohormones and enzymes [13]. On the other hand, decreased intracellular carbohydrate content in *E. gracilis* was observed, implying the phenols treatment induced the conversion of carbon flux from carbohydrate to lipids, which might be mainly attributed to the competition mechanism between carbohydrate and lipid synthesis. Generally, they are both the major energy storage products, sharing the same synthetic precursor triacylglycerols, and they can be converted into each other in response to metabolic changes [6].

5.3.5 Principle component analysis

The FT-IR spectra of *E. gracilis* cells with and without the treatment of phenolic compounds were further analyzed using PCA to find the differences in metabolic patterns and the discrete trends between different treatments. The result was shown in the score plot of Fig. 5-6. PCA clearly resolved the data into four major components, with a cumulative contribution rate of

92.3%. The Q^2 of PCA was 0.904, indicating predictability of the model is good. As seen from the score plot, the controls and the phenol-treated samples were well distinguished. The first principle component (PC1) explained 51.8% of the total variance in the data sets of four different treatments, and the second principle component (PC2) accounted for 30.8% of the variance. Since the other two components contributed little to the model, we focused on the PC1 and PC2 loadings to interpret the differences in metabolic patterns. The spectra of the control group and the phenols-treated group were clearly separated into 3 major cluster groups in the score plot. The spectra of HMA treated samples were mainly clustered in the lower right part of the score plot (positive scores for PC1 and negative scores for PC2), while those of control samples were clustered in a reversed direction. The spectra of HBA and SRA treated samples were clustered together and were not well discriminated, indicating that closely similar changes in biochemical macromolecules composition occurred under the two aromatic aldehydes treatments, but they were still clearly separated from the controls and HMA treatment groups. To interpret the separation between each group, and find the biomarkers which contributed the most to the variance, PC1 and PC2 loadings were analyzed [36]. It revealed that along PC1 the major variation of macromolecules occurred in the lipid regions, and lipid content was more prominent in the groups located in the positive direction of PC1 of the score plot. PC2 loadings indicated that major variation occurred in the lipid and carbohydrate regions, and carbohydrate content are more prominent in the positive direction of PC2, while lipid content are more prominent in the negative direction. Therefore, PCA identified that lipid biosynthesis increased but carbohydrate content decreased under the exposure of phenolic compounds, and these biomarkers content changed most obviously in HMA treatment, which was consistent with the results shown in Fig. 5-5. FT-IR analysis combined with PCA was an effective tool in determining the changes in macromolecule pools under the exposure of different phenolic compounds, and it demonstrated that these three phenolic compounds from the basic structures of lignin could be employed as the growth elicitors of *E. gracilis* and enhance the lipids accumulation. This study provides a preliminary understanding of the roles of phenolic compounds in the cultivation of microalgae, and further exploration of other phenolic growth promotors from the downstream byproducts of

lignin for biomass and biofuel production of microalgae is strongly recommended.

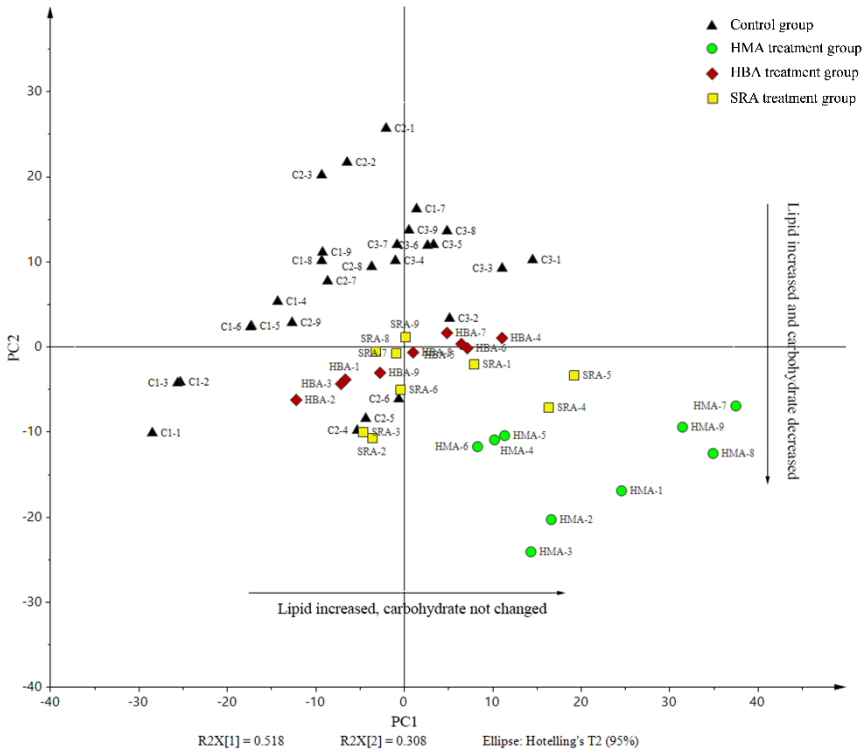

Fig. 5-6. PCA score plot of FT-IR spectra derived from *E. gracilis* cells in response to the optimal dosage of phenols (0.5 g·L^{-1} for HMA, and 0.1 g·L^{-1} for HBA and SRA). $R^2X = 0.923$, $Q^2 = 0.904$. Each sample was analyzed in 9 replicates.

5.4 Conclusion

The current work highlighted the stimulation effect of three major phenolic compounds from basic structures of lignin on the growth and lipid accumulation of *E. gracilis*. At the optimal dosage of HMA, HBA and SRA, the biomass yield was increased by 2.30, 1.30 and 1.21 times, respectively. Morphological changes such as cell elongation and enlargement was observed, accompanied by an increase in photosynthetic pigments content. Lipid biosynthesis was also promoted by phenols without sacrificing microalgae growth, implying the potential of waste stream rich in HMA, HBA and SRA in improving the biomass and biofuel production of *E. gracilis*.

Reference:

1. Esakkimuthu, S., Krishnamurthy, V., Wang, S., Hu, X., Swaminathan, K., & Abomohra, A. E.

F. (2020). Application of p-coumaric acid for extraordinary lipid production in Tetradesmus obliquus: A sustainable approach towards enhanced biodiesel production. *Renewable Energy*. 157, 368-376.

2. Dasan, Y. K., Lam, M. K., Yusup, S., Lim, J. W., & Lee, K. T. (2019). Life cycle evaluation of microalgae biofuels production: Effect of cultivation system on energy, carbon emission and cost balance analysis. *Science of the total environment*, *688*, 112-128.

3. Suzuki, K. (2017). Large-scale cultivation of *Euglena*, in: Schwartzhach, S.D., Shigeoka, S. (Eds.), *Euglena*: *Biochemistry, Cell and Molecular biology*. Springer, Berlin, pp. 285-293.

4. Yamada, K., Suzuki, H., Takeuchi, T., Kazama, Y., Mitra, S., Abe, T., ... & Iwata, O. (2016). Efficient selective breeding of live oil-rich Euglena gracilis with fluorescence-activated cell sorting. *Scientific reports*, *6*, 26327.

5. Lv, J. M., Cheng, L. H., Xu, X. H., Zhang, L., & Chen, H. L. (2010). Enhanced lipid production of Chlorella vulgaris by adjustment of cultivation conditions. *Bioresource technology*, *101*(17), 6797-6804.

6. Sun, H., Ren, Y., Mao, X., Li, X., Zhang, H., Lao, Y., & Chen, F. (2020). Harnessing C/N balance of Chromochloris zofingiensis to overcome the potential conflict in microalgal production. *Communications Biology*, *3*(1), 1-13.

7. Sun, X. M., Ren, L. J., Zhao, Q. Y., Zhang, L. H., & Huang, H. (2019). Application of chemicals for enhancing lipid production in microalgae-a short review. *Bioresource technology*, *293*, 122135.

8. Yamane, Y. I., Utsunomiya, T., Watanabe, M., & Sasaki, K. (2001). Biomass production in mixotrophic culture of Euglena gracilis under acidic condition and its growth energetics. *Biotechnology Letters*, *23*(15), 1223-1228.

9. Nogami, R., Ushijima, K., Nishida, H., & Wakisaka, M. (2017). Enhancement of Growth and Lipid Production of *Botryococcus braunii* by Steel Slags. *Journal of the Japan Institute of Energy*, *96*(9), 372-375.

10. Li, P., Miao, X., Li, R., & Zhong, J. (2011). In situ biodiesel production from fast-growing and high oil content Chlorella pyrenoidosa in rice straw hydrolysate. *Journal of Biomedicine*

and Biotechnology, *2011*.

11. Freudenberg, K., & Neish, A. C. (1968). Molecular biology, Biochemistry and biophysics. 2. Constitution and biosynthesis of lignin. *Molecular biology, Biochemistry and biophysics. 2. Constitution and biosynthesis of lignin.*
12. Zhu, J., & Wakisaka, M. Application of lignosulfonate as the growth promotor for freshwater microalga Euglena gracilis to increase productivity of biomass and lipids. *Fuel*, *283*, 118920.
13. Ertani, A., Francioso, O., Tugnoli, V., Righi, V., & Nardi, S. (2011). Effect of commercial lignosulfonate-humate on Zea mays L. metabolism. *Journal of agricultural and food chemistry*, *59*(22), 11940-11948.
14. Cramer, M., & Myers, J. (1952). Growth and photosynthetic characteristics of Euglena gracilis. *Archiv für Mikrobiologie*, *17*(1-4), 384-402.
15. Chi, Z., Xie, Y., Elloy, F., Zheng, Y., Hu, Y., & Chen, S. (2013). Bicarbonate-based integrated carbon capture and algae production system with alkalihalophilic cyanobacterium. *Bioresource technology*, *133*, 513-521.
16. Toyama, T., Kasuya, M., Hanaoka, T., Kobayashi, N., Tanaka, Y., Inoue, D., ... & Mori, K. (2018). Growth promotion of three microalgae, Chlamydomonas reinhardtii, Chlorella vulgaris and Euglena gracilis, by in situ indigenous bacteria in wastewater effluent. *Biotechnology for biofuels*, *11*(1), 176.
17. Lichtenthaler, H.K., Wellburn, A.R. (1983). Determinations of total carotenoids and chlorophylls a and b of leaf extracts in different solvents. *Biochemical Society Transactions,* 11(5), 591–592.
18. Driver, T., Bajhaiya, A. K., Allwood, J. W., Goodacre, R., Pittman, J. K., & Dean, A. P. (2015). Metabolic responses of eukaryotic microalgae to environmental stress limit the ability of FT-IR spectroscopy for species identification. *Algal research*, *11*, 148-155.
19. Meng, Y., Yao, C., Xue, S., & Yang, H. (2014). Application of Fourier transform infrared (FT-IR) spectroscopy in determination of microalgal compositions. *Bioresource technology*, *151*, 347-354.
20. Nakai, S., Inoue, Y., & Hosomi, M. (2001). Algal growth inhibition effects and inducement

modes by plant-producing phenols. *Water Research*, *35*(7), 1855-1859.

21. Larson, L. J. (1989). Effect of phenolic acids on growth of Chlorella pyrenoidosa. *Hydrobiologia*, *183*(3), 217-222.
22. Bajguz, A., Czerpak, R., Piotrowska, A., & Polecka, M. (2001). Effect of isomers of hydroxybenzoic acid on the growth and metabolism of Chlorella vulgaris Beijerinck (Chlorophyceae). *Acta societatis botanicorum Poloniae*, *70*(4), 253-259.
23. Jusoh, M., Loh, S. H., Chuah, T. S., Aziz, A., & San Cha, T. (2015). Elucidating the role of jasmonic acid in oil accumulation, fatty acid composition and gene expression in Chlorella vulgaris (Trebouxiophyceae) during early stationary growth phase. *Algal Research*, *9*, 14-20.
24. Raman, V., & Ravi, S. (2011). Effect of salicylic acid and methyl jasmonate on antioxidant systems of Haematococcus pluvialis. *Acta Physiologiae Plantarum*, *33*(3), 1043-1049.
25. Kefeli, V., & Kutáček, M. (1979). Effects of phenolic compounds on auxin biosynthesis and vice versa. In *Regulation of Secondary Product and Plant Hormone Metabolism* (pp. 13-23). Pergamon.
26. Docquier, S., Kevers, C., Lambe, P., Gaspar, T., & Dommes, J. (2007). Beneficial use of lignosulfonates in in vitro plant cultures: stimulation of growth, of multiplication and of rooting. *Plant cell, tissue and organ culture*, *90*(3), 285-291.
27. Frébortová, J., Fraaije, M. W., Galuszka, P., Šebela, M., Peč, P., Hrbáč, J., ... & Frébort, I. (2004). Catalytic reaction of cytokinin dehydrogenase: preference for quinones as electron acceptors. *Biochemical Journal*, *380*(1), 121-130.
28. Li, M., Muñoz, H. E., Goda, K., & Di Carlo, D. (2017). Shape-based separation of microalga Euglena gracilis using inertial microfluidics. *Scientific reports*, *7*(1), 1-8.
29. Jeon, M. S., Oh, J. J., Kim, J. Y., Han, S. I., Sim, S. J., & Choi, Y. E. (2019). Enhancement of growth and paramylon production of Euglena gracilis by co-cultivation with Pseudoalteromonas sp. MEBiC 03485. *Bioresource technology*, *288*, 121513.
30. Park, W. K., Yoo, G., Moon, M., Kim, C. W., Choi, Y. E., & Yang, J. W. (2013). Phytohormone supplementation significantly increases growth of Chlamydomonas reinhardtii cultivated for biodiesel production. *Applied biochemistry and biotechnology*, *171*(5), 1128-1142.

31. Noble, A., Kisiala, A., Galer, A., Clysdale, D., & Emery, R. N. (2014). Euglena gracilis (Euglenophyceae) produces abscisic acid and cytokinins and responds to their exogenous application singly and in combination with other growth regulators. *European journal of phycology*, *49*(2), 244-254.

32. Yu, Z., Song, M., Pei, H., Jiang, L., Hou, Q., Nie, C., Zhang, L., 2017. The effects of combined agricultural phytohormones on the growth, carbon partitioning and cell morphology of two screened algae. Bioresour. Technol. 239, 87-96.

33. Wijffels, R. H., & Barbosa, M. J. (2010). An outlook on microalgal biofuels. *Science*, *329*(5993), 796-799.

34. Dale, M. P., & Causton, D. R. (1992). Use of the chlorophyll a/b ratio as a bioassay for the light environment of a plant. *Functional Ecology*, 190-196.

35. Xuan, T. D., & Khang, D. T. (2018). Effects of exogenous application of protocatechuic acid and vanillic acid to chlorophylls, phenolics and antioxidant enzymes of rice (Oryza sativa L.) in submergence. *Molecules*, *23*(3), 620.

36. Dean, A. P., Sigee, D. C., Estrada, B., & Pittman, J. K. (2010). Using FTIR spectroscopy for rapid determination of lipid accumulation in response to nitrogen limitation in freshwater microalgae. *Bioresource technology*, *101*(12), 4499-4507.

37. Dao, L., Beardall, J., & Heraud, P. (2017). Characterisation of Pb-induced changes and prediction of Pb exposure in microalgae using infrared spectroscopy. *Aquatic Toxicology*, *188*, 33-42.

38. Braunwald, T., Schwemmlein, L., Graeff-Hönninger, S., French, W. T., Hernandez, R., Holmes, W. E., & Claupein, W. (2013). Effect of different C/N ratios on carotenoid and lipid production by Rhodotorula glutinis. *Applied Microbiology and Biotechnology*, *97*(14), 6581-6588.

39. Li, Z., Ling, X., Zhou, H., Meng, T., Zeng, J., Hang, W., ... & He, N. (2019). Screening chemical modulators of benzoic acid derivatives to improve lipid accumulation in Schizochytrium limacinum SR21 with metabolomics analysis. *Biotechnology for biofuels*, *12*(1), 1-11.

Chapter 6. Summary and prospect

Effects of different growth elicitors from lignocellulose were summarized in Table. 6-1. Although the highest promotion effect was achieved by sugar alcohols from hemicellulose, the required dosages are too high. Phenolic compounds are more practical since growth promotion could be obtained at lower concentrations. Compared with phenolic aldehydes, phenolic acids had superior growth promotion effect on *E. gracilis*. We have already investigated the effects of different types of growth promotors on *E. gracilis*, and it is necessary to use these compounds in a combined form or the waste water from lignocellulose downstream industries after simple treatments to cultivate microalgae. We are also improving our work in this regard to expand its practical application.

Table. 6-1 Summary of the growth elicitors from lignocellulosic materials on the growth and metabolism of *E. gracilis*

Supplements	Category	Source	Optimal dosage	Impact on growth	Impact on metabolism
Mannitol	Sugar alcohol	Hemicellulose	4 $g \cdot L^{-1}$	4.64-fold	Lipid content increased, carbohydrate content decreased
Xylitol	Sugar alcohol	Hemicellulose	4 $g \cdot L^{-1}$	3.18-fold	Lipid content increased, carbohydrate content decreased
LIGNs	Lignin byproduct	Lignin	5 $g \cdot L^{-1}$	1.95-fold	Lipid content increased, carbohydrate content decreased
SA	Phenolic acid	Lignin	0.5 $g \cdot L^{-1}$	1.63-fold	Lipid content increased, carbohydrate content increased
p-CA	Phenolic acid	Lignin	0.3 $g \cdot L^{-1}$	1.93-fold	Lipid content increased, carbohydrate content decreased
HMA	Phenolic acid	Lignin	0.5 $g \cdot L^{-1}$	2.30-fold	Lipid content increased, carbohydrate content decreased
HBA	Aromatic aldehyde	Lignin	0.1 $g \cdot L^{-1}$	1.30-fold	Lipid content increased, carbohydrate content decreased
SRA	Aromatic aldehyde	Lignin	0.1 $g \cdot L^{-1}$	1.21-fold	Lipid content increased, carbohydrate content decreased

List of achievements

1. Research Articles:

1. **Zhu, J.**, Tan, X., Hafid, H. S., & Wakisaka, M. (2020). Enhancement of biomass yield and lipid accumulation of freshwater microalga Euglena gracilis by phenolic compounds from basic structures of lignin. Bioresource Technology, 124441.
2. **Zhu, J**., & Wakisaka, M. (2020). Finding of phytase: Understanding growth promotion mechanism of phytic acid to freshwater microalga *Euglena gracilis*. Bioresource Technology, 296, 122343.
3. **Zhu, J**., & Wakisaka, M. (2020). Effect of two lignocellulose related sugar alcohols on the growth and metabolites biosynthesis of *Euglena gracilis*. Bioresource Technology, 303, 122950.
4. **Zhu, J**., & Wakisaka, M. (2020). Application of lignosulfonate as the growth promotor for freshwater microalga Euglena gracilis to increase productivity of biomass and lipids. Fuel, 283, 118920.
5. **Zhu, J**., & Wakisaka, M. (2018). Growth promotion of Euglena gracilis by ferulic acid from rice bran. AMB Express, 8(1), 1-7.
6. **Zhu, J**., & Wakisaka, M. (2020). Harvesting of *Arthrospira platensis* by flocculation with phytic acid from rice bran. Bioscience, Biotechnology, and Biochemistry, 1-9.
7. **Zhu, J**., Hong, D. D., & Wakisaka, M. (2019). Phytic acid extracted from rice bran as a growth promoter for *Euglena gracilis*. Open Chemistry, 17(1), 57-63.
8. **Zhu, J**., Hu, B., Lu, J., & Xu, S. (2018). Analysis of metabolites in cabernet sauvignon and shiraz dry red wines from Shanxi by 1H NMR spectroscopy combined with pattern recognition analysis. Open Chemistry, 16(1), 446-452.
9. **Zhu, J**., & Wakisaka, M. (2019). Effect of Air Nanobubble Water on the Growth and Metabolism of Haematococcus lacustris and Botryococcus braunii. Journal of nutritional science and vitaminology, 65(Supplement), S212-S216.
10. **Zhu, J.,** Wakisaka, M. (2020). Biological Response of Protozoans *Haematococcus lacustris*

and *Euglena gracilis* to Conductive Polymer Poly (3,4-ethylenedioxythiophene) Polystyrene Sulfonate, Letters in Applied Microbiology.

11. **Zhu, J.,** Tan, X., Hafid, H., Wakisaka, M. (November, 2020): Enhanced lipid accumulation in freshwater microalga Euglena gracilis without sacrificing growth by supplementation of syringic acid and p-coumaric acid, Renewable Energy. **(Under review)**

2. Coauthored articles:

12. Tan, X., **Zhu, J.,** & Wakisaka, M. (2020). Effect of Protocatechuic Acid on Euglena gracilis Growth and Accumulation of Metabolites. Sustainability, *12*(21), 9158.
13. Tam, L. T., Ha, N. C., **Zhu, J. Y.**, Wakisaka, M., & Hong, D. D. (2020). Ferulic acid extracted from rice bran as a growth promoter for the microalga Nannochloropsis oculata. Journal of Applied Phycology, 1-9.
14. Xu, S., **Zhu, J**., Zhao, Q., Hardie, J., & Hu, B. (2017). Changes in the profile of aroma compounds in vitis vinifera l. cv merlot from grapes to wine. Bangladesh Journal of Botany, 46(3), 1089-1098.
15. Hu, B., Gao, J., Xu, S., **Zhu, J**., Fan, X., & Zhou, X. (2020). Quality evaluation of different varieties of dry red wine based on nuclear magnetic resonance metabolomics. Applied Biological Chemistry, 63(1), 1-8.
16. Hu, B., Cao, Y., **Zhu, J**., Xu, W., & Wu, W. (2019). Analysis of metabolites in chardonnay dry white wine with various inactive yeasts by 1 H NMR spectroscopy combined with pattern recognition analysis. AMB Express, 9(1), 140.
17. Hafid, H. S., Omar, F. N., **Zhu, J**., & Wakisaka, M. (2021). Enhanced Crystallinity and Thermal Properties of Cellulose from Rice Husk Using Acid Hydrolysis Treatment. Carbohydrate Polymers, 117789.
18. Xu, S., **Zhu, J**., Zhao, Q., Gao, J., Zhang, H., Hu, B. (2021). Quality Evaluation of Cabernet Sauvignon Wines in Different Vintages by 1H Nuclear Magnetic Resonance-Based Metabolomics. Open Chemistry.

3. Academic conferences:

1. 2020.11, The 9th Joint Conference on Renewable Energy and Nanotechnology: Growth promotion of freshwater microalga *Euglena gracilis* by three phenolic compounds from lignin basic structures **(JCREN 2020, Khon Kae, Thailand, Oral presentation)**; **Outstanding Presentation Award.**
2. 2019.09, The 13th International Congress on Engineering and Food: Application of air nanobubble water for the improvement of microalgae culture **(ICEF 13, Melbourne, Australia, Oral presentation)**;
3. 2019.09, The 12th International Marine Biotechnology Conference & the 12th Asia Pacific Marine Biotechnology Conference: Application Potential of Phytic Acid in the Harvest of Arthrospira platensis **(MBC 2019, Shizuoka, Japan, Poster presentation)**;
4. 2018.12, The 6th International Symposium on Applied Engineering and Sciences: Effect of Ferulic Acid from Rice Bran on Haematococcus lacustris and Euglena gracilis **(SAES 2018, Fukuoka, Japan, Oral presentation)**;
5. 2018.12, The 7th Joint Conference on Renewable Energy and Nanotechnology: Effect of Air Nanobubble Water on the Growth and Metabolism of Haematococcus lacustris and Botryococcus braunii **(JCREN 2018, Yamaguchi, Japan, Oral presentation)**; **Best Presentation Award.**
6. 2018.11, The 3rd International Symposium on Rice Science in Global Health: Phytic acid and ferulic acid from rice bran as growth promoters for Euglena gracilis **(ISRGH 2018, Kyoto, Japan, Poster presentation)**;
7. 2017.10, The 6th Joint Conference on Renewable Energy and Nanotechnology: Phytic acid as regulators of growth and metabolism of Euglena gracilis **(JCREN 2017, Kyoto, Japan, Oral presentation)**;
8. 2017.08, The 18th Annual Conference on Japanese Society for Food Engineering: Effect of phytic acid to growth and metabolites of various microalgae **(JSFE 2017, Osaka, Japan, Oral presentation)**;